PHENOMENOLOGICAL ANALYSIS OF HIGH-ENERGY HADRONIC PROCESSES

by

BRIAN JOHN HARTLEY

A thesis presented for the degree of

Doctor of Philosophy of the

University of London

and

the Diploma of Membership of Imperial College

Physics Department,

Imperial College of Science and Technology,

London S.W.7.

June 1971

ABSTRACT

A Reggeized absorption model is applied to 2-body and quasi-2-body hadronic scattering processes. The incorporation of U(6,6) ⊗ O(3,1) symmetry and the assumption of strong exchange degeneracy fix uniquely the relevant pole graphs in terms of the known pion-nucleon coupling constant and the known $\rho \to 2\pi$ decay width. Using the experimentally observed elastic scattering data absorption corrections are applied to these amplitudes. By appealing to a number of plausible assumptions we are able to obtain a model with no further adjustable parameters to be fitted to the data.

This model is applied to meson-baryon scattering processes which fall in the following categories

$$0^- \; 1/2^+ \to 0^- \; 1/2^+$$
$$0^- \; 1/2^+ \to 0^- \; 3/2^+$$
$$0^- \; 1/2^+ \to 1^- \; 1/2^+$$

and baryon-baryon scattering processes of the type

$$1/2^+ \; 1/2^+ \to 3/2^+ \; 1/2^+$$
$$1/2^+ \; 1/2^+ \to 3/2^+ \; 3/2^+$$

and which proceed by the exchange of non-strange mesons. The predictions of the model are compared with representative data on differential cross sections, polarizations and spin density matrix elements for a wide variety of such processes. Although detailed comparison is not always good, it is extremely encouraging that for the processes considered there are no drastic failures and a substantial number of successes.

PREFACE

The work presented in this thesis was carried out in the Department of Physics, Imperial College, London between October 1967 and September 1970 under the supervision of Professor P.T. Matthews, to whom the author is grateful for guidance and constant encouragement.

Except where explicit reference is made to the work of others, the material discussed is original and has not been submitted for a degree in this or any other University.

The author wishes to thank many members of the Theoretical Physics group, in particular Dr. R.W. Moore, P.A. Collins and K.J.M. Moriarty, with whom he collaborated for parts of this and similar work.

The financial support of the University of London in the form of Postgraduate Studentships during the academic years 1967-69 and the award of the George William Britt (Junior) Studentship during 1969-70 is gratefully acknowledged.

CONTENTS

		Page
ABSTRACT		2
PREFACE		3
CHAPTER I.	THE REGGEIZED ABSORPTION MODEL	
1.1	The Peripheral Model	6
1.2	Regge Poles	7
1.3	Difficulties with Regge Pole Models	9
1.4	The Absorption Model	12
1.5	Regge Cuts	16
1.6	Use of Absorption Corrections	19
1.7	Comparison with Other Models	20
CHAPTER II.	THE MODEL	
2.1	U(6,6) Formalism	24
2.2	Reggeization	34
2.3	Higher-Spin Exchange	37
2.4	Regge Trajectories	38
2.5	Absorption Effects	39
CHAPTER III.	APPLICATION TO MESON-BARYON SCATTERING	
3.1	Introduction	46
3.2	Formalism	46
3.3	Discussion and Results (i) $0^- 1/2^+ \to 0^- 1/2^+$	49
	(ii) $0^- 1/2^+ \to 0^- 3/2^+$	61
	(iii) $0^- 1/2^+ \to 1^- 1/2^+$	63

Page

CHAPTER IV. APPLICATION TO BARYON-BARYON SCATTERING

4.1 Introduction 93

4.2 Formalism 93

4.3 Discussion and Results (i) $1/2^+ \; 1/2^+ \to 3/2^+ \; 1/2^+$ 96

(ii) $1/2^+ \; 1/2^+ \to 3/2^+ \; 3/2^+$ 98

CHAPTER V. CONCLUSIONS

5.1 Summary 106

5.2 Calculational Procedure 109

APPENDIX A. NOTATION 110

APPENDIX B. DENSITY MATRIX AND POLARIZATION 112

APPENDIX C. ROTATION FUNCTIONS 115

APPENDIX D. HELICITY AMPLITUDES 120

APPENDIX E. NUMERICAL PROCEDURE 144

REFERENCES 147

CHAPTER I

THE REGGEIZED ABSORPTION MODEL

1.1 The Peripheral Model

The scattering amplitude for the 2-body process $1 + 2 \rightarrow 3 + 4$ may be expressed as a function of the three Mandelstam variables

$$s = (p_1 + p_2)^2$$

$$t = (p_1 - p_3)^2$$

$$u = (p_1 - p_4)^2$$

which are related by

$$s + t + u = \sum_{i=1}^{4} m_i^2 ,$$

where the p_i and m_i are the 4-momenta and masses, respectively, of the particles. Now, one of the empirical facts which has emerged from experimental high-energy 2-body inelastic scattering data is that an accumulation of events near the forward direction occurs when, and only when, the quantum numbers of the crossed t-channel reaction correspond to some known meson. This indicates a simple model for such processes, namely, an interaction mechanism based on the exchange of single particles in the t channel [1].

Early attempts to utilize this idea considered elementary particles as the intermediaries. Evaluation of the Feynman diagram for the exchange in the t channel of a particle of mass M leads to a scattering amplitude with a propagator containing a term of the form

$1/(t-M^2)$. Since this is singular at the (unphysical) value $t = M^2$, a general peaking of the differential cross section may be obtained at small values of momentum transfer. The idea of the peripheral model is that the scattering amplitude can be approximated by a sum of such 1-particle-exchange amplitudes, the particles of smallest mass giving rise to singularities lying closest to the physical region and thus dominating the interaction.

However, calculations involving the exchange of a particle of fixed spin J result in a momentum transfer distribution with an asymptotic energy dependence

$$\frac{d\sigma}{dt} \propto s^{2J-2}.$$

Since at sufficiently high incident momenta all cross sections are observed to decrease with energy, only spin-0 exchange can possibly give agreement at all energies, while higher-spin exchange inevitably fails except over a severely limited range. Theoretically, the total cross section should not diverge more rapidly than allowed by the Froissart bound [2] i.e. it can behave at most like $\ln^2 s$ as s tends to infinity.

1.2 Regge Poles

Following an original suggestion of Regge [3], the spin of the exchanged particle may be made a function of the momentum transfer i.e.

$$J \rightarrow \alpha(t).$$

The amplitude is then dominated asymptotically by a singularity in the

crossed channel which moves along the Regge trajectory $\alpha(t)$ [4]. As for elementary particles, each such moving pole has associated with it definite quantum numbers, in particular, isotopic spin, parity, hypercharge, baryon number, and (for non-strange mesons) G-parity, and an additional quantity known as signature $\tau = \pm 1$.

The Regge amplitude has the general asymptotic form

$$A(s,t) \sim \beta(t) \frac{1 + \tau e^{-i\pi\alpha(t)}}{2} \frac{1}{\sin\pi\alpha(t)} \left(\frac{s}{s_o}\right)^{\alpha(t)},$$

where s_o is a scale factor and the residue $\beta(t)$ is related to the coupling constants at the vertices. The term $1/\sin\pi\alpha(t)$ is similar to the elementary-particle propagator , but gives poles at all integer values of $\alpha(t)$. However, the signature factor gives zeros at wrong-signature points i.e. integer values of $\alpha(t)$ for which $\tau = -(-1)^{\alpha(t)}$, thus cancelling alternate poles. Therefore poles occur only at right-signature points i.e. integer values of $\alpha(t)$ for which $\tau = (-1)^{\alpha(t)}$. For $t > 0$ these poles correspond to particles with the appropriate spin, mass and internal quantum numbers. To avoid poles in the physical region $t < 0$, appropriate factors of $\alpha(t)$ must be inserted into the residue to eliminate these "ghosts". Owing to the $s^{\alpha(t)}$ term, those trajectories for which $\alpha(t)$ is greatest in the physical region tend to dominate the interaction.

For the exchange of such a Regge pole the momentum transfer distribution behaves like

$$\frac{d\sigma}{dt} \propto s^{2\alpha(t)-2}.$$

With $\alpha(t) < 1$ in the scattering region for all exchanges, qualitative

agreement with experiment is possible, thus overcoming the difficulty of energy dependence inherent in the exchange of fixed-spin particles [5].

The presence or absence of peaks in the backward direction may similarly be correlated with the exchange of baryons in the u-channel [1].

1.3 Difficulties with Regge Pole Models

However, particularly with the accumulation of more extensive and more detailed experimental data, it became apparent that there were a number of difficulties associated with simple Regge pole models [6]. In particular, it became necessary to introduce Regge trajectories corresponding to no known particles in order to account for certain important experimental features.

Pion-exchange reactions were a source of difficulty. The experimental differential cross-section data on certain processes which permit π exchange has an s^{-2} energy dependence and exhibits a sharp forward peak of width in t of the order of the square of the pion mass, suggesting π-exchange dominance.

A typical process of this type is $pn \to np$. The π contributes predominantly to two s-channel helicity amplitudes traditionally known as

$$\phi_2 = \langle ++|\phi|--\rangle$$

$$\phi_4 = \langle +-|\phi|-+\rangle .$$

Parity imposes the condition

$$\phi_2^{\pi} = \phi_4^{\pi}$$

since the pion has unnatural parity i.e. parity and spin related by $P = -(-1)^J$. Now, ϕ_4 is a net helicity flip amplitude and must therefore vanish in the forward direction for angular momentum conservation. Hence, ϕ_2 vanishes at $t = 0$, although, being a net helicity nonflip amplitude, it need not vanish at this point. A forward zero is therefore obtained rather than a peak.

In a pure Regge-pole framework a parity doublet of the π, known as the pion conspirator, is introduced. Since this has natural parity i.e. $P = (-1)^J$,

$$\phi_2^{c} = -\phi_4^{c}.$$

By arranging that at $t = 0$

$$\phi_2^{c} = \phi_2^{\pi}$$

to give

$$\phi_2 = \phi_2^{\pi} + \phi_2^{c}$$

$$= 2\,\phi_2^{\pi}$$

$$\phi_4 = \phi_4^{\pi} + \phi_4^{c}$$

$$= \phi_2^{\pi} - \phi_2^{c}$$

$$= 0$$

angular momentum is conserved without having ϕ_2 vanish at $t = 0$.

However, no candidate for this particle has been found, and Le Bellac showed, using factorization, that a consistent extension of the conspiracy solution predicts dips in the forward direction for reactions reactions such as

$$\pi N \to \rho \Delta$$
$$KN \to K^{*} \Delta$$
$$\pi N \to f \Delta,$$

whereas forward peaks are observed experimentally [4].

A second source of trouble was the type of process where only one known pole can be exchanged, notably the process $\pi^{-}p \to \pi^{o}n$, which proceeds by ρ exchange. Theoretically, the polarization of the recoil neutron depends on the term [7]

$$P(t) \sim \text{Im}\ (\phi_{++}\phi_{-+}^{*}),$$

where ϕ_{++} and ϕ_{-+} are the s-channel helicity nonflip and helicity flip amplitudes, respectively. Since both amplitudes have the same phase, zero polarization is predicted. However, high-energy experimental data shows that the polarization is about 15% for small momentum transfers.

A solution in a pure Regge-pole framework is to invoke the existence of another particle with the appropriate quantum numbers to be exchanged, known as the ρ'. Polarization is then generated by interference between the two poles. However, searches for this particle proved unsuccessful [4].

Elastic scattering also presented difficulties. High-energy

pp and $\bar{p}p$ elastic scattering should be dominated by the P + P' $\pm$ ω Regge poles, respectively. Experimentally, the differential cross section for $\bar{p}p$ is larger at t = 0 but more steeply t dependent than that for pp, so that they intersect at $t_o \simeq -.15$. In terms of a pure Regge-pole model this crossover requires the ω residue to change sign at this point. Then, by factorization, all ω residue functions must contain a zero at t_o.

This agrees with the crossover in $K^{\pm}p$ elastic scattering, which is also dominated by P, P' and ω, but it does not show up universally. For example, the reaction $\gamma p \to \pi^o p$ should be dominated by ω exchange, but it does not exhibit a minimum at t_o.

One solution is to introduce another ω-like term, the ω'. The crossover is then accounted for by having the $\omega+\omega'$ amplitude change sign at t_o without having to insert a zero in the ω residue. However, there is no known particle corresponding to the ω'.

1.4 The Absorption Model

These difficulties with pure Regge pole models can, at least in principle, be overcome by employing a model used very successfully for elementary-particle exchange in pion-dominated reactions, namely the absorption model.

The absorption model is based on the characteristics of high-energy elastic scattering [8]. At high energies many inelastic channels are open. When a collision takes place it is likely to result in a transition to one of these other channels. With respect to the elastic channel, such a transition results in the loss or absorption of a beam

particle. This absorption is greatest at small impact parameters, since the more complex inelastic reactions take place in the more violent "head-on" collisions. The target particle therefore appears as a diffuse absorbing disc to the particles in the beam.

For the elastic scattering of spinless particles of 3-momentum p, the partial wave expansion of the scattering amplitude, defined by

$$\frac{d\sigma}{d\Omega} = |f(\theta)|^2,$$

where θ is the center-of-mass scattering angle, is

$$f(\theta) = \frac{1}{2ip} \sum_{\ell=0}^{\infty} (2\ell+1)\ a^{\ell}\ P_{\ell}(\cos\theta),$$

where

$$a_{\ell} = 1 - S^{\ell}.$$

Introducing the impact parameter b, defined by

$$pb = \ell + \tfrac{1}{2},$$

low partial waves are seen to correspond to collisions at small impact parameters. The elastic waves are then largely absorbed i.e.

$$S^{\ell} \to 0$$

$$a^{\ell} \to 1.$$

Since the incident particles must "hit" the target for scattering to take place i.e.

$$\ell + \tfrac{1}{2} < pR,$$

where R is the radius of the interaction, no scattering takes place for high partial waves, and hence

$$S^{\ell} \to 1$$

$$a^{\ell} \to 0.$$

Since at high energies a large number of partial waves contribute to the partial-wave expansion, the sum over ℓ may be replaced by an integral over b i.e.

$$\sum_{\ell=0}^{\infty} \to \int_0^{\infty} p\, db.$$

In the Gaussian model it is assumed that

$$a(b) = C\, e^{-b^2/2R^2}.$$

Using the small-angle approximation

$$P_{\ell}(\cos\theta) = J_o(b\sqrt{|t|}),$$

we obtain

$$f(\theta) = \frac{pC}{i} R^2\, e^{\frac{1}{2}R^2 t},$$

and hence

$$\left(\frac{d\sigma}{dt}\right)_{\text{elastic}} \Big/ \left(\frac{d\sigma}{dt}\right)_{\text{elastic}} \Bigg|_{t=0} = e^{\frac{1}{2}R^2 t}.$$

This gives the falling exponential observed experimentally at small angles for elastic scattering. The quantity C may be obtained from the Optical Theorem, giving

$$C = \frac{\sigma_{tot}}{2\pi R^2} .$$

Similar considerations apply in the case of inelastic scattering. When the particles interact with impact parameter less than R, they are likely to be absorbed into another channel. Low partial waves are therefore absorbed out.

The absorption model takes into account the strong elastic interaction of the particles in the initial and final states. Sopkovich [9] and later authors [10,11] used the distorted-wave Born approximation to solve the Schrödinger equation for scattering in the presence of a potential with an imaginary part to simulate the effects of the competing channels. This part of the potential was chosen to give an adequate representation of the elastic scattering.

Sopkovich[9] obtained the formula

$$T'_{ba}{}^{\ell} = \sqrt{S_{bb}{}^{\ell}}\, T_{ba}{}^{\ell} \sqrt{S_{aa}{}^{\ell}},$$

where $T_{ba}{}^{\ell}$ is the Born term for scattering from channel a to channel b, $S_{aa}{}^{\ell}$ and $S_{bb}{}^{\ell}$ are the elastic scattering S-matrix elements in the initial and final states, respectively, and $T'_{ba}{}^{\ell}$ is the corrected amplitude. A similar formula, namely

$$T'_{ba}{}^{\ell} = \tfrac{1}{2}\left[S_{bb}{}^{\ell}\, T_{ba}{}^{\ell} + T_{ba}{}^{\ell}\, S_{aa}{}^{\ell}\right],$$

was obtained by Durand and Chiu [10]. These two equations become identical when $S_{bb}^{\ell} = S_{aa}^{\ell}$.

We see that these formulae do have the effect of absorbing out the low partial waves. Taking equal initial-state and final-state elastic scattering parameterized by a Gaussian, the above formulae become

$$T'_{ba}{}^{\ell} = \left[1 - Ce^{-\ell(\ell+1)/R^2p^2}\right] T_{ba}^{\ell} .$$

The high partial waves are unaffected, but the low partial waves are reduced. Indeed, when C = 1 the S-wave (ℓ=0) is completely eliminated. The modified amplitude is then different from the original amplitude. It was for this reason that the absorption model was originally developed. The 1-particle-exchange model, in paying no attention to the requirements of unitarity, allows the unitarity limit on the low partial waves to be violated. This leads to differential cross sections which are generally too large and not sufficiently peaked in the forward direction.

However, the assumptions made in the derivation of the various absorption formulae apply only at high energies. The use of the non-relativistic Schrödinger equation is therefore dubious. Despite this shakey theoretical basis, this model has been widely and successfully employed.

1.5 Regge Cuts

Assuming the elastic scattering to be described by a pole in the complex angular momentum plane, these corrections generate Regge-cut contributions to the scattering amplitudes. In particular, they have

the same general cut properties as those deduced from Feynman diagram models [6].

The existence of cuts in the complex angular momentum plane was first proposed by Amati, Fubini and Stangehellini [12] from a study of perturbation theory. Mandelstam [13] later showed that in fact the 2-Reggeon AFS cut is cancelled by other contributions, but he also showed how to generate cut diagrams which were not cancelled, the essential difference between the two diagrams being that, unlike the AFS diagram, the Mandelstam diagrams have a third double spectral function.

Although no one knows how to calculate the cut contributions, some general properties are known [6].

1. When n Regge poles $\alpha_i(t)$ are exchanged, the branch point of the leading cut is given by

$$\alpha_c(t) = \max\left[\sum_{i=1}^{n} \alpha_i(t_i)\right] - n + 1,$$

where $\sqrt{-t}$ and $\sqrt{-t_i}$ form a closed polygon. In particular, for two linear trajectories the 2-Reggeon branch point is also linear and is given by

$$\alpha_c(t) = \alpha_1(0) + \alpha_2(0) - 1 + \frac{\alpha_1' \alpha_2'}{\alpha_1' + \alpha_2'} t .$$

If all the Reggeons except one, $\alpha_1(t)$, are pomerons, with $\alpha_p(t) = 1$, the branch points of all the cuts coincide with α_1 at $t = 0$ and lie above it for $t < 0$. We therefore expect pomeron-induced cuts to dominate over poles asymptotically for $t < 0$. At $t = 0$ they are unfavoured logarithmically.

2. The discontinuity across the n-Reggeon cut near $j = \alpha_c$ has the form

$$\text{disc} \sim \left[\alpha_c(t) - j\right]^{n-2},$$

with the cut contribution to the amplitude having the energy dependence

$$A \sim \frac{s^{\alpha_c(t)}}{\ln s^{n-1}} .$$

Since this logarithmic energy dependence is slow, it cannot be detected at presently available energies.

3. Although a Regge pole belongs to a unique spin-parity class a 2-Reggeon cut does not. It can contribute to both parities and can therefore conspire with itself.

4. Cut contributions are non-factorizable. This overcomes the difficulties arising from factorizing pole residues and relating different processes.

The main difficulty in including cut contributions is the lack of knowledge about the discontinuity function. The usual practical approach is to employ a model such as the absorption model, since the absorption corrections result in contributions with the known properties of cuts [14], the Gaussian parameterization of the elastic scattering being equivalent asymptotically to a fixed-pole pomeron.

We can see how cuts arise in the absorption model by taking the absorption formula

$$T'^{\ell} = \tfrac{1}{2}\left[T_{ex}^{\ell}\, S_{el}^{\text{initial } \ell} + S_{el}^{\text{final } \ell}\, T_{ex}^{\ell}\right]$$

and, ignoring density of states factors, writting

$$S_{el}^{\ell} = 1 - i\, T_{el}^{\ell},$$

and expanding to obtain

$$T'^{\ell} = T_{ex}^{\ell} - \tfrac{1}{2}i\left[T_{ex}^{\ell}\, T_{el}^{\text{initial } \ell} + T_{el}^{\text{final } \ell}\, T_{ex}^{\ell}\right].$$

The first term may then be thought of as representing the pure Regge pole exchange, while the other two terms represent, respectively, elastic scattering in the initial state followed by an exchange, and an exchange followed by elastic scattering in the final state.

1.6 Use of Absorption Corrections

The sharp forward peaking observed in certain π-exchange reactions may be obtained by applying absorption corrections to the amplitudes [15]. The rotation functions in the partial-wave expansions ensure that the helicity flip amplitude ϕ_4 vanishes in the forward direction but imposes no such condition on the helicity nonflip amplitude ϕ_2. Now, for small t

$$\phi_2^{\pi} \sim \frac{t}{t - m_\pi^2}$$

$$= 1 + \frac{m_\pi^2}{t - m_\pi^2}\,.$$

The first term, being S-wave, is largely removed by the absorption, while the other partial waves are largely unaltered. Hence, after absorption

$$\phi_2^{\pi} \sim \frac{m_\pi^2}{t - m_\pi^2},$$

which gives the desired peak in the forward direction.

Absorption corrections produce relative changes of phase in the Regge amplitudes, thus generating non-zero polarization, and may be used to obtain destructive interference with the pole term to produce crossovers rather than having zeros in the residues. The Reggeized absorption model has thus eliminated many of the difficulties associated with models based solely on poles.

1.7 Comparison with Other Models

Basically, there are two currently popular models [16] which may be adopted for the introduction of Pomeron-Reggeon cuts by means of absorption corrections to pole-graph amplitudes.

In the "weak-cut" model, the approach adopted by the Argonne [17] and Imperial College [18,19] groups, the input Regge-pole amplitudes are "traditional" in that they contain appropriate factors to cause them to vanish at "nonsense" α values i.e. values of α less than the net helicity flip at either vertex. The presence of such a factor in the flip amplitude is the customary explanation of the dip near $t = -.5$ in the πN charge-exchange differential cross section. Because of the presence of these α factors the resulting cut contribution tends to be small. The absorption corrections therefore cause, for the most part, only modest changes to the pure pole term. The idea of wrong-signature nonsense zeros is supported by the sucess of the Veneziano model [20].

An alternative view, incorporated in the "strong-cut" model of the Michegan group [21], is that in the presence of cut corrections all prior notions concerning sense-nonsense factors should be discarded, since the standard arguments for the existence of these factors fail in the presence of a third double spectral function. The absence of α factors in this model then leads to a much larger cut term and the mechanism for generating dips in differential cross sections becomes the destructive interference between the pole and the cut amplitudes. This model also attempts to incorporate inelastic diffraction contributions by enhancing the contribution of the cut by a factor λ above that given by the standard absorption formula. Arguments are put forward to justify $\lambda \sim 2$ but in pratice it is taken as an arbitrary parameter to be fitted to the data, often with a value higher than this. Although the following remark in no way invalidates the concepts behind this approach, in a test of the systematics of dip generation by this model Drago et al [22] found it possible with a suitable choice of λ parameters to generate dips over a very wide range of momentum transfers and, in one case, found it necessary to take $\lambda \sim 3.5$ to obtain a dip in the correct position. They felt entitled to ask whether such a large λ was physically reasonable or just parameter fitting. Indeed the weak point of this model is the considerable number of free parameters which are introduced to parameterize the cuts in addition to those required in the pole amplitudes. Such flexibility permits the relatively easy fitting of available data but at the expense of a considerable loss of predictive power [23].

The model used here is the "weak-cut" type of model i.e. input Regge-pole amplitudes with wrong-signature nonsense zeros and cuts generated by the traditional absorption formula i.e. $\lambda = 1$. This does not add any parameters beyond those already present in simple Regge-pole

models. However there is still a considerable amount of arbitrariness, thus permitting a certain amount of flexibility. In particular, there is usually considerable freedom in the calculation of the pole graphs since there are frequently several different particles which may be exchanged, with often alternative couplings possible at the vertices and with the magnitudes of the coupling constants unknown. The Reggeization is also arbitrary in that it allows different ghost-eliminating mechanisms and exponential factors in the residues, with trajectories which are frequently unconstrained.

Rather than employ this arbitrariness to advantage by introducing free parameters which can then be fitted to the experimental data, it seems preferable to use some higher symmetry scheme in which the couplings are uniquely determined. We employ the $U(6,6) \otimes O(3,1)$ symmetry scheme [24] to calculate the pole graphs. This determines the vertex couplings and their magnitude and thus the amplitudes for the t-channel exchange of $\underline{35}$ mesons for $\underline{35} + \underline{56} \to \underline{35} + \underline{56}$ and $\underline{56} + \underline{56} \to \underline{56} + \underline{56}$ and the u-channel exchange of $\underline{56}$ baryons for $\underline{35} + \underline{56} \to \underline{56} + \underline{35}$. Since the $\underline{35}$ contains the meson 0^- octet and 1^- nonet and the $\underline{56}$ contains the baryon $1/2^+$ octet and $3/2^+$ decuplet, this accounts for a large section of 2-body and quasi-two-body processes on which data is presently available. Higher multiplets are regarded as angular-momentum-excited recurrences of lower ones [25]. We then take a single ghost-eliminating mechanism and a constant value of the scale factor s_o for all exchanges and obtain the Regge trajectories from the known masses of the particles lying on these trajectories.

Bearing in mind that the model contained no free parameters,

previous work with the U(6,6) peripheral absorption model with elementary-particle exchange [26,27,28] gave extremely good results for π (spin-0) exchange. Owing to the bad asymptotic energy dependence of the Born graphs for higher-spin exchange, this approach did not work except in the intermediate energy range for the exchange of spin other than zero. By Reggeization of these amplitudes the problem of energy dependence associated with high-spin exchange is eliminated. It is well known that for small momentum transfer elementary and Reggeized π exchange give essentially similar results [19]. We therefore retain the good results of the U(6,6) absorption model for π exchange but improve the results for higher-spin exchange.

CHAPTER II

THE MODEL

2.1 U(6,6) Formalism

The fact that the known meson and baryon particle spectrum is well described by the lower representations of SU(6) is the motivation for using an absorption model with the couplings related by U(6,6), the relativistic generalization of U(6).

The U(6,6) algebra [24] has 144 generators

$$\left[J_{Ri} \right]_A^{\ B} = \left[T_i \right]_a^{\ b} \left[\gamma_R \right]_\alpha^{\ \beta}$$

with A, B = 1 - 12, a, b = 1 - 3 and α, β = 1 - 4. The γ_R are the 16 Dirac matrices

$$1,\ \gamma_\mu,\ \sigma_{\mu\nu} = i\tfrac{1}{2}\left[\gamma_\mu, \gamma_\nu\right],\ \gamma_5 = \gamma_0\gamma_1\gamma_2\gamma_3,\ i\gamma_\mu\gamma_5$$

forming the generators of U(2,2), while the $T_i = \frac{1}{2}\lambda_i$, where the λ_i are the 9 Gell-Mann matrices forming the generators of U(3).

The basic spinor representation (quark), of multiplicity 12, transforms under the group according to

$$\psi_A \rightarrow S_A^{\ B}\ \psi_B$$

with

$$S_A^{\ B} = \left[e^{i\varepsilon_{Ri} J_{Ri}} \right]_A^{\ B}.$$

However, this does not correspond to any known physical particles. Higher representations are constructed by taking products of quark representations and reducing to irreducible representations. The product of quark and antiquark gives

$$\underline{12} \otimes \underline{\bar{12}} = \underline{1} \oplus \underline{143}$$

and the product of three quarks gives

$$\underline{12} \otimes \underline{12} \otimes \underline{12} = \underline{220} \oplus \underline{364} \oplus \underline{572} \oplus \underline{572} \ ,$$

where the representations are denoted by their multiplicities.

Two of the above multispinor representations are of interest, namely the traceless meson tensor $\Phi_A{}^B(\underline{143})$, which reduces to $(6,\bar{6})$ under the rest symmetry group U(6) ⊗ U(6) decomposition, and the fully symmetric baryon tensor $\Psi_{(ABC)}(\underline{364})$, which reduces to (56,1) under the U(6) ⊗ U(6) decomposition.

For a given J^P assignment SU(3) relates mesons and baryons among themselves. Under SU(3) ⊗ U(2,2) the above tensors decompose as

$$\underline{143} = (8,15) \oplus (1,15) \oplus (8,1)$$

$$\underline{364} = (10,20) \oplus (8,20) \oplus (1,4).$$

The $\underline{143}$ therefore contains the pseudoscalar meson octet and the vector meson nonet, while the $\underline{364}$ contains the baryon octet with spin 1/2 and the baryon decuplet with spin 3/2.

Written explicitly the decomposition of the meson tensor is

$$\Phi_A{}^B(p) = \left[\gamma_R \, T_i \right]_A{}^B \, \phi_R{}^i(p)$$

$$= \left[T_i \right]_a{}^b \left[\phi^i(p) + \gamma_5 \phi_5{}^i(p) + i\gamma_\mu \gamma_5 \phi_{\mu 5}{}^i(p) \right.$$

$$\left. + \gamma_\mu \phi_\mu{}^i(p) + \tfrac{1}{2}\sigma_{\mu\nu}\phi_{\mu\nu}{}^i(p) \right]_\alpha{}^\beta,$$

where the $\phi_R{}^i$ are the free meson fields of momentum p and mass μ. The trace term has been included.

Taking the fields on-shell, the Bargmann-Wigner equations

$$(\not{p}-\mu)_A{}^B \, \Phi_B{}^C(p) = \Phi_A{}^B(p) \, (\not{p}+\mu)_B{}^C = 0$$

lead to the relations

$$\phi^i(p) = 0$$

$$ip_\mu \, \phi_{\mu 5}{}^i(p) = \mu \, \phi_5{}^i(p)$$

$$i\mu \, \phi_{\mu 5}{}^i(p) = p_\mu \, \phi_5{}^i(p)$$

$$ip_\mu \, \phi_{\mu\nu}{}^i(p) = \mu \, \phi_\nu{}^i(p)$$

$$i\mu \, \phi_{\mu\nu}{}^i(p) = p_\mu \, \phi_\nu{}^i(p) - p_\nu \, \phi_\mu{}^i(p).$$

Substituting these relations, and using the equation of continuity of the vector field

$$p_\mu \, \phi_\mu{}^i(p) = 0,$$

gives

$$\Phi_A{}^B(p) = \frac{1}{2\mu} \left[T^i \right]_a{}^b \left[(\not{p}+\mu) \left(\gamma_\mu \, \phi_\mu{}^i(p) - \gamma_5 \, \phi_5{}^i(p) \right) \right]_\alpha{}^\beta,$$

where ϕ_5 is the nonet of pseudoscalar meson fields and ϕ_μ is the nonet of vector meson fields.

The baryon tensor is similarly decomposed to give

$$\Psi_{(ABC)}(p) = \varepsilon_{abc} \, V_{(\alpha\beta\gamma)}(p) + \frac{\sqrt{3}}{2\sqrt{2}} D_{(abc)(\alpha\beta\gamma)}(p)$$

$$+ \frac{1}{2\sqrt{6}} \left[\varepsilon_{abd} \, N_c{}^d{}_{(\alpha\beta)\gamma}(p) + \varepsilon_{bcd} \, N_a{}^d{}_{(\beta\gamma)\alpha}(p) \right.$$

$$\left. + \varepsilon_{cad} \, N_b{}^d{}_{(\gamma\alpha)\beta}(p) \right],$$

where

$$V_{(\alpha\beta\gamma)} = C_{\alpha\beta} \, V'_\gamma + (\gamma_5 \, C)_{\alpha\beta} \, V_\gamma + i \, (\gamma_\mu \, \gamma_5 \, C)_{\alpha\beta} \, V_{\mu\gamma}$$

$$D_{(\alpha\beta\gamma)} = (\gamma_\mu \, C)_{\alpha\beta} \, D_{\mu\gamma} + \tfrac{1}{2} \, (\sigma_{\mu\nu} \, C)_{\alpha\beta} \, D_{\mu\nu\gamma}$$

$$N_{(\alpha\beta)\gamma} = C_{\alpha\beta} \, N'_\gamma + (\gamma_5 \, C)_{\alpha\beta} \, N_\gamma + i \, (\gamma_\mu \, \gamma_5 \, C)_{\alpha\beta} \, N_{\mu\gamma},$$

with C the charge-conjugation matrix

$$C^{-1} \, \gamma_0 \, C = - \gamma_0$$

and

$$V = \gamma_5 V'$$

$$V_\mu = -i \gamma_\mu \gamma_5 V'$$

$$N' = \gamma_5 N + i \gamma_\mu \gamma_5 N_\mu$$

$$\gamma_\mu D_\mu = \gamma_\mu D_{\mu\nu} + i D_\nu = 0.$$

Applying the Bargmann-Wigner equations

$$(\not{p}-m)_A^B \Psi_{(BCD)}(p) = 0,$$

where m is the baryon mass, gives

$$V = N' = 0$$

$$(\not{p}-m) N(p) = 0$$

$$im N_\mu(p) = p_\mu N(p)$$

$$(\not{p}-m) D_\mu(p) = 0$$

$$im D_{\mu\nu}(p) = p_\mu D_\nu(p) - p_\nu D_\mu(p).$$

We therefore obtain

$$\Psi_{(ABC)}(p) = \frac{\sqrt{3}}{2\sqrt{2}m} \left((\not{p}+m)\ \gamma_\mu\ C \right)_{\alpha\beta} D_{\mu\gamma(abc)}(p)$$

$$+ \frac{1}{2\sqrt{6}m} \Big[\left((\not{p}+m)\ \gamma_5\ C \right)_{\alpha\beta} \varepsilon_{abd}\ N_c{}^d{}_\gamma(p)$$

$$+ \left((\not{p}+m)\ \gamma_5\ C \right)_{\beta\gamma} \varepsilon_{bcd}\ N_a{}^d{}_\alpha(p)$$

$$+ \left((\not{p}+m)\ \gamma_5\ C \right)_{\gamma\alpha} \varepsilon_{cad}\ N_b{}^d{}_\beta(p) \Big] ,$$

with N_μ and $D_{\mu\gamma}$ the fields corresponding to the $1/2^+$ octet and $3/2^+$ decuplet, respectively.

The 3-meson vertex is described by the unique interaction Lagrangian

$$\mathcal{L} = \Phi_A{}^B(-Q)\ J_B{}^A(p,p')$$

with

$$J_A{}^B(p,p') = h \left[\Phi_A{}^C(p)\ \Phi_C{}^B(-p') + \Phi_A{}^C(-p')\ \Phi_C{}^B(p) \right] ,$$

where h is the meson-meson-meson coupling constant, p and p' are the 4-momenta of the incoming and outgoing particles, respectively, and $Q = p - p'$.

There is also a unique baryon-baryon-meson interaction Lagrangian

$$\mathcal{L} = \Phi_A{}^B(-Q)\ J_B{}^A(p,p')$$

with

$$J_A^B(p,p') = g\,\bar{\Psi}^{(BCD)}(p')\,\Psi_{(ACD)}(p),$$

where g is the baryon-baryon-meson coupling constant.

On evaluating the traces, we obtain the pseudoscalar current

$$j_5 = g\left(1+\frac{2m}{\mu}\right)\Big[\frac{P^2}{4m^2}(\bar{N}\gamma_5 N)_{D+\frac{2}{3}F-S} + \frac{Q_\lambda}{m}(\bar{D}_\lambda N)_G$$

$$+\frac{3P^2}{4m^2}\bar{D}_\lambda\gamma_5 D_\lambda + \frac{3}{2m^2}Q_\lambda\bar{D}_\lambda\gamma_5 Q_\kappa D_\kappa + \text{h.c.}\Big]$$

$$-\frac{3h}{2\mu}\varepsilon_{\mu\nu\kappa\lambda}Q_\mu P_\nu(\bar{\phi}_\kappa\phi_\lambda)_D - 3hQ_\lambda(\bar{\phi}_\lambda\phi_5-\bar{\phi}_5\phi_\lambda)_F,$$

and the vector current

$$j_\mu = g\,\frac{P_\mu}{2m}\left(1+\frac{Q^2}{2m\mu}\right)(\bar{N}N)_{F+3S} + g\left(1+\frac{2m}{\mu}\right)\left(\bar{N}\frac{r_\mu}{4m^2}N\right)_{D+\frac{2}{3}F-S}$$

$$-\frac{g}{2m^2}\left(1+\frac{2m}{\mu}\right)\varepsilon_{\mu\nu\kappa\lambda}P_\nu Q_\kappa(\bar{D}_\lambda N)_G$$

$$+\frac{3gP^2}{4m^2}\bar{D}_\lambda\Big[\left(1+\frac{2m}{\mu}\right)\gamma_\mu - \frac{P_\mu}{\mu}\Big]D_\lambda$$

$$+\frac{3g}{2m^2}Q_\lambda\bar{D}_\lambda\Big[\left(1+\frac{2m}{\mu}\right)\gamma_\mu - \frac{P_\mu}{\mu}\Big]Q_\kappa D_\kappa + \text{h.c.}$$

$$+h\left(1+\frac{Q^2}{2\mu^2}\right)P_\mu(\bar{\phi}_5\phi_5-\bar{\phi}_\lambda\phi_\lambda)_F + \frac{h}{\mu^2}P_\mu Q_\nu Q_\lambda(\bar{\phi}_\nu\phi_\lambda)_F$$

$$+3hQ_\nu(\bar{\phi}_\nu\phi_\mu-\bar{\phi}_\mu\phi_\nu)_F + \frac{3h}{2\mu}\varepsilon_{\mu\nu\kappa\lambda}P_\nu Q_\kappa(\bar{\phi}_\lambda\phi_5-\bar{\phi}_5\phi_\lambda)_{D+2S},$$

where

$$r_\mu = \epsilon_{\mu\nu\kappa\lambda} P_\nu Q_\kappa \gamma_\lambda \gamma_5$$

with P and Q the sum and difference, respectively, of the momenta of the incoming and outgoing external particles at the vertex.

The subscripts D, F, S and G represent the U(3) Clebsch-Gordan coefficients. Taking the baryon-baryon-meson vertex as an example, and normalizing to $\bar{p}p\pi^o$, we have, for the coupling of three octets the symmetric coupling

$$(\bar{B}BM)_D = \sqrt{2}(\bar{B}_b{}^c B_a{}^b M_c{}^a + \bar{B}_a{}^b B_b{}^c M_c{}^a),$$

and the antisymmetric coupling

$$(\bar{B}BM)_F = \sqrt{2}(\bar{B}_b{}^c B_a{}^b M_c{}^a - \bar{B}_a{}^b B_b{}^c M_c{}^a),$$

for the coupling of two octets and a singlet

$$(\bar{B}BM_o)_S = \frac{\sqrt{2}}{\sqrt{3}} \bar{B}_b{}^a B_a{}^b M_o,$$

and for the coupling of the baryon decuplet and baryon and meson octets

$$(\bar{D}BM)_G = \sqrt{2}\, \bar{D}^{rst} M_r{}^u \epsilon_{usv} B_t{}^v.$$

These interactions are used to calculate 1-particle-exchange diagrams in which the exchanged particle is off the mass-shell in the region of physical scattering. Since the Bargmann-Wigner equations are

used in the derivation, these interactions, strictly speaking, apply only to free fields. For this reason we take the P^2 and Q^2 terms appearing explicitly in the currents as on-shell i.e.

$$P^2 = \left(1 - \frac{\mu^2}{4m^2}\right)$$

$$Q^2 = \mu^2.$$

The relevant parts of these currents required for the processes considered here are, for the pseudoscalar current

$$J_5(0) = g\left(1 + \frac{2m}{\mu}\right)\left(1 - \frac{\mu^2}{4m_B^2}\right)(\bar{N}\gamma_5 N)_{D+\frac{2}{3}F-S}$$

$$J_5(D) = g\left(1 + \frac{2m}{\mu}\right)\frac{Q_\lambda}{m_B}(\bar{D}_\lambda N)_G$$

$$J_5(V) = -3hQ_\lambda(\bar{\phi}_\lambda\phi_5)_F,$$

and for the vector current

$$J_\mu(0) = g\left[\frac{P_\mu}{2m_B}\left(1 + \frac{\mu}{2m}\right)(\bar{N}N)_{F+3S} + \left(1 + \frac{2m}{\mu}\right)\left(\bar{N}\frac{r_\mu}{4m_B^2}N\right)_{D+\frac{2}{3}F-S}\right]$$

$$J_\mu(D) = -\frac{g}{2m_B^2}\left(1 + \frac{2m}{\mu}\right)\varepsilon_{\mu\nu\kappa\lambda}P_\nu Q_\kappa(\bar{D}_\lambda N)_G$$

$$J_\mu(P) = \frac{3}{2}hP_\mu(\bar{\phi}_5\phi_5)_F$$

$$J_\mu(V) = \frac{3h}{2m_M}\varepsilon_{\mu\nu\kappa\lambda}P_\nu Q_\kappa(\bar{\phi}_\lambda\phi_5)_{D+2S}.$$

Since there is no definitive procedure for mass splitting in higher symmetry schemes, we have adopted a simple prescription which seems physically reasonable. For the group-theoretic baryon mass we take m = 1.27 GeV/c^2, the average of the $1/2^+$ octet and $3/2^+$ decuplet, and for the group-theoretic meson mass we take μ = .63 GeV/c^2, the average of the 0^- nonet and 1^- nonet. Where shown we use the average physical mass of the incoming and outgoing external particles at the baryon and meson vertices, m_B and m_M, respectively. In the kinematics and the evaluation of $\bar{N}N$ etc. we use the physical masses of the particles.

The two coupling constants which appear in the currents are obtained from the known pion-nucleon coupling constant [29], giving

$$\frac{g^2_{NN\pi}}{4\pi} = 14.9 = \frac{g^2}{4\pi}\left(1 + \frac{2m}{\mu}\right)^2 \left(1 - \frac{\mu^2}{4m_N^2}\right)^2 \left(\frac{5}{3}\right)^2,$$

where m_N is the nucleon mass, and from the $\rho \to 2\pi$ decay width [30], giving

$$\frac{g^2_{\rho\pi\pi}}{4\pi} = 2.09 = \frac{(3h)^2}{4\pi} .$$

It is now a straight-forward matter to calculate the 1-particle-exchange diagrams using second-order perturbation theory. For pseudoscalar exchange the amplitude is

$$\langle p_3 p_4 | T | p_1 p_2 \rangle = \langle p_3 p_4 | J_5 \frac{1}{t-M^2} J_5 | p_1 p_2 \rangle,$$

and for vector exchange the amplitude is

$$\langle p_3 p_4 | T | p_1 p_2 \rangle = \langle p_3 p_4 | J'_\mu \frac{-g_{\mu\nu} + Q_\mu Q_\nu / M^2}{t-M^2} J_\nu | p_1 p_2 \rangle,$$

where the primed and unprimed currents distinguish the two vertices, M is the mass of the exchanged particle, and the diagonal metric is $g_{\mu\nu} = (+1;-1,-1,-1)$.

2.2 Reggeization

The Reggeization of the elementary-particle-exchange amplitudes is accomplished in the following manner.

Consider the exchange of a 0^- meson. By expanding in a Taylor series about $t = M^2$

$$\sin\pi(\alpha-J) \simeq \sin\pi(\alpha-J)\Big|_{t=M^2} + \frac{d}{dt}\sin\pi(\alpha-J)\Big|_{t=M^2} (t-M^2)$$

$$\simeq \pi \frac{d\alpha}{dt}\Big|_{t=M^2} (t-M^2),$$

since $\alpha(t=M^2) = 0$. Therefore, near $t = M^2$

$$\frac{1}{t-M^2} = \frac{d\alpha}{dt}\Big|_{t=M^2} \frac{\pi}{\sin\pi\alpha(t)} .$$

Using the identity

$$\frac{\pi}{\sin\pi x} = \Gamma(x)\,\Gamma(1-x),$$

we obtain

$$\frac{1}{t-M^2} = -\alpha' \Gamma(-\alpha)\, \Gamma(1+\alpha).$$

We then insert the signature factor

$$\frac{1 + e^{-i\pi\alpha}}{2},$$

and the factor

$$\left(\frac{s - \tfrac{1}{2}t - \tfrac{1}{2}\sum_{i=1}^{4} m_i^2}{s_o}\right)^{\alpha}.$$

This second term changes the asymptotic energy dependence of the elementary-exchange amplitudes from $s^J = s^0$ into the Regge dependence $s^{\alpha(t)}$. Both these factors are unity at the pole $t = M^2$.

The Gell-Mann ghost-eliminating mechanism [4] is introduced by dividing by $\Gamma(1+\alpha)$ in all amplitudes. We select this mechanism because it is required by exchange degeneracy and is supported by the sucess of the Veneziano formula [20]. It is easily introduced into the formalism and retains the same ratio between the helicity amplitudes when they are extrapolated from the pole.

Hence, the replacement for 0^- exchange is

$$\frac{1}{t-M^2} \to -\left.\frac{d}{dt}\right|_{t=M^2} \Gamma(-\alpha)\, \frac{1 + e^{-i\pi\alpha}}{2} \left(\frac{s + \tfrac{1}{2}t - \tfrac{1}{2}\sum_{i=1}^{4} m_i^2}{s_o}\right)^{\alpha}.$$

Similarly, for 1^- exchange

$$\sin\pi\alpha(t) \simeq \sin\pi\alpha(t)\Big|_{t=M^2} + \frac{d}{dt}\Big|_{t=M^2} \sin\pi\alpha(t)\Big|_{t=M^2} (t-M^2)$$

$$\simeq - \pi \frac{d\alpha}{dt}\Big|_{t=M^2} (t-M^2),$$

since $\alpha(t=M^2) = 1$. Therefore, near $t = M^2$

$$\frac{1}{t-M^2} = - \frac{d\alpha}{dt}\Big|_{t=M^2} \frac{\pi}{\sin\pi\alpha}$$

$$= - \alpha' \Gamma(\alpha) \Gamma(1-\alpha).$$

The signature factor

$$\frac{1 - e^{-i\pi\alpha}}{2},$$

and the factor

$$\left(\frac{s + \frac{1}{2}t - \frac{1}{2} \sum_{i=1}^{4} m_i^2}{s_o} \right)^{\alpha-1},$$

which changes the asymptotic energy dependence from $s^J = s^1$ into $s^{\alpha(t)}$, are inserted. The Gell-Mann mechanism is introduced by dividing by $\Gamma(\alpha)$ in all amplitudes.

The replacement for 1^- exchange is therefore

$$\frac{1}{t-M^2} \to -\alpha' \Gamma(1-\alpha) \frac{1 - e^{-i\pi\alpha}}{2} \left(\frac{s + \frac{1}{2}t - \frac{1}{2}\sum_{i=1}^{4} m_i^2}{s_o} \right)^{\alpha-1} .$$

In summary, the Reggeization of the amplitudes is accomplished by making the replacement

$$\frac{1}{t-M^2} \to \left.\frac{d\alpha}{dt}\right|_{t=M^2} \frac{\pi}{\sin\pi(\alpha-J)} \frac{1 + \tau e^{-i\pi\alpha}}{2} \left(\frac{s + \frac{1}{2}t - \frac{1}{2}\sum_{i=1}^{4} m_i^2}{s_o} \right)^{\alpha-J} ,$$

where $\alpha = J$ at the pole $t = M^2$ and τ is the signature, and substituting

$$\frac{\pi}{\sin\pi\alpha} = \Gamma(\alpha)\,\Gamma(1-\alpha)$$

and dividing by $\Gamma(\alpha)$ for natural-parity exchange, and substituting

$$\frac{\pi}{\sin\pi\alpha} = -\Gamma(-\alpha)\,\Gamma(1+\alpha)$$

and dividing by $\Gamma(1+\alpha)$ for unnatural-parity exchange in all amplitudes.

The scale factor s_o is taken to have the value 1 $(\text{GeV})^2$ since any other choice is equivalent to the introduction of an exponential factor into the residue. The coupling constants g and h retain the values at the poles.

2.3 Higher-Spin Exchange

We also wish to cosider the exchange of the A_2 meson ($J^P=2^+$), which does not belong to the ($\underline{35}$, $\ell=0$). By employing the representation of U(6,6) which contains the A_2, namely the $\underline{4212}$, we have forced upon us

exotics, for which no experimental evidence has been found. However, employing U(6,6) ⊗ O(3,1) we obtain mesons not belonging to the ($\underline{35}$,ℓ=0) by angular-momentum excitating this representation of U(6,6) ⊗ O(3,1). This has the effect of only changing the spin and parity of the particles. Using a spin-2 field-theoretic propagator then gives amplitudes which are similar to those for 1^- exchange but containing one more power of s and, in some cases, extra terms which are non-leading in s. If we ignore these extra terms, we may obtain the Reggeized 2^+-exchange amplitudes from the 1^--exchange amplitudes simply by changing the signature and Clebsch-Gordan coefficients. This is the procedure we adopt, since we wish to obtain the coupling strength from the additional assumption of strong exchange degeneracy. The 1^+-exchange amplitudes are obtained from the 0^--exchange amplitudes in a similar manner. Since previous authors have shown the applicability of ρ-A_2 exchange degeneracy and SU(3) symmetry to $0^-\ 1/2^+ \to 0^-\ 1/2^+$ charge-exchange reactions [31], we consider this is a reasonable prescription.

2.4 Regge Trajectories

The Regge exchanges considered here correspond to the π, η, ρ, ω, ϕ, B and A_2 mesons. We assume linearly rising trajectories

$$\alpha(t) = \alpha_o + \alpha' t,$$

where α_o and α' are the intercept and slope, respectively.

To avoid the introduction of free parameters we make the plausible assumption [32] that the following pairs of particles

$\rho(765)$ - $A_2(1300)$

$\omega(784)$ - $f(1264)$

$\phi(1019)$ - $f'(1514)$

$\pi(140)$ - $B(1235)$

$\eta(549)$ - $D(1285)$

lie on exchange-degenerate trajectories. There were obtained by constraining the trajectories to pass through the positions of the relevant physical particles on the Chew-Frautschi plot, as shown in Fig. 1. The values obtained for these trajectories are given in Table 1.

In Ref. 18 almost exchange-degenerate ρ-A_2 and $K^*(890)$-$K_N(1420)$ trajectories were found to arise from fitting data, although this was not imposed as a constraint. We note that the ρ-A_2 trajectory used here extrapolates to pass extremely closely to the probable ρ-Regge recurrence, the g-meson. The predicted mass is 1673 compared with the experimental mass of 1663. Similarly, the ω-f trajectory extrapolates to give a mass of 1604 for the possible ω-Regge recurrence, the $\phi(1650)$. The π-B trajectory, when extrapolated, predicts a mass for the suggested π-Regge recurrence, the π_A, of 1740 compared with the experimental value of 1633. The Regge recurrences of the ϕ and η are not yet well established.

2.5 Absorption Effects

Now, the partial-wave expansion of the s-channel helicity amplitudes is [33]

$$\langle\lambda_3\lambda_4|\phi(s,t)|\lambda_1\lambda_2\rangle = \sum_{j=j_{min}}^{\infty} (2j+1)\, \langle\lambda_3\lambda_4|T^j(s)|\lambda_1\lambda_2\rangle\, d_{\lambda\mu}{}^j(\cos\theta),$$

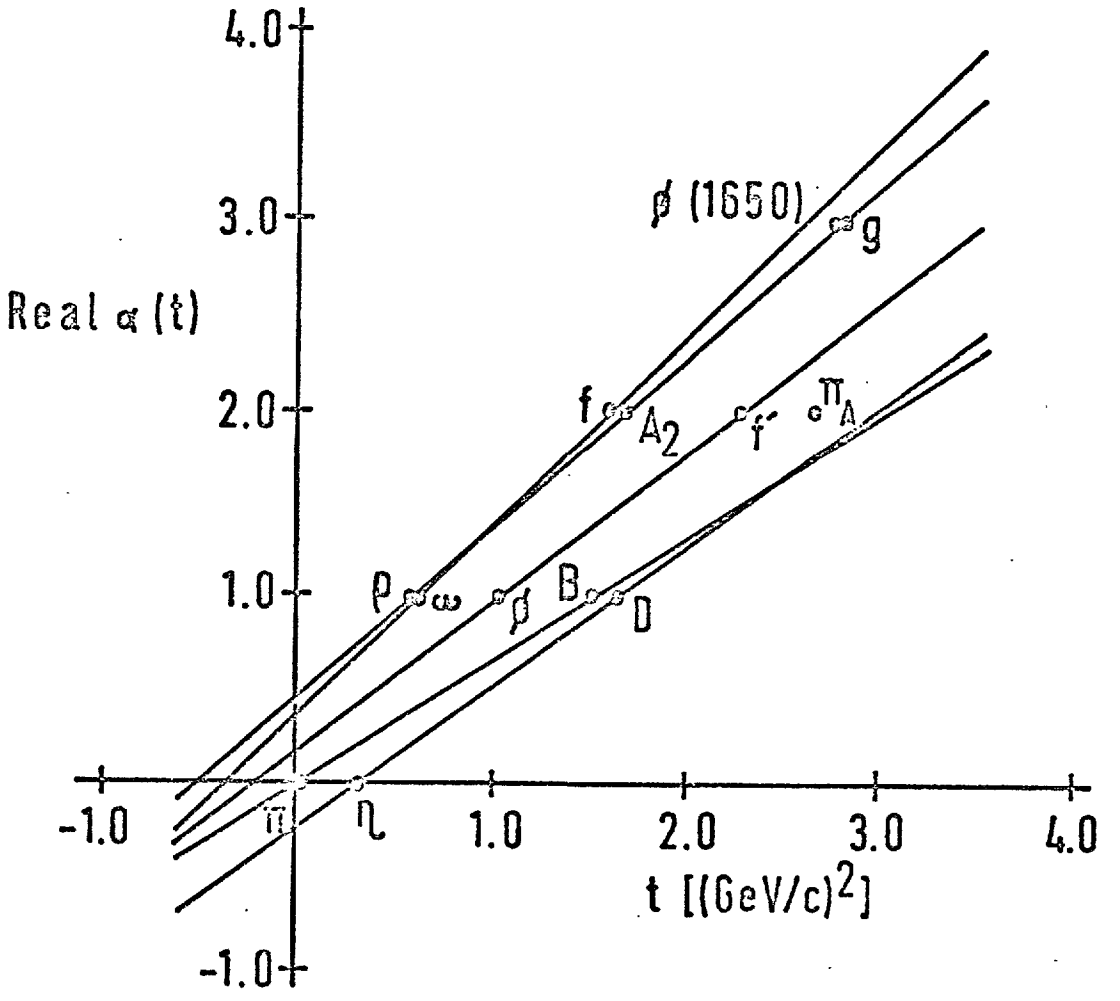


Fig. 1

Chew-Frautschi plot. The trajectories are given in Table 1.

Trajectory	α_o	$\alpha'\{(GeV/c)^{-2}\}$
π,B	- .013	.665
η	- .222	.737
ρ,A_2	.470	.905
ω	.386	1.017
ϕ	.172	.798

Table 1

Regge trajectories

where j is the total angular momentum, $j_{min} = \max(|\lambda|, |\mu|)$, $\lambda = \lambda_1 - \lambda_2$, $\mu = \lambda_3 - \lambda_4$, and θ is the c.m. scattering angle. By making use of the orthogonality property of the rotation functions,

$$\int_{-1}^{+1} d_{\lambda\mu}{}^{j}(\cos\theta)\, d_{\lambda\mu}{}^{j'}(\cos\theta)\, d(\cos\theta) = \frac{2}{2j+1}\,\delta_{jj'}\ ,$$

we obtain the partial-wave amplitudes

$$\langle\lambda_3\lambda_4|T^j(s)|\lambda_1\lambda_2\rangle = \tfrac{1}{2}\int_{-1}^{+1} \langle\lambda_3\lambda_4|\phi(s,t)|\lambda_1\lambda_2\rangle\, d_{\lambda\mu}{}^{j}(\cos\theta)\, d(\cos\theta).$$

We employ the Watson absorption formula [11], according to which the corrected partial-wave amplitude for scattering from channel a to channel b, $T'_{ba}{}^{j}$, is related to the Born partial-wave amplitude, $T_{ba}{}^{j}$, by

$$\langle\lambda_3\lambda_4|T'_{ba}{}^{j}|\lambda_1\lambda_2\rangle = \tfrac{1}{2}\sum_{\alpha,\beta}\big[\langle\lambda_3\lambda_4|S_{bb}{}^{j}|\alpha\beta\rangle\langle\alpha\beta|T_{ba}{}^{j}|\lambda_1\lambda_2\rangle + \langle\lambda_3\lambda_4|T_{ba}{}^{j}|\alpha\beta\rangle\langle\alpha\beta|S_{aa}{}^{j}|\lambda_1\lambda_2\rangle\big],$$

where α, β and λ_i are the helicities of the particles, and $S_{aa}{}^{j}$ and $S_{bb}{}^{j}$ are the S-matrix elements for elastic scattering in the initial and final states, respectively.

We assume a Gaussian model for the elastic scattering of spinless particles [8]

$$S^{\ell} = 1 - Ce^{-\ell(\ell+1)/R^2p^2},$$

where ℓ is the orbital angular momentum and p is the c.m. 3-momentum. Making the replacement $\ell \to j$ in this formula assumes the same form for S^j as for S^ℓ. This association is reasonable since, for example, for $0\ \frac{1}{2}$ elastic scattering the amplitude for total angular momemtum j is a weighted mean of the amplitudes with orbital angular momentum $\ell = j \pm \frac{1}{2}$. Similarly for $\frac{1}{2}\ \frac{1}{2}$ elastic scattering $\ell = j, j \pm 1$. We also assume that S^j involves only helicity nonflip terms. This is the conventional assumption, which is justified on the grounds that the elastic scattering amplitude is experimentally largest in the forward direction. Since the helicity flip amplitudes vanish at this point they are hopefully relatively unimportant in general.

The quantity R, the radius of the interaction, is determined from the observed exponential slope of the elastic scattering data

$$\left(\frac{d\sigma}{dt}\right)_{el} \Big/ \left(\frac{d\sigma}{dt}\right)_{el}\Bigg|_{t=0} = e^{\frac{1}{2}R^2 t},$$

while the opacity C is obtained using the Optical Theorem

$$C = \frac{\sigma_{tot}}{2\pi R^2}\ .$$

The final-state absorption coefficients, C and R, cannot generally be determined experimentally. To obviate the need to introduce free parameters we assume that the coefficients are the same in the final state as in the initial state. We note that since the initial-state and final-state c.m. 3-momenta are usually unequal, this means that $S_{final}{}^j$ and $S_{initial}{}^j$ are slightly different. The absorption

coefficients used [28,34,35] are shown in Table 2. No data exists on K^+n elastic differential cross sections at high energies. However, K^+n and K^+p total cross sections are almost the same, so hopefully the absorption coefficients are not too different. We have therefore used the K^+p coefficients to describe K^+n elastic scattering. We have also used the π^+p coefficients to describe π^+n elastic scattering.

With the above assumptions the absorption formula simplifies to

$$\langle\lambda_3\lambda_4|T'_{ba}{}^{j}|\lambda_1\lambda_2\rangle = \tfrac{1}{2}\,(S_{final}{}^{j}+S_{initial}{}^{j})\,\langle\lambda_3\lambda_4|T_{ba}{}^{j}|\lambda_1\lambda_2\rangle.$$

The partial waves are modified according to this prescription and resummed to obtain the modified scattering amplitudes

$$\langle\lambda_3\lambda_4|\phi'(s,t)|\lambda_1\lambda_2\rangle = \sum_{j=j_{min}}^{\infty}(2j+1)\,\langle\lambda_3\lambda_4|T'^{j}(s)|\lambda_1\lambda_2\rangle\, d_{\lambda\mu}{}^{j}(\cos\theta).$$

It is these modified amplitudes which are to be compared with experiment by means of differential cross sections, polarizations[7] and density matrix elements [36]. These are discussed in Appendices A and B.

Explicit expressions for the rotation functions $d_{\lambda\mu}{}^{j}(\cos\theta)$ are given in Appendix C.

Channel	p_{lab} (GeV/c)	C	(R^{-1}) (GeV/c)
$\pi^- p$	4.2	.83	.26
	5.9	.79	.26
	8.0	.76	.26
	9.8	.74	.26
	11.2	.73	.26
	13.3	.72	.26
	16.0	.71	.26
	18.2	.70	.26
$\pi^+ p$	3.54	.90	.27
	4.0	.87	.27
	5.1	.84	.27
	8.0	.78	.27
	9.0	.77	.27
$K^- p$	4.1	.77	.26
	5.0	.74	.26
	5.5	.73	.26
	6.0	.72	.26
	7.1	.70	.26
	9.5	.67	.26
	10.1	.66	.26
	12.3	.65	.26
$K^+ p$	5.0	.71	.32
	5.5	.68	.31
	7.3	.58	.29
	12.0	.51	.27
	12.7	.51	.27
pp	5.0 - 6.92	1.000	.247
	8.1	.989	.245
	10.0	.963	.245
	13.0	.926	.240
	15.0	.911	.239
	16.08	.904	.237
	18.1	.883	.236
	21.1	.844	.232
	24.2	.830	.230

Table 2

Absorption coefficients

CHAPTER III

APPLICATION TO MESON-BARYON SCATTERING

3.1 Introduction

We consider 2-body and quasi-2-body inelastic meson-baryon scattering processes which fall in the following categories

$$0^-1/2^+ \to 0^-1/2^+$$
$$0^-1/2^+ \to 0^-3/2^+$$
$$0^-1/2^+ \to 1^-1/2^+$$

and which proceed by the exchange of non-strange mesons [37]. Since the conservation of angular momentum and parity forbids the coupling of three pseudoscalar mesons, only 1^- and 2^+ exchanges are possible in the first two types of process, whereas generally 0^- exchange, in particular the pion, is permitted in the third class.

3.2 Formalism

Denoting the pseudoscalar-exchange and vector-exchange amplitudes by T_P and T_V, respectively, we have for $0^-1/2^+ \to 0^-1/2^+$

$$T_V = J_\mu'(P) \frac{-g_{\mu\nu} + Q_\mu Q_\nu/M^2}{t-M^2} J_\nu(O),$$

for $0^-1/2^+ \to 0^-3/2^+$

$$T_V = J_\mu'(P) \frac{-g_{\mu\nu} + Q_\mu Q_\nu/M^2}{t-M^2} J_\nu(D),$$

and for $0^-1/2^+ \to 1^-1/2^+$

$$T_P = J_5'(V) \frac{1}{t-M^2} J_5(0)$$

$$T_V = J_\mu'(V) \frac{-g_{\mu\nu} + Q_\mu Q_\nu/M^2}{t-M^2} J_\nu(0),$$

where the primed and unprimed quantities distinguish the meson and baryon vertices, respectively.

We note that between spinors

$$\frac{r_\mu}{4m_B^2} = \frac{P^2}{4m_B^2} \gamma_\mu - \frac{P_\mu}{2m_B},$$

and take P^2 and Q^2 on-shell.

The $1/M^2$ term in the propagator vanishes identically for $0^-3/2^+$ and $1^-1/2^+$ production from the properties of the ε function. For $0^-1/2^+$ production we eliminate this term by ignoring the slight p-n mass difference. This term, which is non-leading in s, would otherwise lead to a 1/t singularity since $M^2 \to t$ on Reggeization.

These amplitudes are Reggeized and the 1^+ and 2^+ exchanges introduced. We then obtain for $0^-1/2^+ \to 0^-1/2^+$

$$T = \Big[\, h_F\ \alpha'_V\ \Gamma(1-\alpha_V)\ \frac{1 - e^{-i\pi\alpha_V}}{2}\ \left(\frac{s + \frac{1}{2}t - \frac{1}{2}\sum_{i=1}^{4} m_i^2}{s_o}\right)^{\alpha_V - 1}$$

$$+\ h_D\ \alpha'_T\ \Gamma(1-\alpha_T)\ \frac{1 + e^{-i\pi\alpha_T}}{2}\ \left(\frac{s + \frac{1}{2}t - \frac{1}{2}\sum_{i=1}^{4} m_i^2}{s_o}\right)^{\alpha_T - 1}\ \Big]$$

$$\times\ \frac{3}{2}\ g\ h\ \Big[\ \frac{1}{2m_B}\Big[\Big(1 + \frac{\mu}{2m}\Big)g_F - \Big(1 + \frac{2m}{\mu}\Big)g_{D+\frac{2}{3}F}\Big]\bar{u}u$$

$$+\ \Big(1 - \frac{t}{4m_B^2}\Big)\Big(1 + \frac{2m}{\mu}\Big)\ g_{D+\frac{2}{3}F}\ \bar{u}\not{P}'u\ \Big]\ ,$$

for $0^-1/2^+ \to 0^-3/2^+$

$$T = -\Big[\, h_F\ \alpha'_V\ \ \Gamma(1-\alpha_V)\ \frac{1 - e^{-i\pi\alpha_V}}{2}\ \left(\frac{s + \frac{1}{2}t - \frac{1}{2}\sum_{i=1}^{4} m_i^2}{s_o}\right)^{\alpha_V - 1}$$

$$+\ h_D\ \alpha'_T\ \ \Gamma(1-\alpha_T)\ \frac{1 + e^{-i\pi\alpha_T}}{2}\ \left(\frac{s + \frac{1}{2}t - \frac{1}{2}\sum_{i=1}^{4} m_i^2}{s_o}\right)^{\alpha_T - 1}\ \Big]$$

$$\times\ 3\ g\ h\ g_G\ \frac{1}{4m_B^2}\ \Big(1 + \frac{2m}{\mu}\Big)\ \varepsilon_{\mu\kappa\lambda\rho}P'_\mu P_\kappa Q_\lambda \bar{\psi}_\rho u\ ,$$

and for $0^-1/2^+ \to 1^-1/2^+$

$$T = \Big[\, h_F\ \alpha'_P\ \ \Gamma(-\alpha_P)\ \frac{1 + e^{-i\pi\alpha_P}}{2}\ \left(\frac{s + \frac{1}{2}t - \frac{1}{2}\sum_{i=1}^{4} m_i^2}{s_o}\right)^{\alpha_P}$$

$$+\ h_D\ \alpha'_A\ \ \Gamma(-\alpha_A)\ \frac{1 - e^{-i\pi\alpha_A}}{2}\ \left(\frac{s + \frac{1}{2}t - \frac{1}{2}\sum_{i=1}^{4} m_i^2}{s_o}\right)^{\alpha_A}\ \Big]$$

$$\times\ 3\ g\ h\ g_{D+\frac{2}{3}F-S}\left(1+\frac{2m}{\mu}\right)\left(1-\frac{\mu^2}{4m_B^2}\right)Q'_\lambda\bar{\varepsilon}_\lambda\bar{u}\gamma_5 u$$

$$+\Big[h_{D+2S}\alpha'_V\ \ \Gamma(1-\alpha_V)\ \frac{1-e^{-i\pi\alpha_V}}{2}\left(\frac{s+\frac{1}{2}t-\frac{1}{2}\sum_{i=1}^{4}m_i^2}{s_o}\right)^{\alpha_V-1}$$

$$+\ h_F\ \alpha'_T\ \ \Gamma(1-\alpha_T)\ \frac{1+e^{-i\pi\alpha_T}}{2}\left(\frac{s+\frac{1}{2}t-\frac{1}{2}\sum_{i=1}^{4}m_i^2}{s_o}\right)^{\alpha_T-1}\Big]$$

$$\times\ 3\ g\ h\ \frac{1}{2m_M}\Big[\ \frac{1}{2m_B}\Big[\Big(1+\frac{\mu}{2m}\Big)g_{F+3S}-\Big(1+\frac{2m}{\mu}\Big)g_{D+\frac{2}{3}F-S}\Big]$$

$$\times\ \varepsilon_{\mu\kappa\lambda\rho}P_\mu\bar{\varepsilon}_\kappa P'_\lambda Q'_\rho\bar{u}u$$

$$+\ \Big(1-\frac{t}{4m_B^2}\Big)\Big(1+\frac{2m}{\mu}\Big)\ g_{D+\frac{2}{3}F-S}\ \varepsilon_{\mu\kappa\lambda\rho}\bar{u}\gamma_\mu u\bar{\varepsilon}_\kappa P'_\lambda Q'_\rho\Big]\,.$$

Explicit expressions for the helicity amplitudes are evaluated using standard techniques and are given in Appendix D.

3.3 Discussion and Results

We now discuss each class of reaction and compare the predictions of the model with representative experimental data on differential cross sections, polarizations and spin density matrix elements.

(i) $0^-1/2^+ \to 0^-1/2^+$

There is an abundance of experimental data on the four charge-exchange processes

$$\pi^- p \rightarrow \pi^o n$$

$$\pi^- p \rightarrow \eta n$$

$$K^- p \rightarrow \bar{K}^o n$$

$$K^+ n \rightarrow K^o p$$

at a sufficiently high energy for us to hope that in this region the asymptotic Regge form is a good approximation to the 2-body scattering amplitude. The first two of these processes are important in that for each only one known trajectory has the appropriate quantum numbers to be exchanged, namely the ρ and A_2 trajectories, respectively, thus enabling us to compare with experiment the predictions of the symmetry scheme and strong exchange degeneracy for these particular exchanges.

In Fig. 2 we show the contributions to the momentum transfer distribution from the pole, the cut and the pole+cut for the process $\pi^- p \rightarrow \pi^o n$. Since we are employing the Gell-Mann ghost-eliminating mechanism, the pole amplitudes contain zeros at $\alpha(t) = 0, -2, -4$, etc. The first zero, for our trajectory, corresponds to the point $t = -.52$. The cut has the effect of partially filling in this zero to give a dip lying closer to the forward direction at about $t = -.43$. The absorption also produces the experimentally observed forward turnover, which is not present in the pole differential cross section.

Fig. 3 illustrates the energy dependence of the differential cross section for this process. The decrease in magnitude of the experimental data with increasing energy is well represented. The positions of the dip and particularly the secondary maximum move towards $t = 0$ as the energy increases. Although the forward normalization is reasonable, the differential cross section is too high at wide angles.

However, considering that this is hardly the peripheral region and that we have not "fitted" the data, we consider the result to be extremely good.

Since the pole-graph helicity amplitudes have the same phase, the polarization from the pole graph alone is identically zero. As already mentioned, the motivation for the introduction into simple pole models of the (undetected) ρ' was to allow the generation of the experimentally observed non-zero polarization by interference between ρ and ρ' poles. However, the application of absorption corrections produces polarization from pole-cut interference. The polarization predicted by our model, shown in Fig. 4, is positive and decreases with increasing energy for small t in agreement with the data. We obtain about 90% polarization near $t = -.43$, which corresponds to the dip region in the differential cross section. Although the present data [38] does not go to sufficiently large t values to rule out this possibility, it does not give much indication of this effect, particularly at the higher energy. We note that the dip in the differential cross section occurs near $t = -.43$, whereas the minimum in the data appears to be further out, in the region of $t = -.55$. If the predicted position of this dip could be moved to a larger value of $|t|$, the minimum in the polarization would also move out. Alternatively, since the polarization, particularly near the dip region, is sensitive to the ghost-eliminating mechanism, an alternative to the Gell-Mann scheme may be required to obtain agreement. Lastly, it may well be that a less simple parameterization of the elastic scattering is required. The change in sign near $t = -.3$ of the polarization in $0^-1/2^+ \to 0^-1/2^+$ hypercharge-exchange reactions can be produced by using a moving-pole pomeron rather than a fixed pole [39].

As discussed above, we invoke strong exchange degeneracy to obtain the A_2 contribution to $\pi^- p \to \eta n$. The predicted s and t dependence is compared with the data in Fig. 5. Whereas $\alpha(t) = 0$ is a wrong-signature point for the ρ trajectory, it is a right-signature point for the A_2. Hence, there is no zero in the pole amplitudes near $t = -.5$ and no dip in the absorbed differential cross section. The theoretical distributions exhibit a turnover near $t = 0$, somewhat broader than that obtained for π^o production. There is clear evidence for this broader turnover at 5.9 GeV/c but the data is not too clear on this detail at higher energies. Although a slight breaking of exchange degeneracy would naturally improve the results, our assumption of exchange degeneracy in not only the trajectories but also the residues of the ρ and A_2 appears to be well founded in these two processes.

The polarization given by the model, shown in Fig 6, is consistent with the somewhat sparse data available. We note that the theory does not exhibit a large negative value near $t = -.5$ as in π^o production.

In the other two processes,

$$K^- p \to \bar{K}^o n$$

$$K^+ n \to K^o p,$$

both the ρ and A_2 trajectories can be exchanged. Since we have assumed strong ρ-A_2 exchange degeneracy

$$\frac{d\sigma}{dt}(K^- p \to \bar{K}^o n) = \frac{d\sigma}{dt}(K^+ n \to K^o p)$$

before absorption, with the pole amplitudes complex for $K^- p \to \bar{K}^o n$ and real for $K^+ n \to K^o p$.

Fig. 7 shows the energy dependence of the momentum transfer distribution for $K^- p \to \bar{K}^o n$. The general features of the data, namely a fairly broad turnover intermediate between that for $\pi^- p \to \pi^o n$ and that for $\pi^- p \to \eta n$, and no dip near $t = -.5$ are given by our theoretical predictions, the dip near $t = -.5$ in the ρ-exchange contribution being filled in by the A_2 exchange. The normalization is about correct in the forward direction but the differential cross section does not decrease as rapidly as the data with increasing t. The predicted polarization, for which data is not presently available, is very similar in structure and magnitude to that for $\pi^- p \to \eta n$.

Fig. 8 compares the differential cross section given by our model with the data on the process $K^+ n \to K^o p$. The forward turnover, no dip near $t = -.5$ and about the correct normalization are obtained. Because of our parameterization of the elastic scattering the amplitudes remain real after absorption, thus predicting zero polarization.

Since the data on all four processes exhibits a turnover near $t = 0$ this indicates a large helicity flip amplitude compared with the helicity nonflip amplitude. This is given by the model. It is encouraging that a preliminary application of this model to $0^- 1/2^+ \to 0^- 1/2^+$ hypercharge-exchange reactions gives the forward peaking of the differential cross sections observed for these reactions.

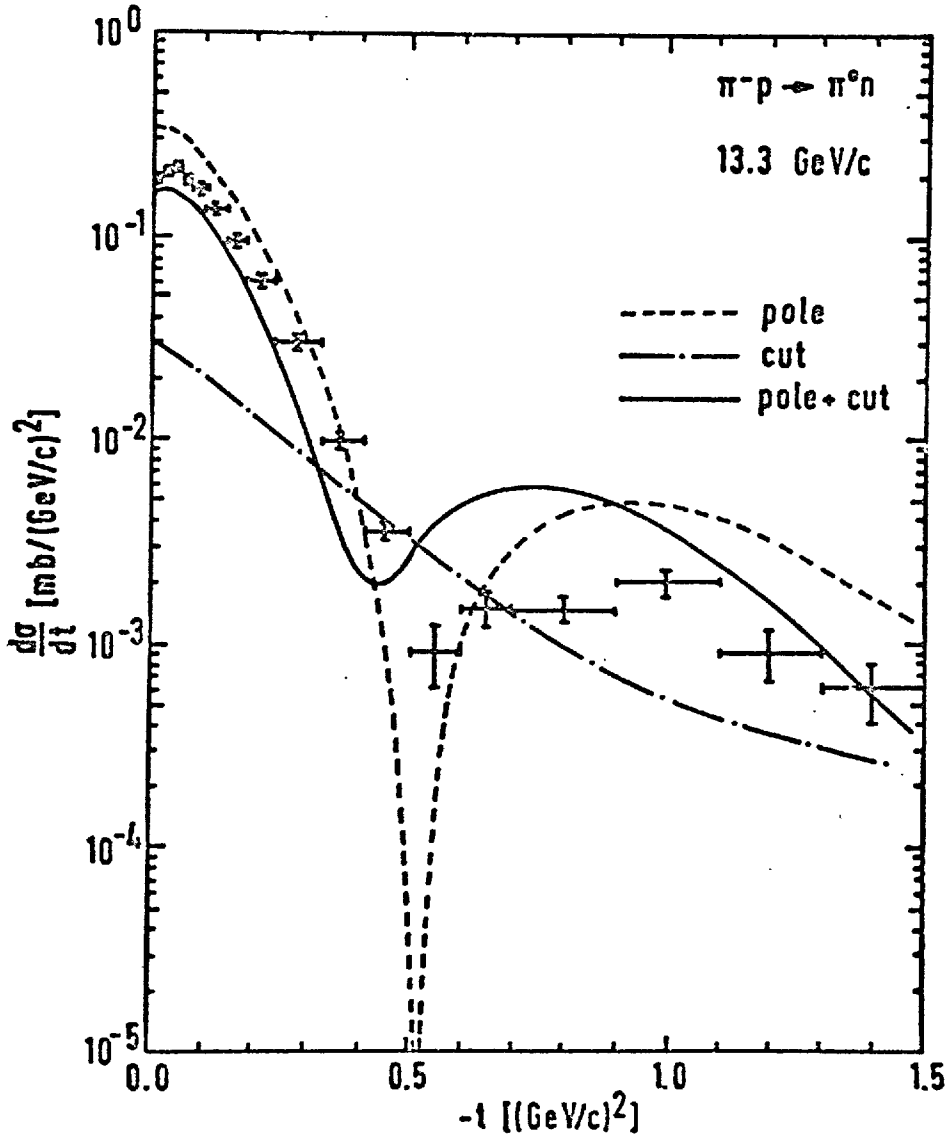


Fig. 2

Contributions to the differential cross section for $\pi^- p \to \pi^0 n$ from the pole, cut and pole+cut. Data from Ref. 40.

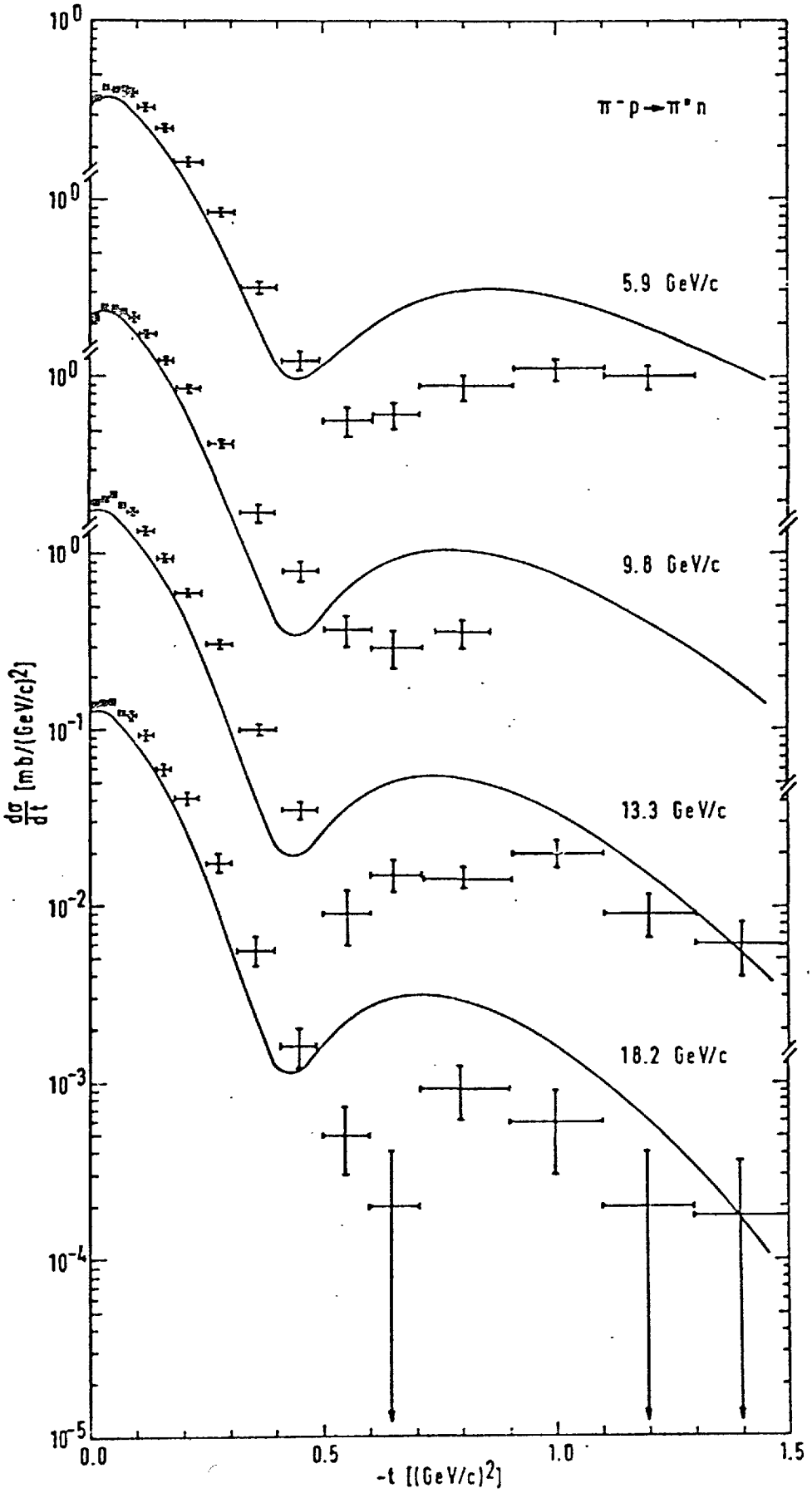


Fig. 3

Differential cross section for $\pi^- p \to \pi^0 n$. Data from Ref. 40.

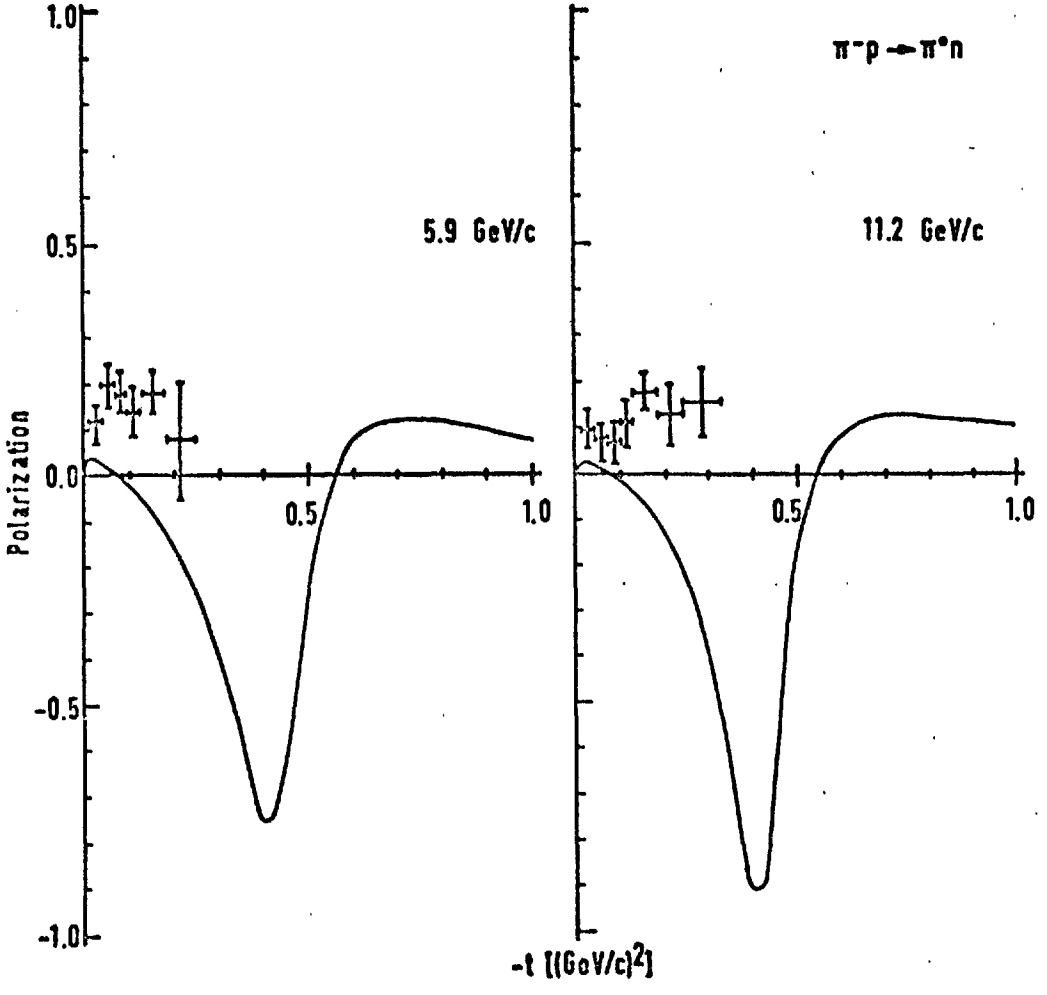


Fig. 4

Polarization of the recoil neutron in $\pi^- p \to \pi^0 n$. Data from Ref. 41.

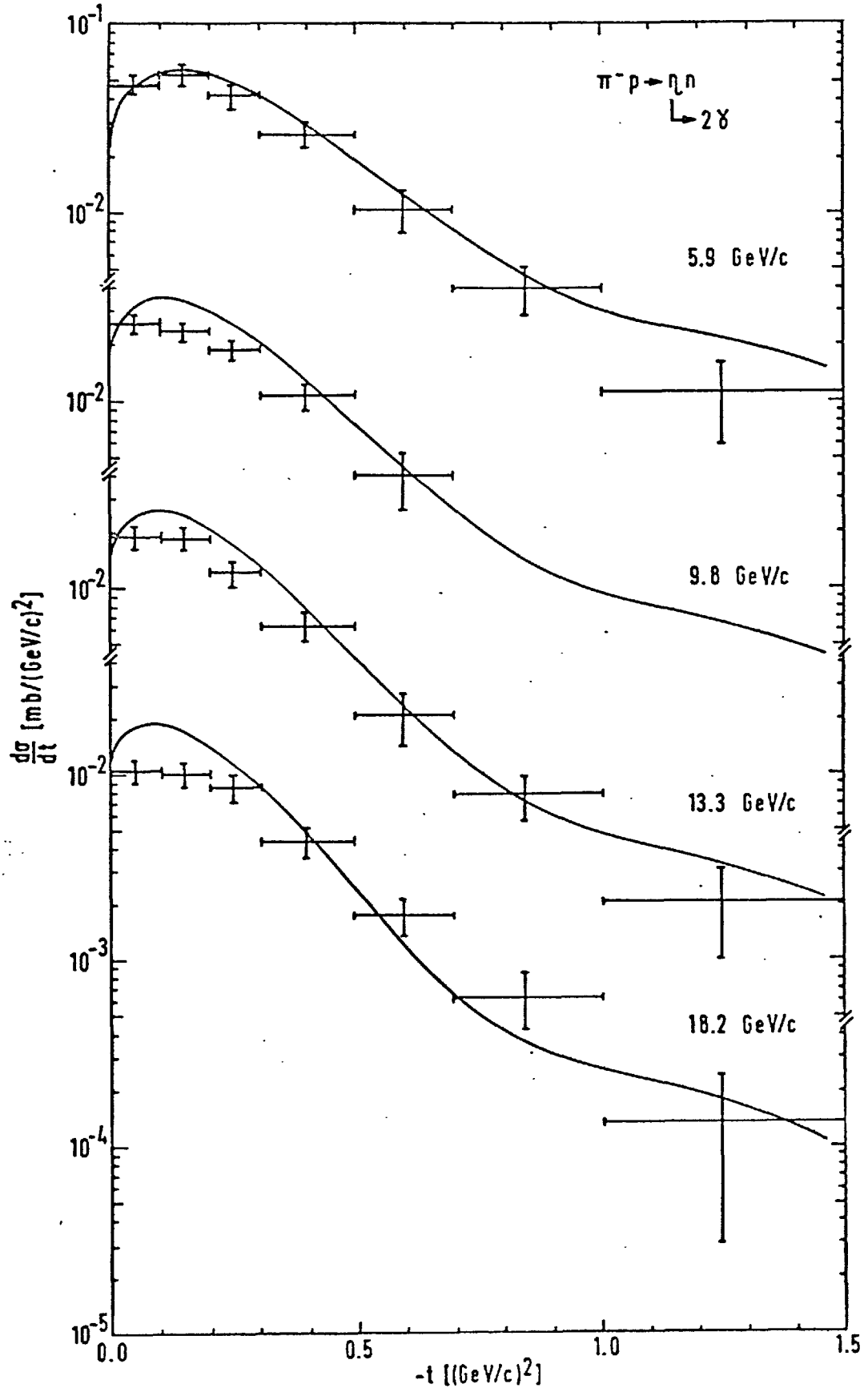


Fig. 5

Differential cross section for $\pi^- p \to \eta n$. The theoretical curve has been multiplied by the branching ratio $\eta \to 2\gamma$, which we took to be 0.381. Data from Ref. 42.

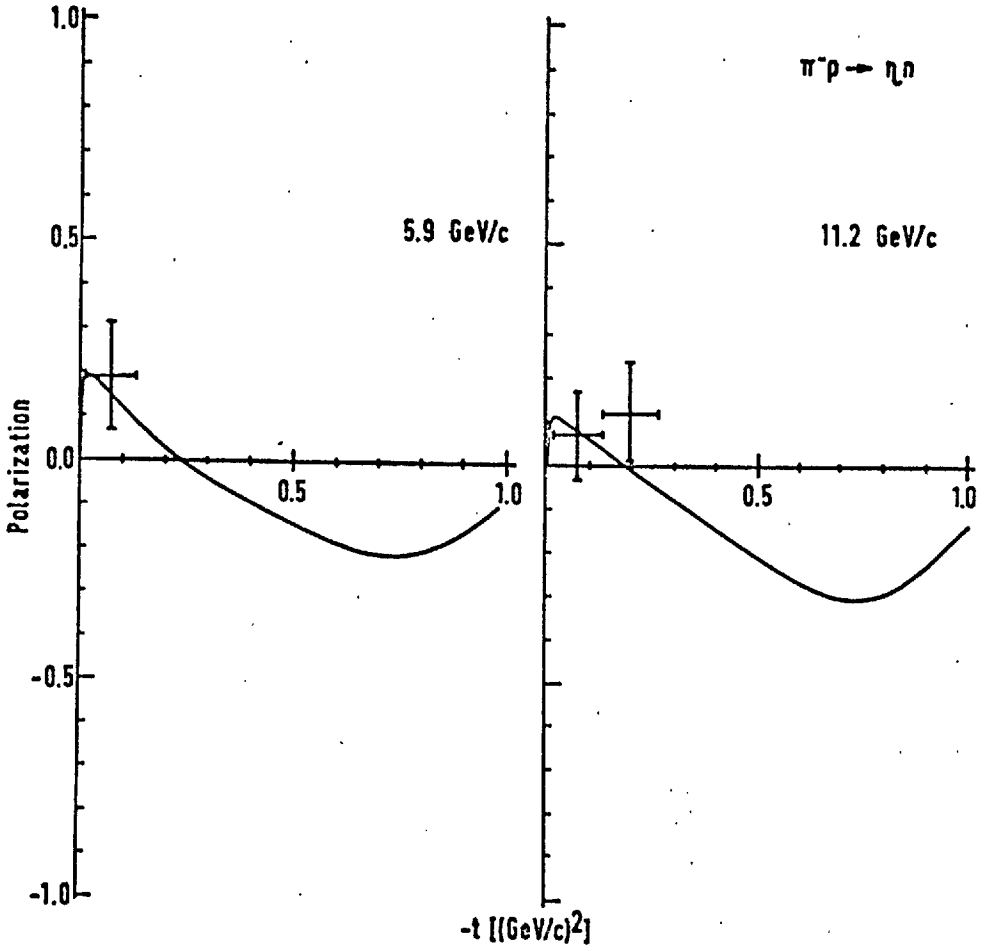


Fig. 6

Polarization of the recoil neutron in $\pi^- p \to \eta n$. Data from Ref. 41.

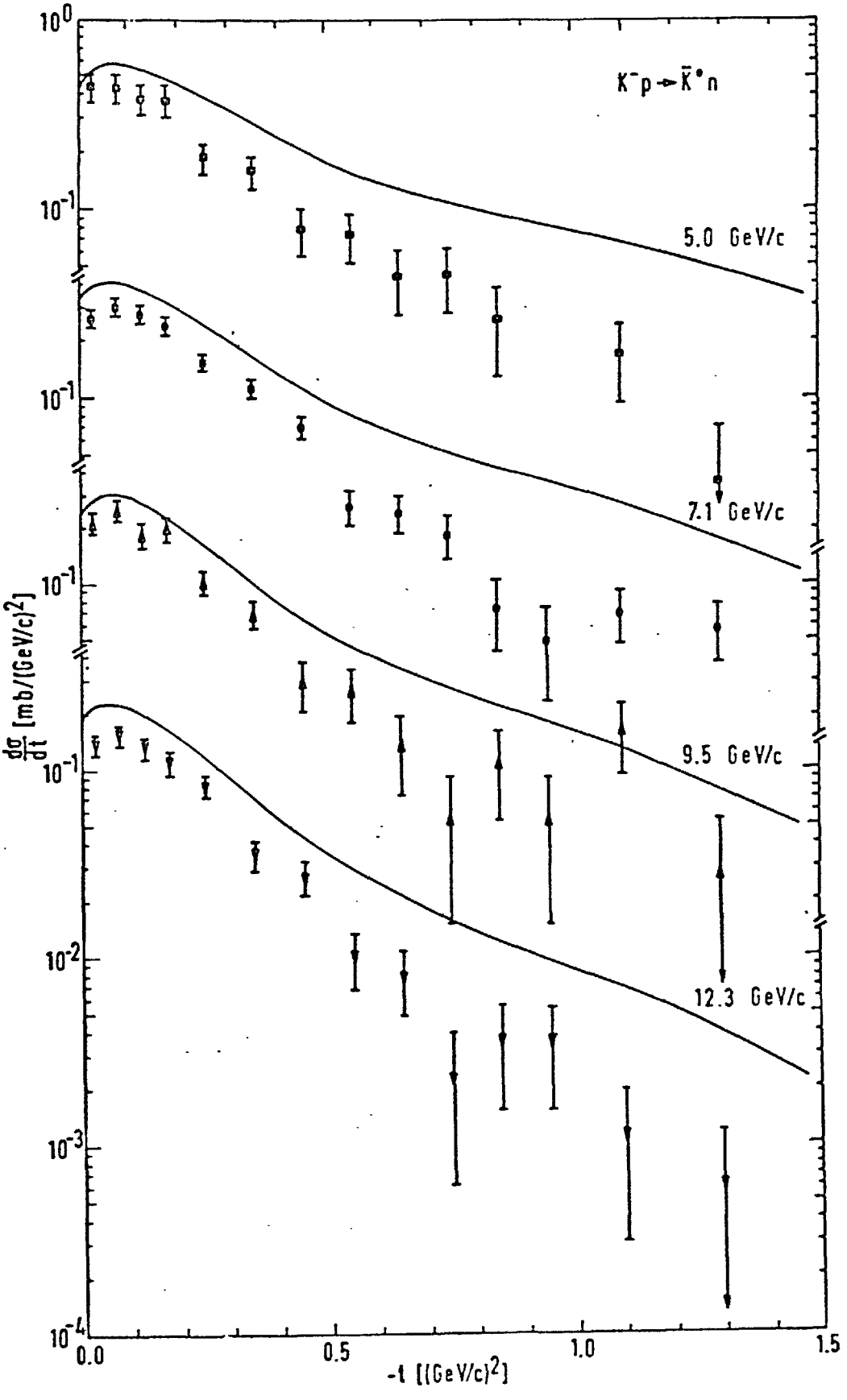


Fig. 7

Differential cross section for $K^-p \to \bar{K}^0 n$. Data from Ref. 43.

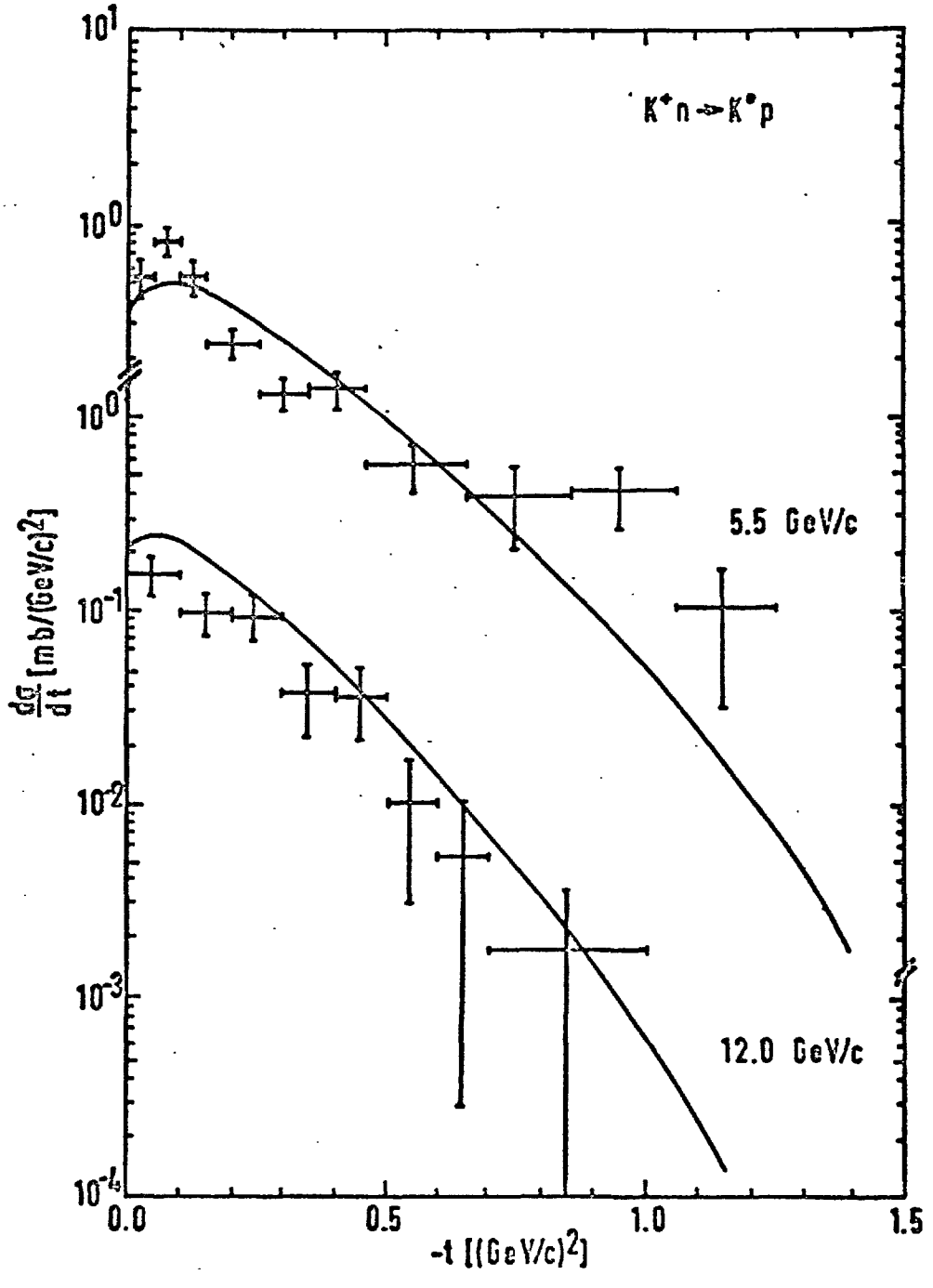


Fig. 8

Differential cross section for $K^+n \to K^0p$. Data from Ref. 44.

(ii) $\underline{0^-1/2^+ \to 0^-3/2^+}$

We have applied our model to the reactions

$$\pi^+ p \to \pi^o \Delta^{++}$$
$$\pi^+ p \to \eta \Delta^{++}$$
$$K^+ p \to K^o \Delta^{++}.$$

These Δ-production reactions are similar to the $0^-1/2^+ \to 0^-1/2^+$ processes discussed above in that they allow only ρ, A_2 and $\rho + A_2$ exchanges, respectively. The $\bar{\Delta}$NM and $\bar{N}$NM vertices are related by the symmetry scheme. Although the data is poorer for these reactions, the evidence appears to point to the same correlation between the shapes of the differential cross sections and the permitted exchanges as in the nucleon-production processes.

Fig. 9 shows our theoretical result for the momentum transfer distribution for $\pi^+ p \to \pi^o \Delta^{++}$. The data indicates a fairly sharp turnover near the forward direction as in the similar process $\pi^- p \to \pi^o n$. Although the pole-graph amplitudes go to zero in the forward direction, when absorbed the helicity nonflip amplitude peaks at this point. The symmetry scheme predicts helicity flip dominance in this region and hence a turnover in the absorbed differential cross section. There is a hint in the 4.0 GeV/c data of the expected dip near $t = -.5$. Our curves are lower than the data near the forward direction, but there appears to be some doubt in the literature about the absolute magnitude of the differential cross section. In particular, a plot of σ_{tot} against p_{lab} is far from smooth. This difficulty is illustrated in the figure, where the 4.0 GeV/c data has a higher normalization than the 3.54 GeV/c data.

With no absorption we obtain the constant values

$$\rho_{33} = 3/8 = .375, \quad \mathrm{Re}\rho_{3,-1} = \sqrt{3}/8 = .216, \quad \mathrm{Re}\rho_{31} = 0,$$

for the spin density matrix elements of the Δ resonance produced in reactions in this category. Our results for the reaction $\pi^+ p \to \pi^o \Delta^{++}$ are shown in Fig. 10. We see that after absorption these values do not change significantly except in the forward direction. The absorbed nonflip amplitude no longer goes to zero at this point thus causing all these density matrix elements to vanish here. The results appear to be consistent with the data but with such wide "bins" a detailed comparison cannot be made.

The predicted differential cross section for $\pi^+ p \to \eta \Delta^{++}$ is shown in Fig. 11. As in the $0^- 1/2^+ \to 0^- 1/2^+$ processes, the theoretical η-production distribution has a broader forward turnover than the π^o production. The data appears to bear this out. Our normalization at the lower energy is too small but at the higher energy it is consistent with the data. The spin density matrix elements of the Δ, for which the data is rather meager, are shown in Fig. 12. The data is adequately represented by the model.

Our results for the differential cross section for the reaction $K^+ p \to K^o \Delta^{++}$ are shown in Fig. 13. The data at 7.3 GeV/c exhibits the turnover near the forward direction given by the model. Our forward normalization is low except at the highest energy. The density matrix elements, shown in Fig. 14, are consistent with the data.

It is apparent from our results that the predicted normalizations for this class of reaction are too low, perhaps by as much as a factor

of four. Although our assumption of equal final-state and initial-state absorption coefficients may be causing some difficulty, it would seem that the symmetry scheme is at fault here, in particular the predicted magnitude of the coupling of the ρ to the Δ and the nucleon.

(iii) $\underline{0^- \; 1/2^+ \to 1^- \; 1/2^+}$

The reactions we have considered in this category are

$$\pi^{\pm} p \to \rho^{\pm} p$$

$$\pi^{-} p \to \rho^{o} n$$

$$K^{\pm} p \to K^{*\pm} p$$

$$K^{-} p \to \bar{K}^{*o} n$$

$$\pi^{+} n \to \omega p \; .$$

In all cases, except ω production, π exchange is allowed. Because of the proximity of the pion pole to the scattering region, elementary and Reggeized π exchange are extremely similar for small values of t. Now π exchange was the forte of the absorption model with elementary particle exchange and so we expect π exchange in a Reggeized model to give similarly good results. Indeed this is the case, as may be seen by comparing the results of these calculations with those obtained in Ref. 26 and 28 with elementary-particle exchange and U(6,6) symmetry.

The $\rho^{\pm}$-production reactions permit π, ω and A_2 exchanges, while ρ^{o} production proceeds by π and A_2 exchanges. Since we have assumed "folk-model" ω-ϕ mixing i.e.

$$\omega_{phys} = \frac{\sqrt{2}}{\sqrt{3}} \omega_0 + \frac{1}{\sqrt{3}} \omega_8$$

$$\phi_{phys} = \frac{1}{\sqrt{3}} \omega_0 - \frac{\sqrt{2}}{\sqrt{3}} \omega_8$$

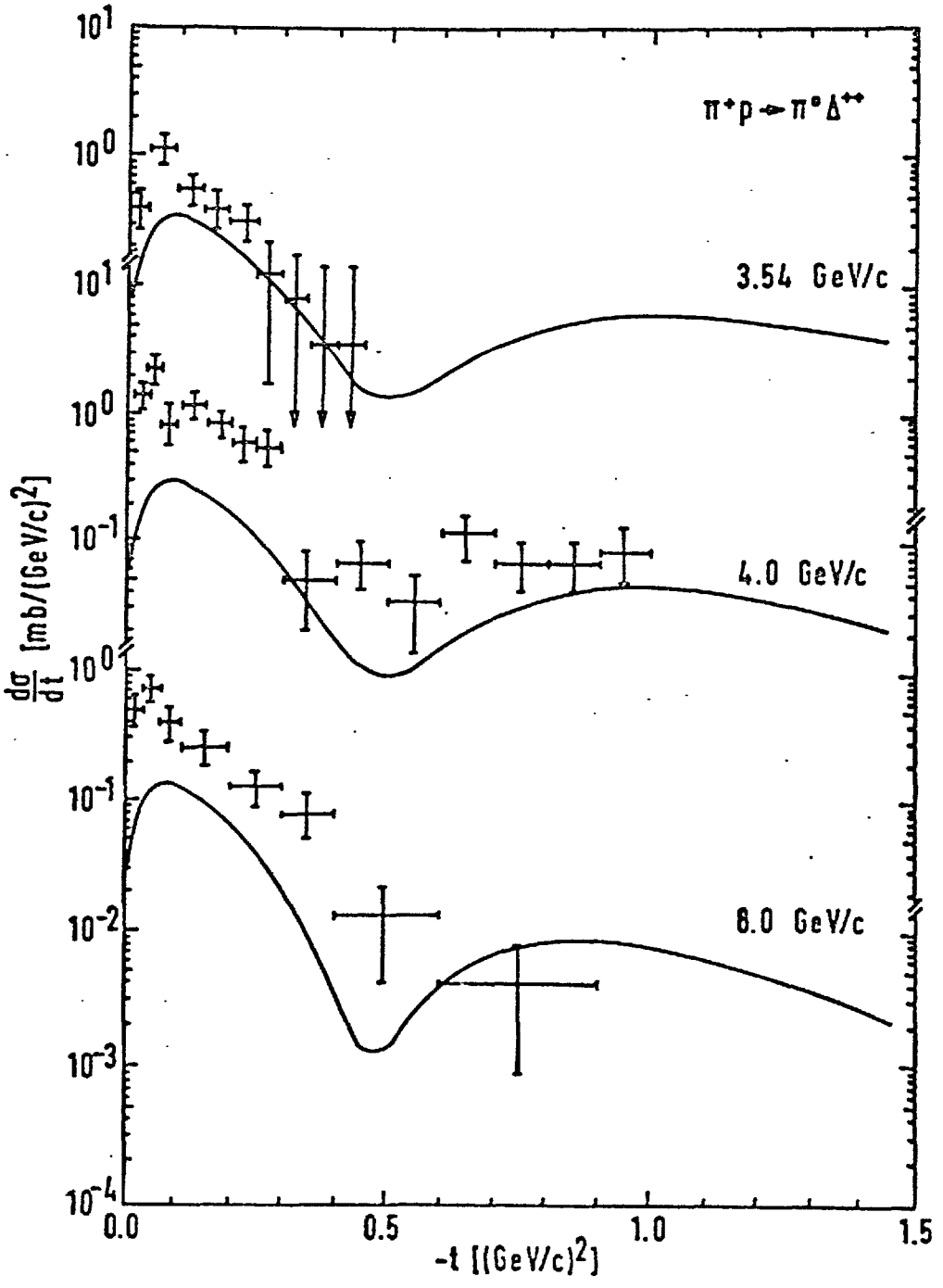


Fig. 9
Differential cross section for $\pi^+p \to \pi^0\Delta^{++}$.
Data from Ref. 45, 46 and 47.

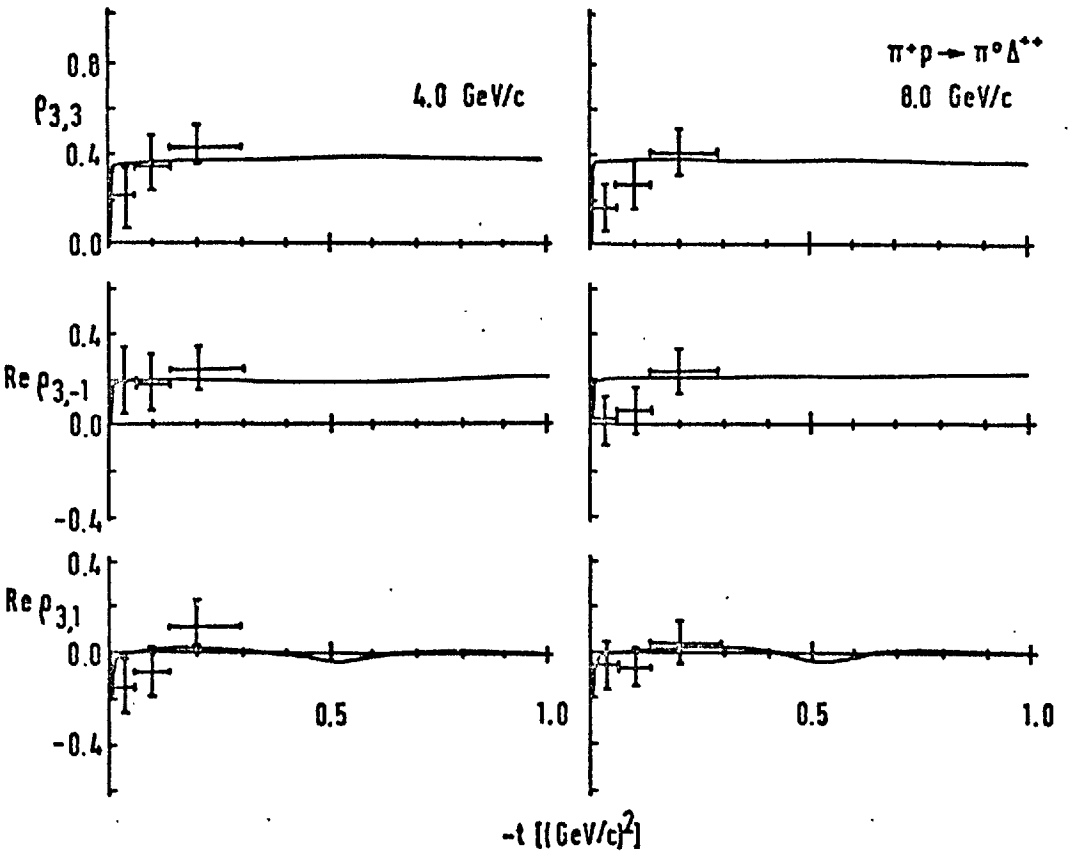


Fig. 10

Density matrix elements of the Δ resonance in $\pi^+p \to \pi^0\Delta^{++}$.

Data from Ref. 48 and 49.

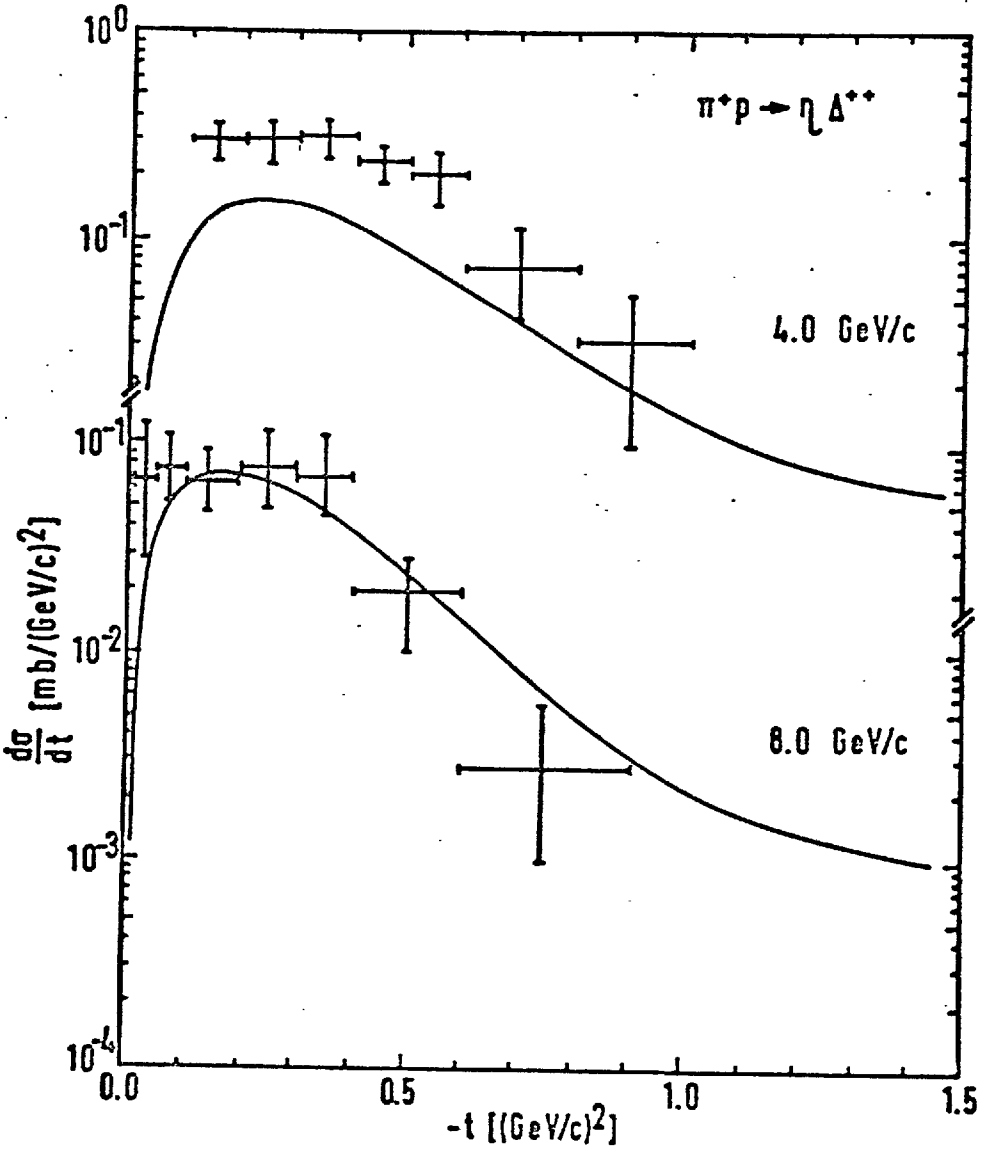


Fig. 11

Differential cross section for $\pi^+p \to \eta\Delta^{++}$.

Data from Ref. 47 and 50.

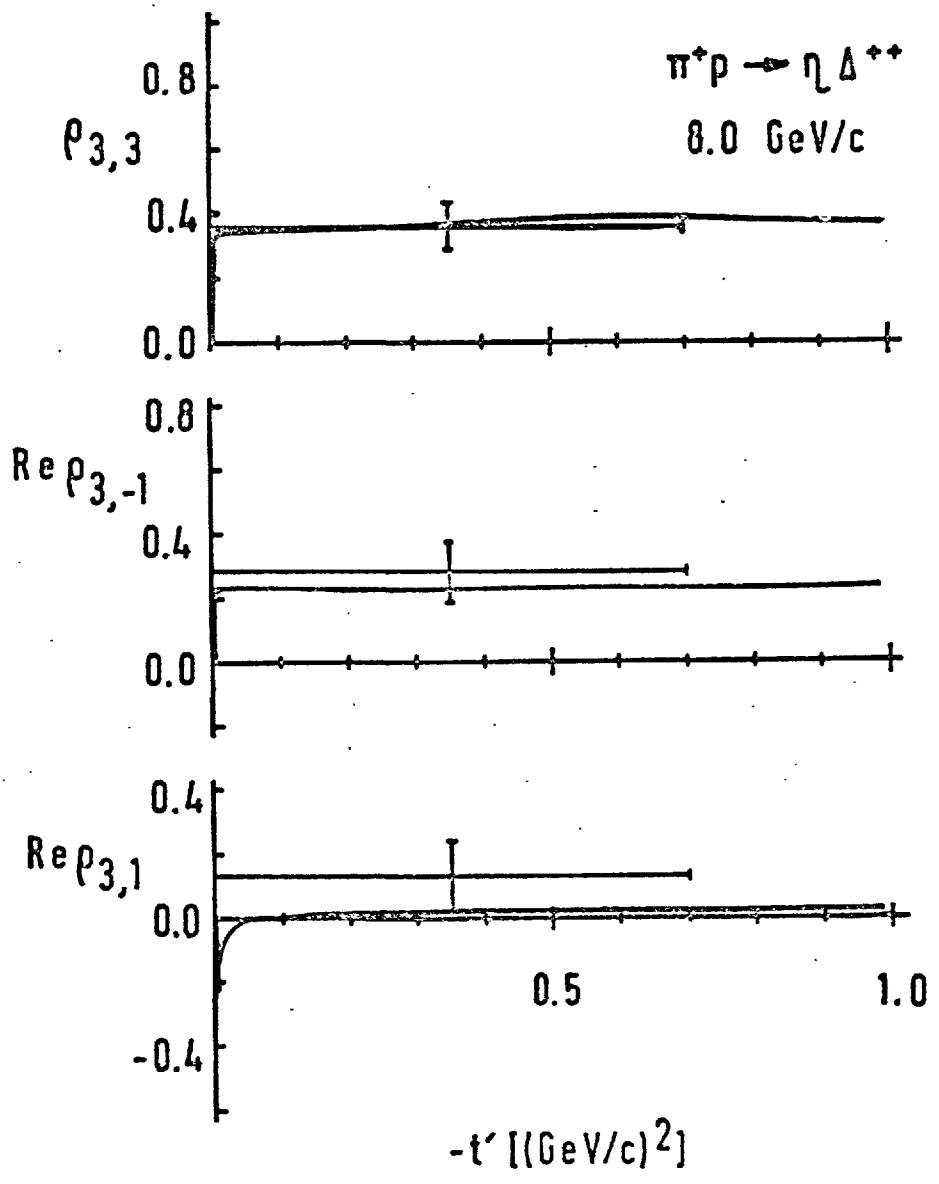


Fig. 12

Density matrix elements of the Δ resonance in $\pi^+p \to n\Delta^{++}$.

Data from Ref. 51.

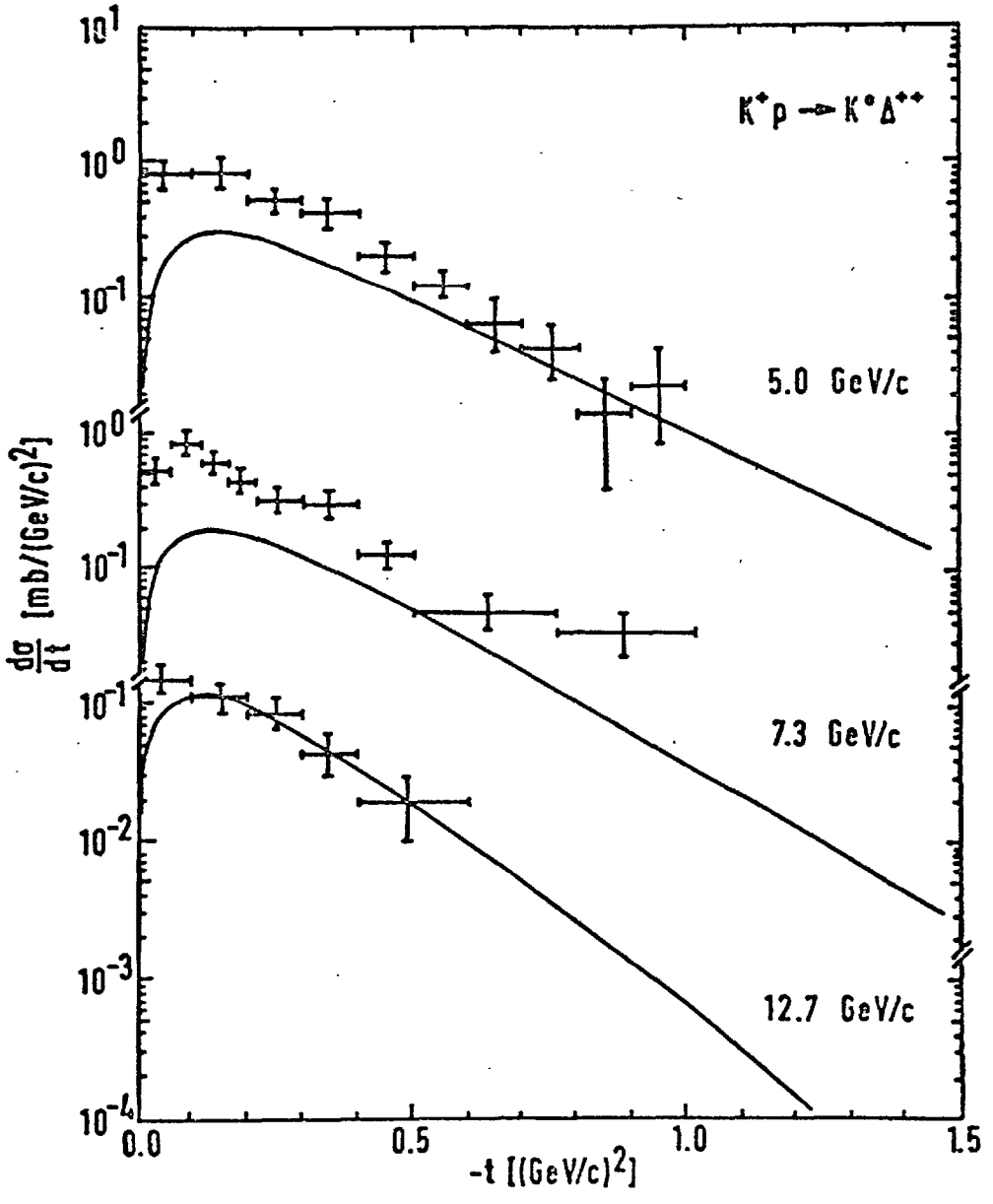


Fig. 13

Differential cross section for $K^+p \rightarrow K^0\Delta^{++}$.

Data from Ref. 52, 53 and 54.

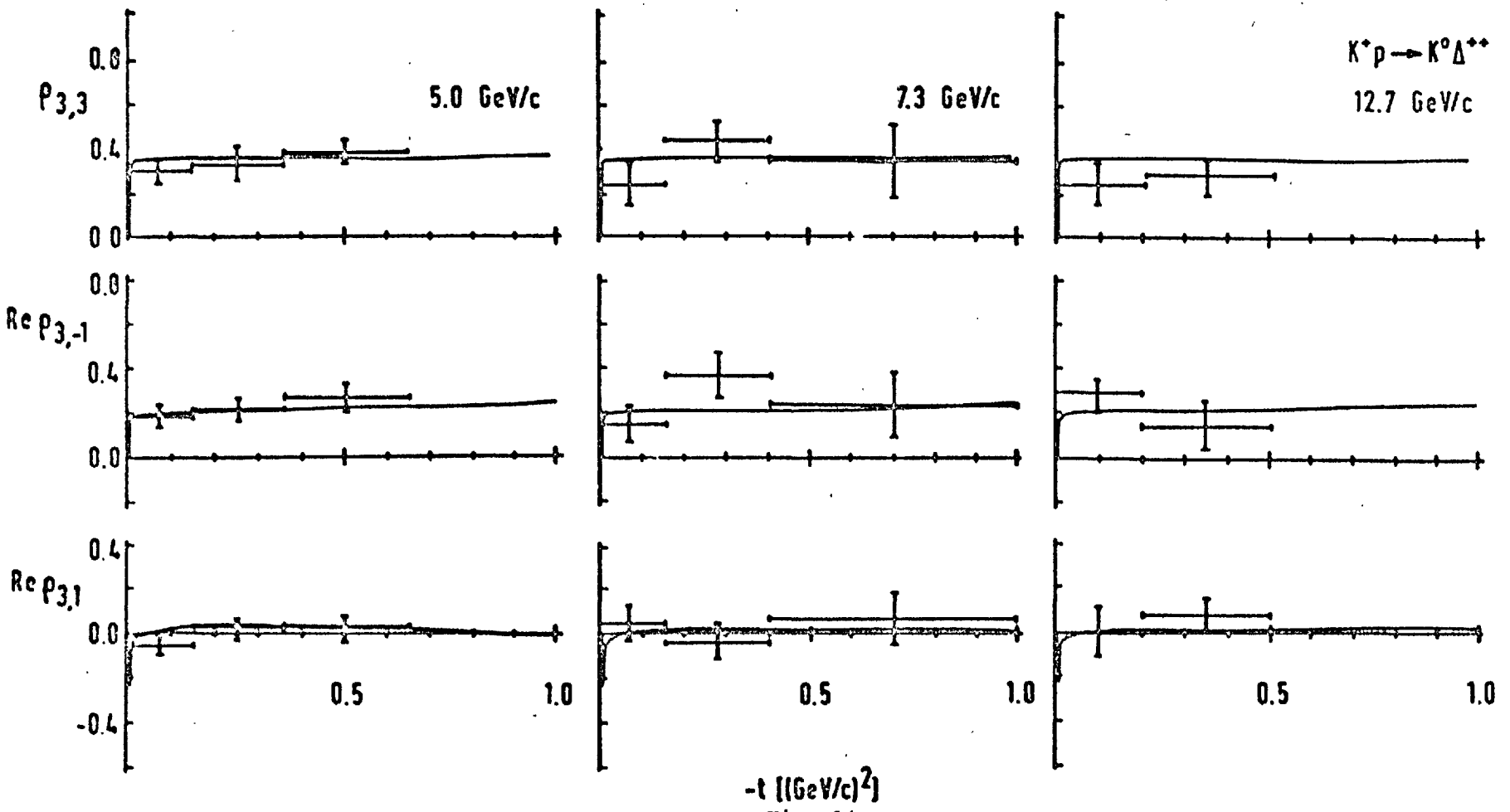


Fig. 14

Density matrix elements of the Δ resonance in $K^+p \to K^0\Delta^{++}$. Data from Ref. 52, 53 and 54.

the ϕ does not couple to the π-ρ vertex. Fig. 15, which shows the contributions to the differential cross section for the reaction $\pi^+ p \to \rho^+ p$ from the absorbed π-exchange amplitudes before and after Reggeization, illustrates their similarity. In the forward direction the contributions agree to within about 20%, but at larger values of t the Reggeized exchange is about an order of magnitude smaller than the elementary-particle exchange. The absorbed ω and A_2 contributions are also shown. We note that the forward differential cross section is almost entirely due to π exchange, while at wider angles the ω and A_2 exchanges dominate.

In order to judge whether the behaviour of an amplitude near $t = 0$ is attributable to a Reggeized pion rather thean to some other contribution unconnected with the pion, Leader discussed minimal requirements for associating a contribution with Reggeized π exchange [55]. These conditions are as follows.

1. The contribution should be associated with a pole at $t = m_\pi^2$ and the pole-like denominator should be largely responsible for the rapid variation with t for $|t| \lesssim$ a few m_π^2.

2. The contribution should reduce to the result for elementary π exchange when continued to the region $t \simeq m_\pi^2$.

3. The energy dependence of $d\sigma/dt$ for small t should be approximately s^{-2}.

Leader's first condition is ensured by constraining the pion

trajectory to pass through the pion pole i.e.

$$\alpha(t=m_\pi^2) = 0.$$

For small t our amplitudes contain the factor

$$\Gamma(-\alpha_\pi) \simeq -\frac{1}{(t - m_\pi^2)\alpha'}$$

near $t = m_\pi^2$, which is singular at $t = m_\pi^2$. This denominator is largely responsible for the rapid variation with t for $|t| \lesssim m_\pi^2$. In fact

$$-\frac{m_\pi^2}{t - m_\pi^2} \simeq e^{t/m_\pi^2} \simeq e^{50t}$$

for small t.

The second condition is trivially satisfied since the Reggeized π-exchange amplitudes are obtained from the elementary π-exchange amplitudes by the replacement discussed in Chapter II. This is exact at the pole $t = m_\pi^2$.

The trajectory of the pion-pomeron cut is given by [12,13]

$$\alpha_c(t) = \alpha_\pi(0) + \alpha_{el}(0) - 1 + \frac{\alpha_\pi' \alpha_{el}'}{\alpha_\pi' + \alpha_{el}'} t .$$

In our case the elastic scattering is described by a fixed-J pole

$$\alpha_{el}(t) = 1,$$

giving

$$\alpha_c(t) = \alpha_\pi(0)$$

$$\simeq 0.$$

Therefore the cut contribution to the differential cross section has an energy dependence of the form

$$\frac{d\sigma}{dt} \sim \left(\frac{s^{\alpha_c(t)-1}}{\ln s}\right)^2$$

$$\sim s^{-2}$$

because of the slow logarithmic variation. This satisfies Leader's third condition.

The momentum transfer distributions for the three ρ-production reactions are compared with the experimental data in Fig. 16, 17 and 18. The t dependence of the differential cross sections is similar in each case, in particular, the sharp turnover near the forward direction produced by the π-exchange contribution. This feature is clearly exhibited by the ρ^+-production data at 8.0 GeV/c, by the ρ^--production data at both energies and by the ρ^o-production data at 11.2 GeV/c. The s dependence is well represented, as is the forward normalization, but the distributions are too high at wide angles. There is a hint of a dip near $t = -.5$ in the ρ^+-production data at 4.0 GeV/c, although this is the only set of data to show such an effect. If this is really present, it is not given by this model. The dip at this point in the ω-exchange contribution is filled in by the A_2 exchange. In fact our

curves exhibit a slight shoulder in the region of t = - .6 due largely to the contribution of the A_2.

Our results for the spin density matrix elements of the ρ-meson produced in these reactions are shown in Fig. 19, 20 and 21. The separate contributions to ρ^+ production from elementary π and Reggeized π, ω and A_2 exchanges are also shown in Fig. 19. With no absorption, we obtain for π (unnatural-parity) exchange

$$\rho_{00} = 1, \quad \rho_{1,-1} = 0, \quad \text{Re } \rho_{10} = 0,$$

and for ω and A_2 (natural-parity) exchange

$$\rho_{00} = 0, \quad \rho_{1,-1} = \tfrac{1}{2}, \quad \text{Re } \rho_{10} = 0.$$

The absorption does not drastically change these values. The data indicates that, particulatly near the forward direction, π exchange is the dominant mechanism. This is given by the model. We note that the values given by elementary and Reggeized π exchanges are generally similar. The addition of the higher-spin exchanges improves the agreement with the data compared with that obtained from pure π exchange to give results which agree extremely favourably with experiment.

The reactions $K^{\pm} p \to K^{*\pm} p$ may proceed by π, η, ρ, ω, ϕ, B and A_2 exchanges, while the reaction $K^- p \to \bar{K}^{*o} n$ permits π, ρ, B and A_2 exchanges. For all three charge modes the differential cross sections have an s^{-2} energy dependence. However, the non-charge-exchange reactions have broad forward turnovers and resonance decay correlations indicating dominance by natural-parity exchange, whereas the charge-exchange reaction

has a momentum transfer distribution which falls much more rapidly with increasing t and resonance decay correlations indicating dominance by unnatural-parity exchange.

Fig. 22 shows the contributions to the differential cross section for the reaction $K^+p \to K^{*+}p$ from the unnatural-parity and natural-parity exchanges. The unnatural-parity exchanges, predominantly the π, give a sharp forward turnover, while the natural-parity exchanges have the broader turnover exhibited by the data. However, the relative couplings predicted by the symmetry scheme lead to pion dominance and hence to a momentum transfer distribution which is too peaked in the forward direction.

Our results for the differential cross sections for these three reactions are compared with the data in Fig. 23, 24 and 25. The π-exchange dominance leads to a good s dependence but it does not reproduce the broad forward turnover in $K^{*\pm}$ production. However, the t dependence of the $\bar{K}^{*o}$-production distribution compares extremely favourably with experiment, although the data at small t is not good enough to test the predicted forward turnover.

The density matrix elements calculated from our model are compared with the data in Fig. 26, 27 and 28. The separate contributions to K^{*+} production from unnatural-parity and natural-parity exchanges are also shown in Fig. 26. The data for the non-charge-exchange reactions strongly suggest natural-parity exchange, whereas the model predicts the dominance of unnatural-parity exchange. The charge-exchange data is strikingly different in that it indicates that unnatural-parity exchange

is the dominant mechanism. Our results for this reaction are therefore extremely satisfactory. We should remark that it may be possible within the confines of the model to enhance the contribution of the natural-parity exchanges relative to that of the unnatural-parity exchanges by means of, for example, a different mass-splitting scheme in order to improve the results for the non-charge-exchange reactions.

The reaction $\pi^+ n \to \omega p$ should be dominated at high energy by ρ exchange. However, experimentally the differential cross section shows no sign of the dip near $t = -.5$ given by this exchange. Previous authors [4] have attempted to eliminate this difficulty by also including B-meson exchange to fill in this minimum. The contributions to the differential cross section from ρ, B and ρ+B exchanges in this model are shown in Fig. 29. The constructive interference between the two exchanges attenuates the dip but not sufficiently to completely remove it. Fig. 30 compares the s dependence of the momentum transfer distribution with representative data. Although the agreement is reasonable in the forward direction, the secondary maximum leads to a distribution which is too high beyond $t = -.5$. The contributions to the density matrix elements of the ω meson from ρ, B and ρ+B exchanges are shown in Fig. 31. The addition of the B seems to improve the results. A slight breaking of the assumed strong exchange degeneracy would enable us to improve the results for this reaction.

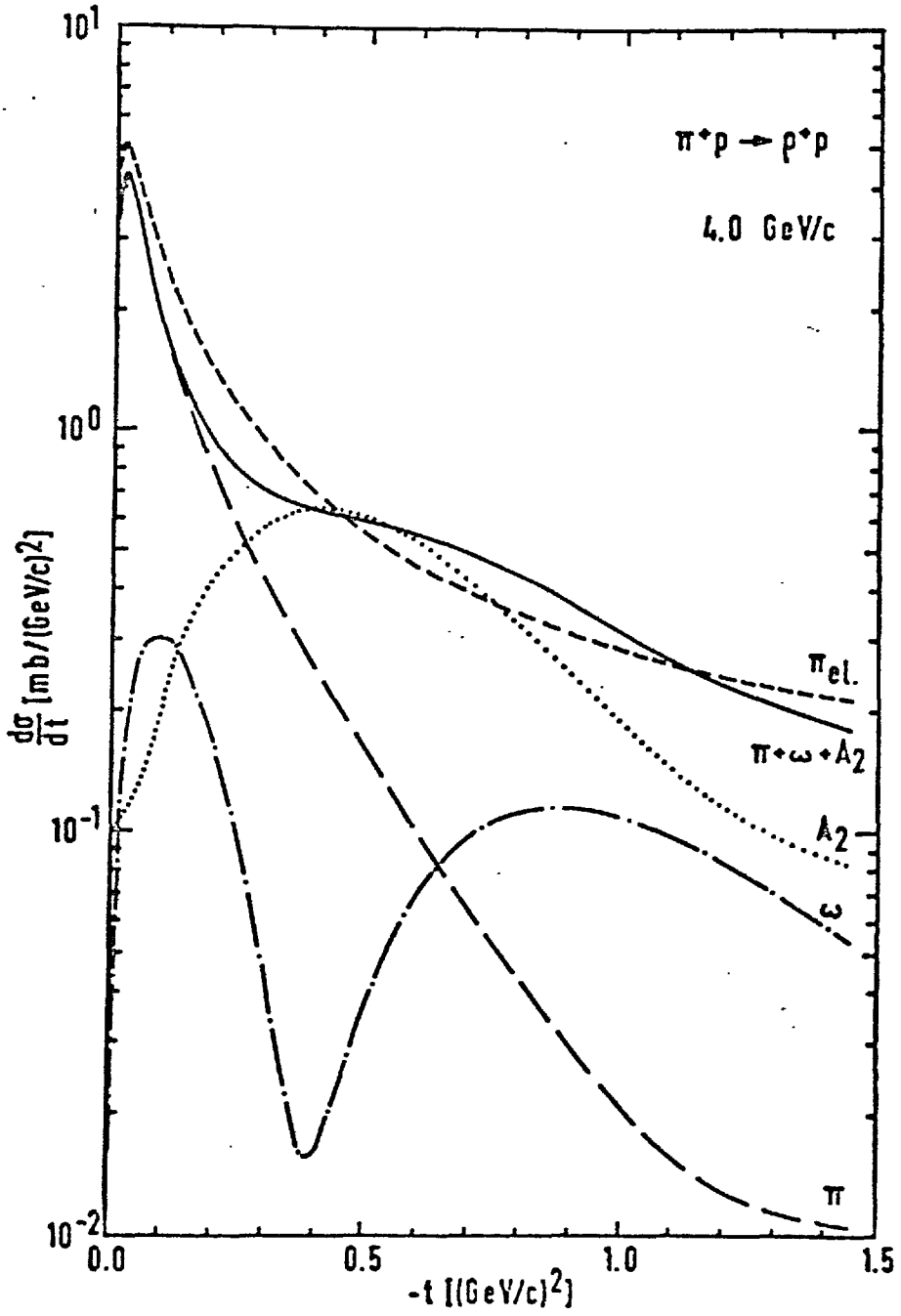


Fig. 15

Contributions to the differential cross section for $\pi^+p \to \rho^+p$ from absorbed elementary π, Reggeized π, ω, A_2 and $\pi+\omega+A_2$ exchanges.

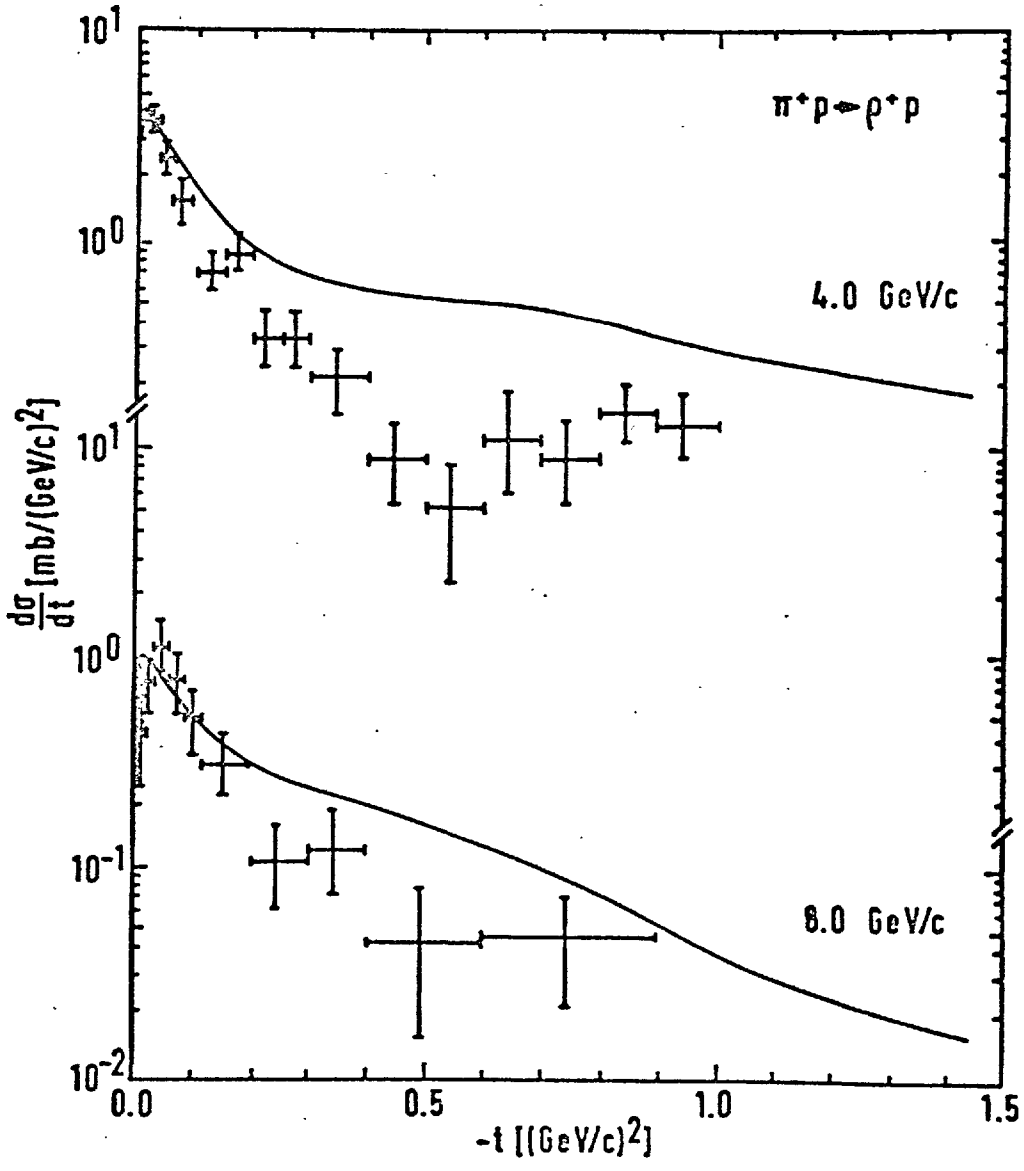


Fig. 16

Differential cross section for $\pi^+p \to \rho^+p$.

Data from Ref. 46 and 47.

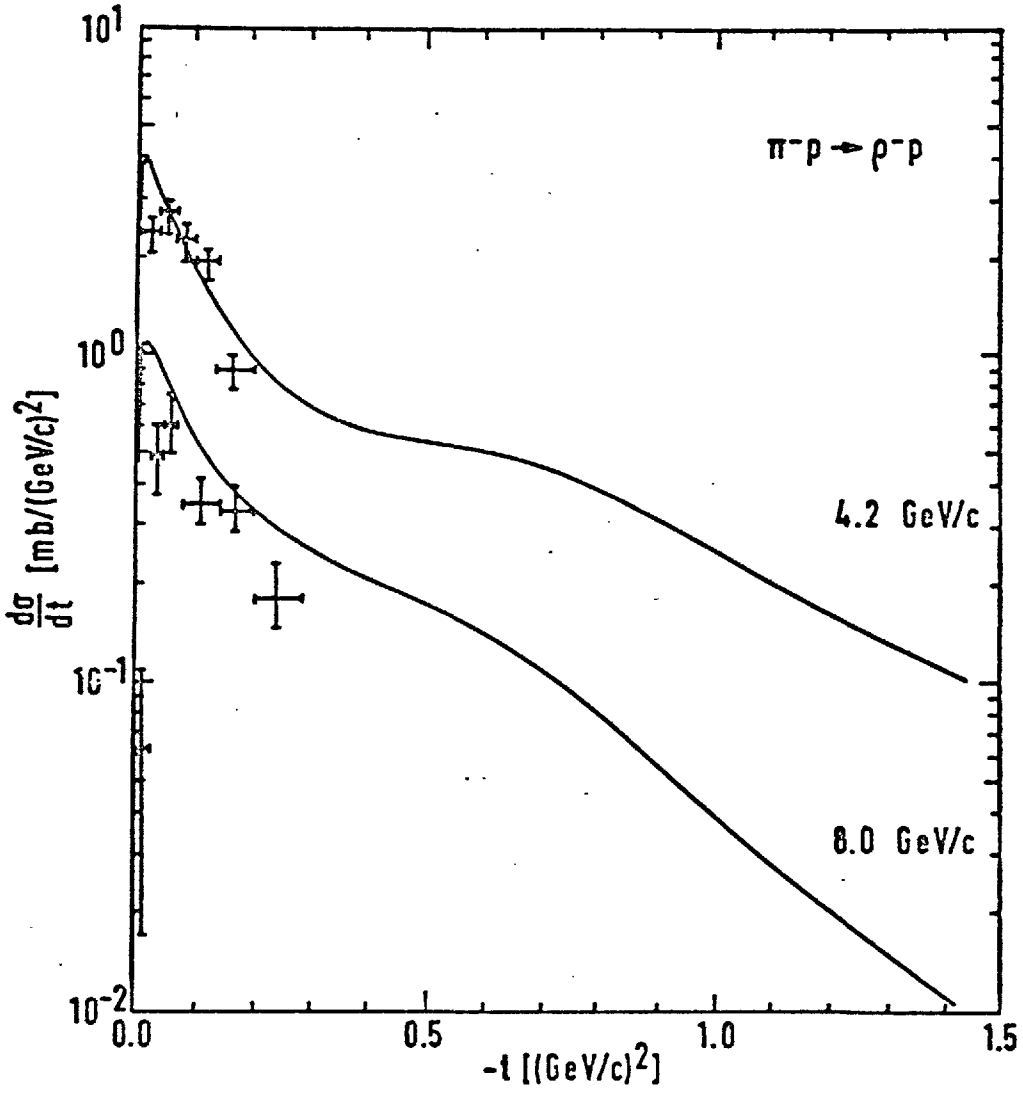


Fig. 17

Differential cross section for $\pi^- p \to \rho^- p$.

Data from Ref. 56 and 57.

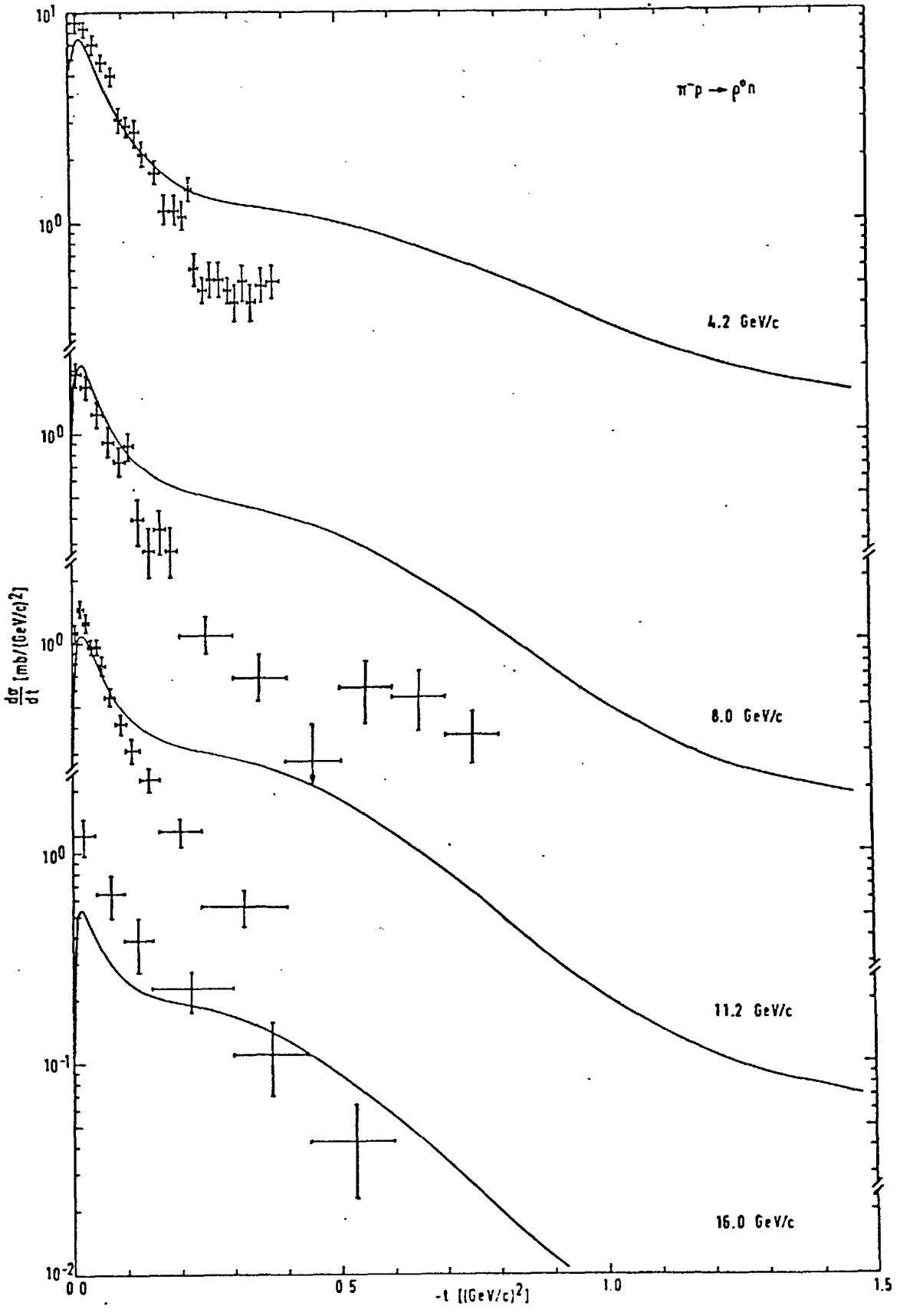


Fig. 18

Differential cross section for $\pi^- p \to \rho^0 n$.

Data from Ref. 56, 58 and 59.

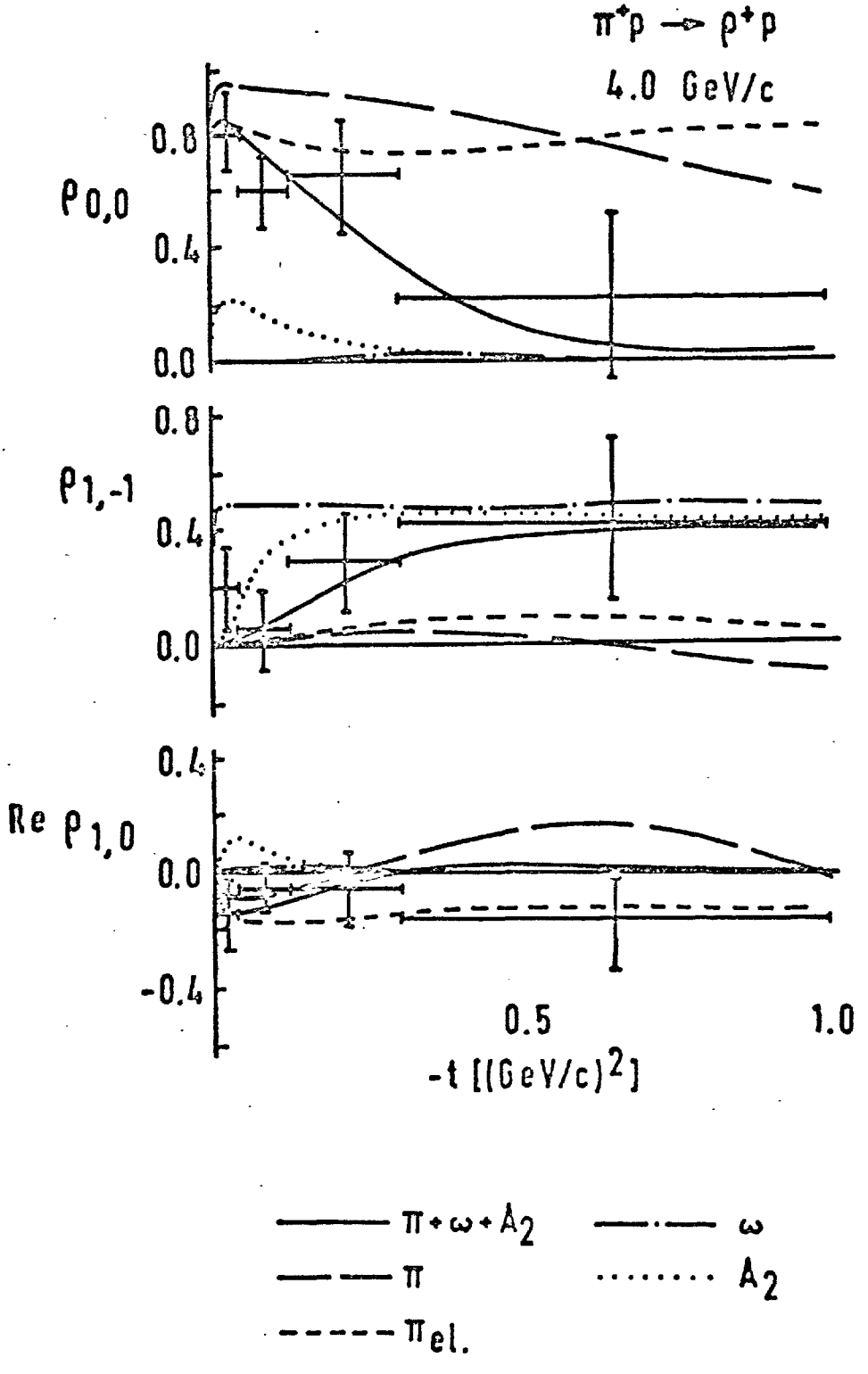


Fig. 19

Density matrix elements of the ρ resonance in $\pi^+p \to \rho^+p$. The contributions from absorbed elementary π, Reggeized π, ω, A_2 and $\pi+\omega+A_2$ exchanges are shown. Data from Ref. 48.

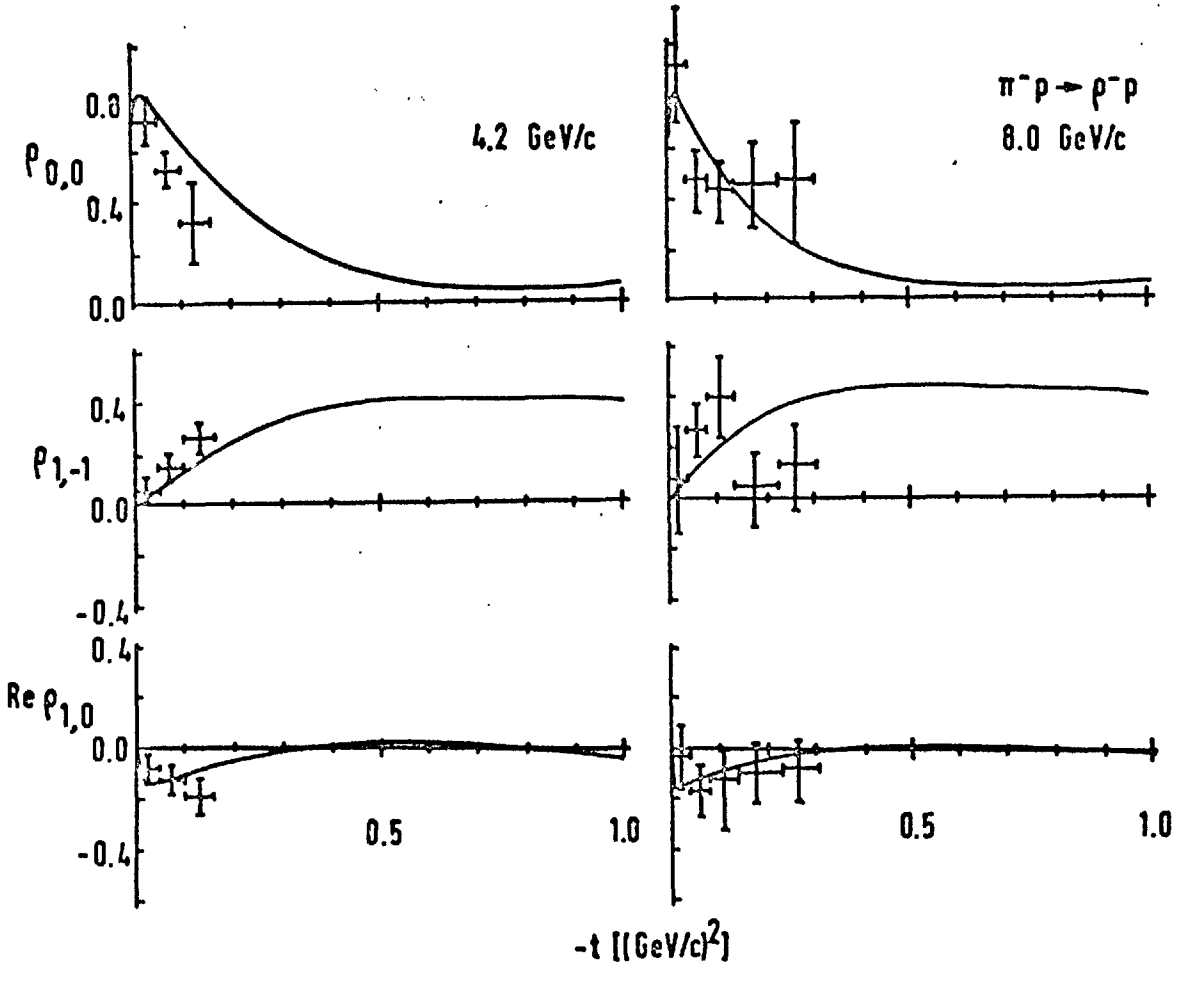


Fig. 20

Density matrix elements of the ρ resonance in $\pi^- p \to \rho^- p$. Data from Ref. 56 and 57.

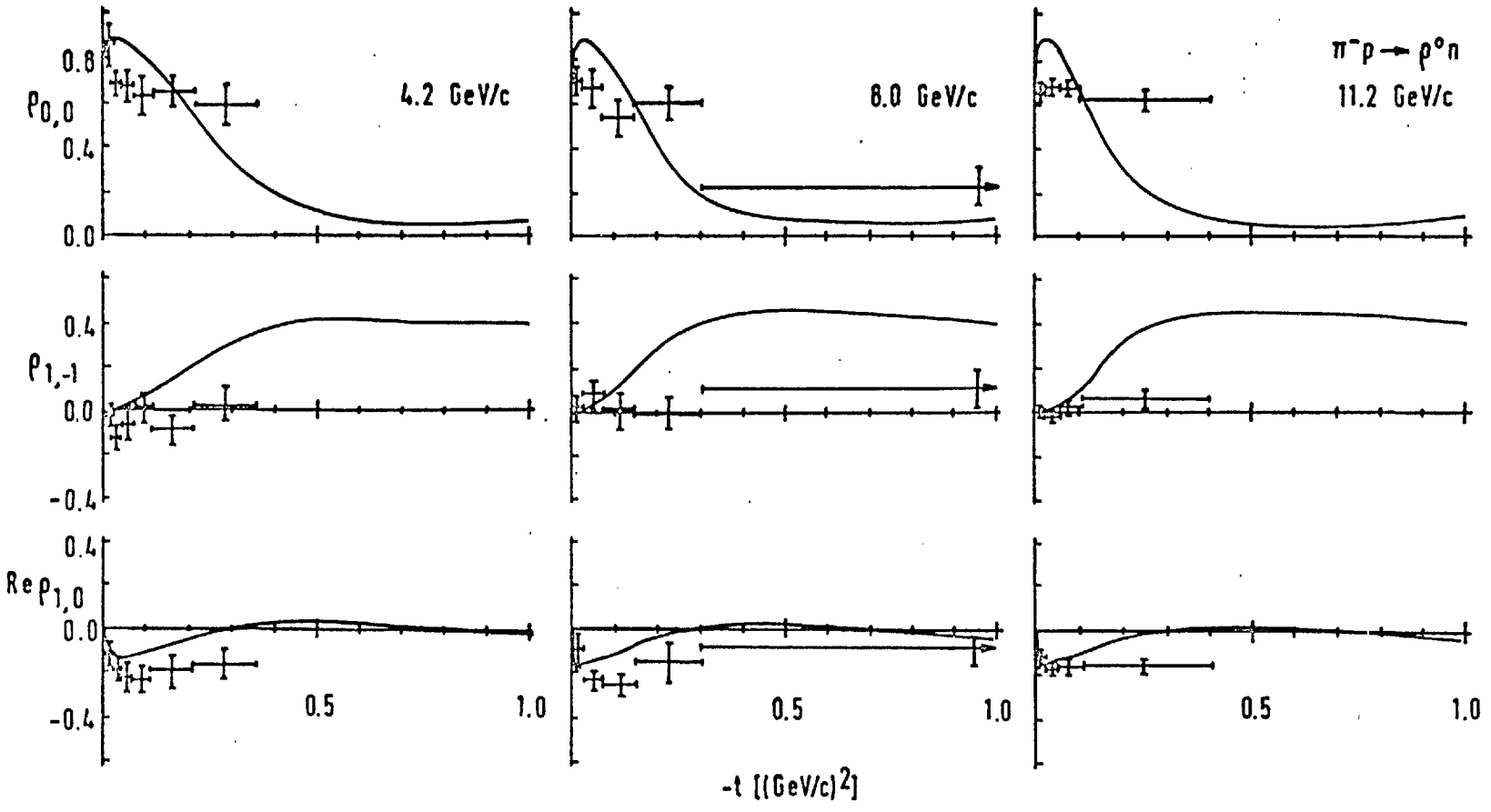


Fig. 21

Density matrix elements of the ρ resonance in $\pi^- p \to \rho^0 n$. Data from Ref. 56 and 58.

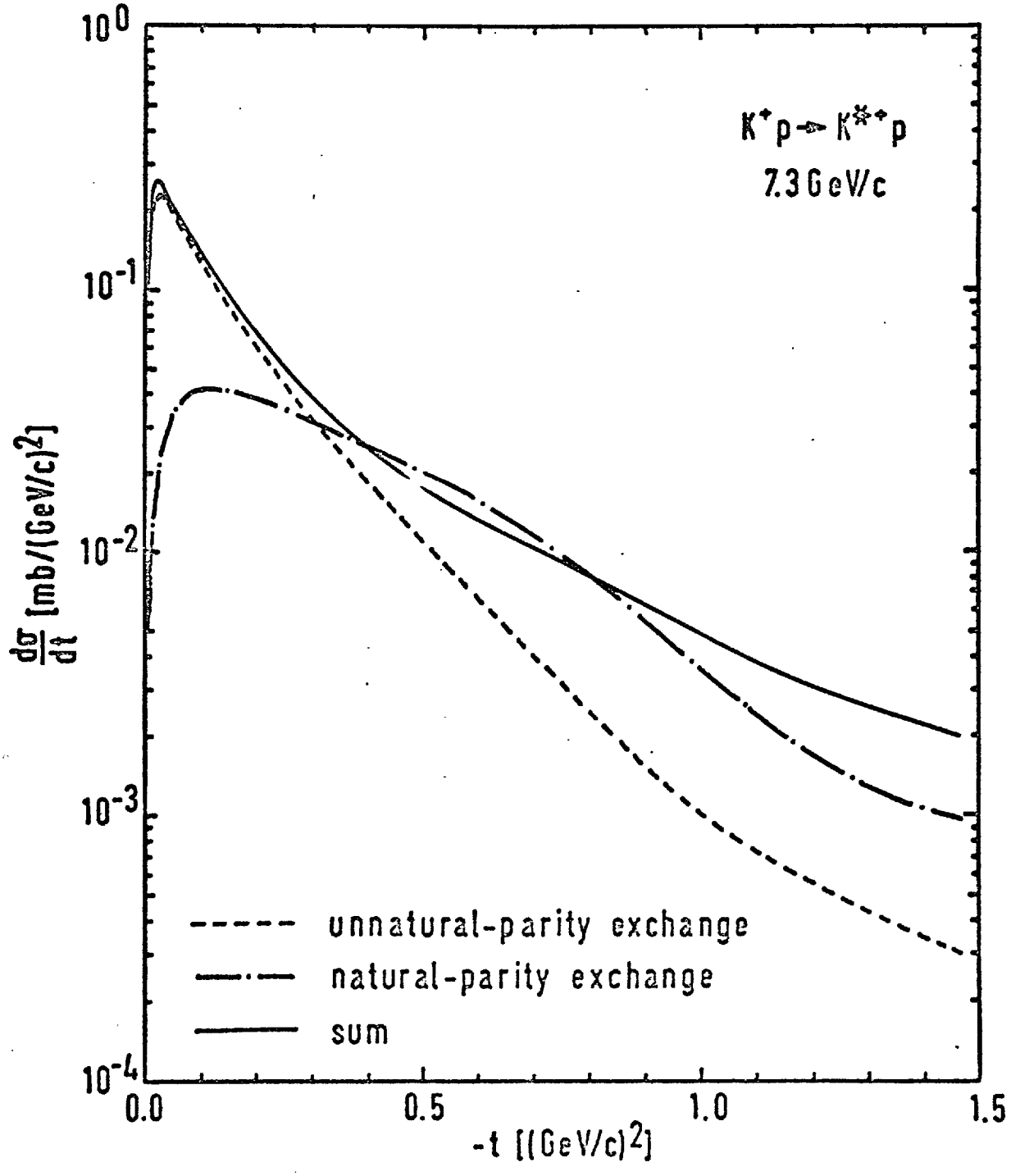


Fig. 22

Contributions to the differential cross section for $K^+p \to K^{*+}p$ from unnatural-parity and natural-parity exchanges.

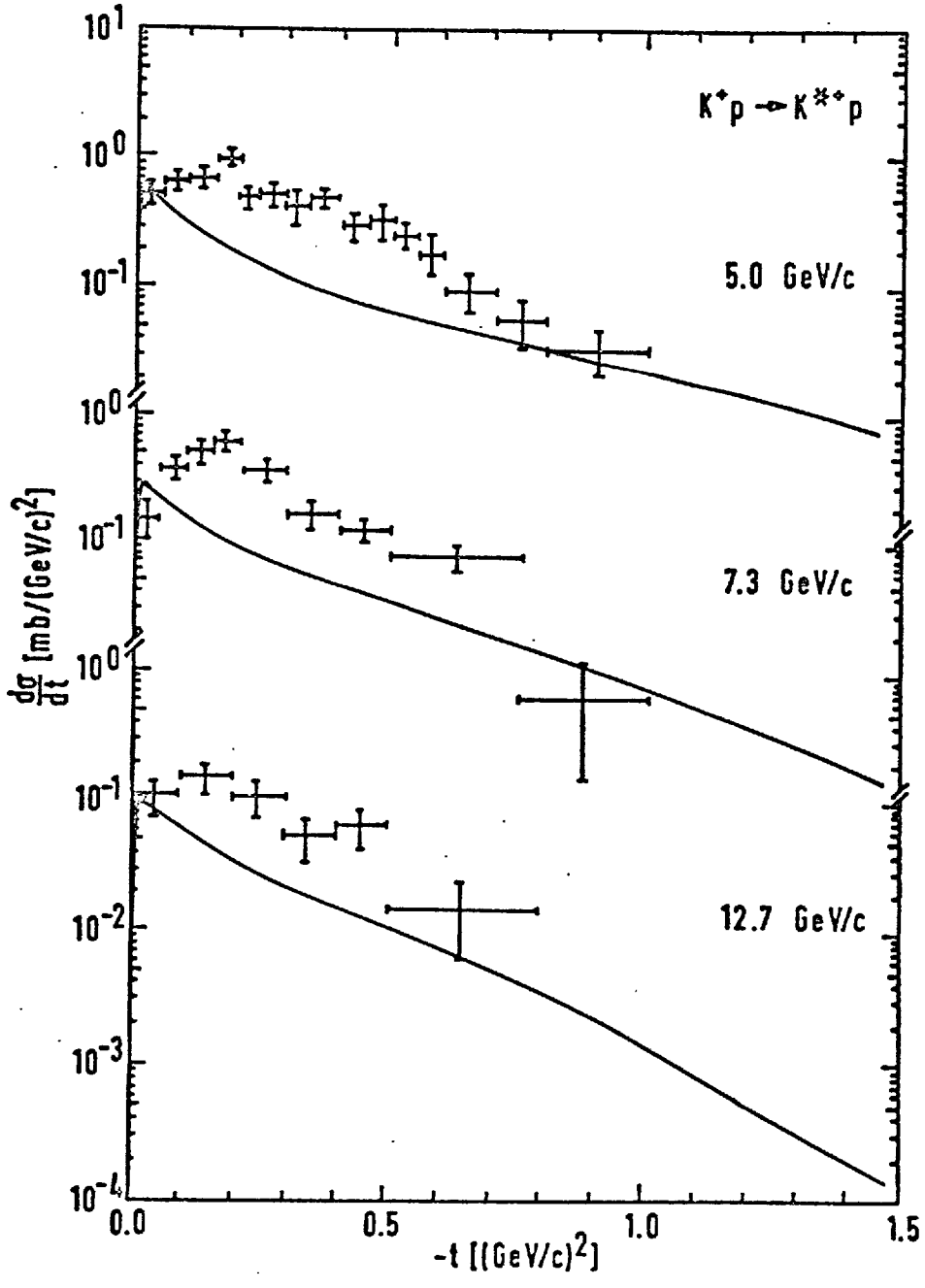


Fig. 23

Differential cross section for $K^+p \to K^{*+}p$.

Data from Ref. 53, 54 and 60.

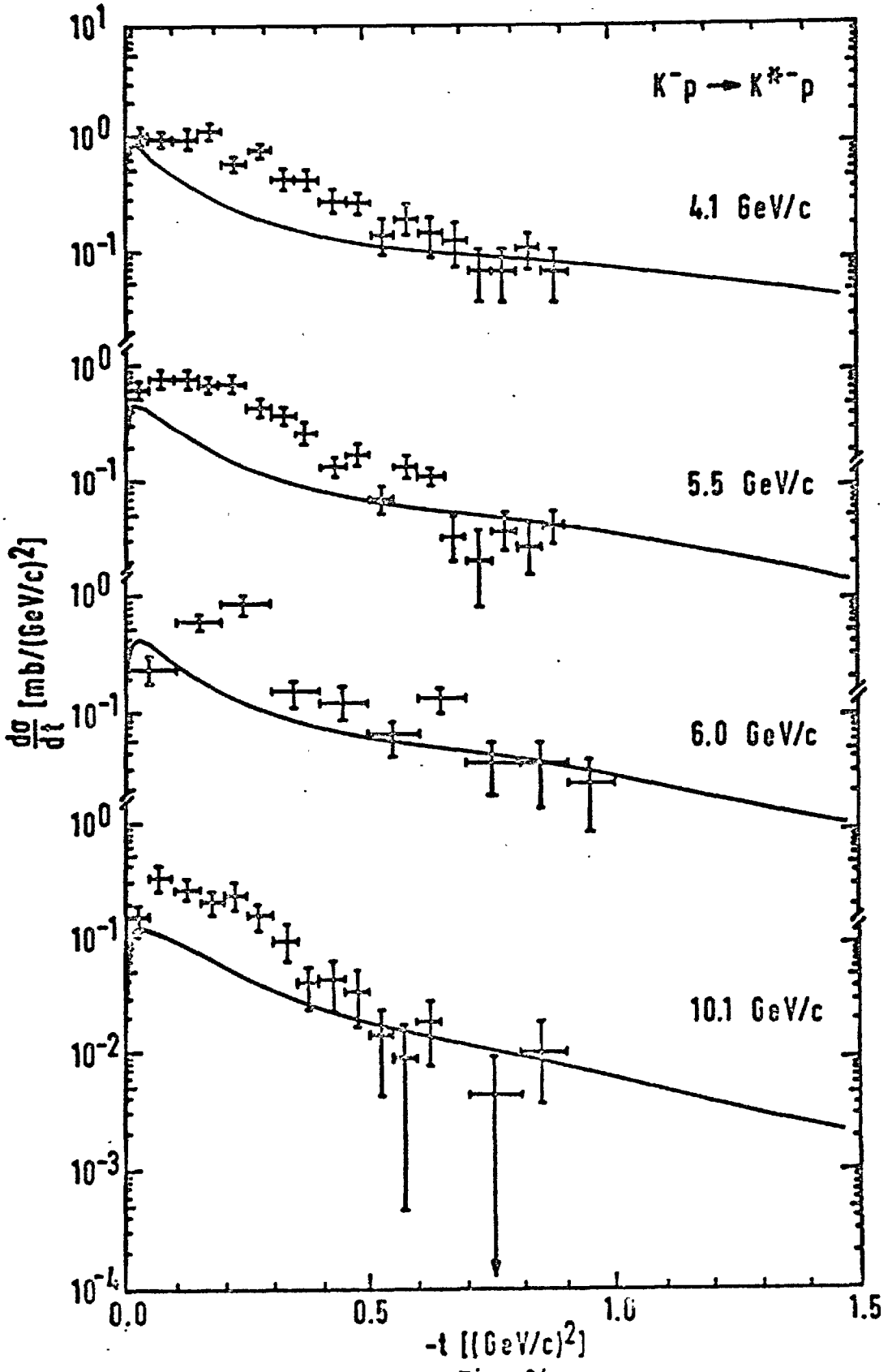


Fig. 24

Differential cross section for $K^-p \rightarrow K^{*-}p$.

Data from Ref. 61, 62 and 63.

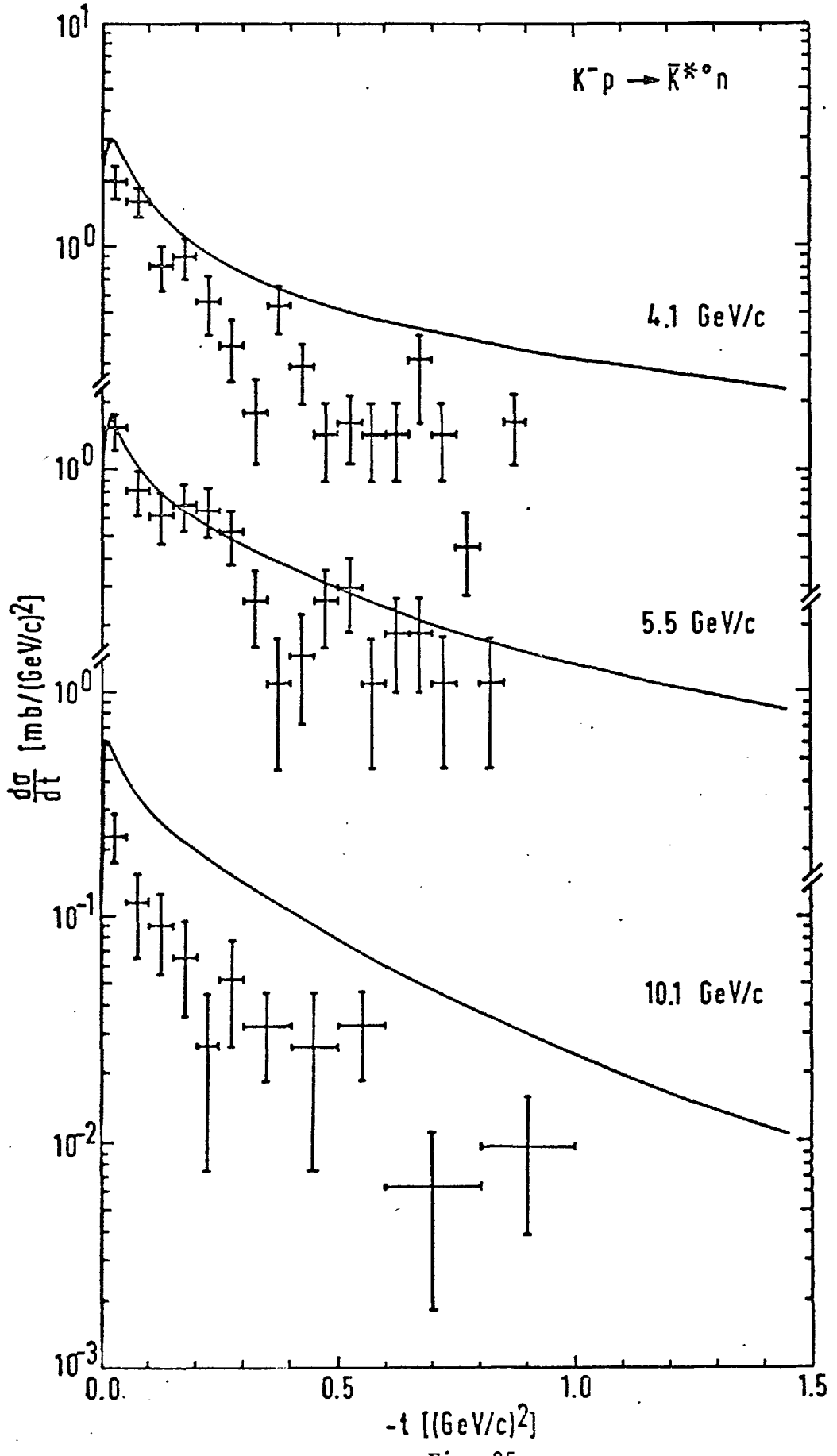


Fig. 25

Differential cross section for $K^- p \rightarrow \bar{K}^{*o} n$. Data from Ref. 61 and 63.

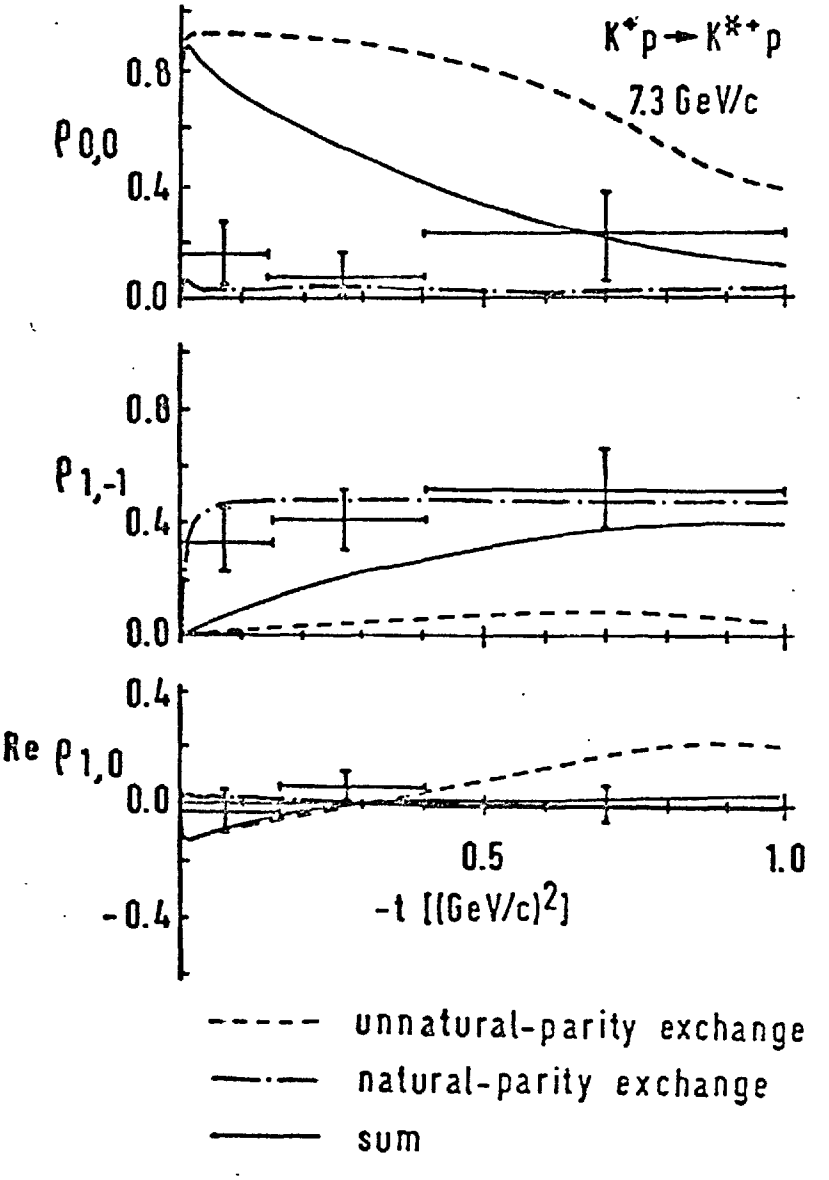


Fig. 26

Density matrix elements of the K^* resonance in $K^+p \to K^{*+}p$. The contributions from unnatural-parity and natural-parity exchanges and the sum are shown. Data from Ref. 53.

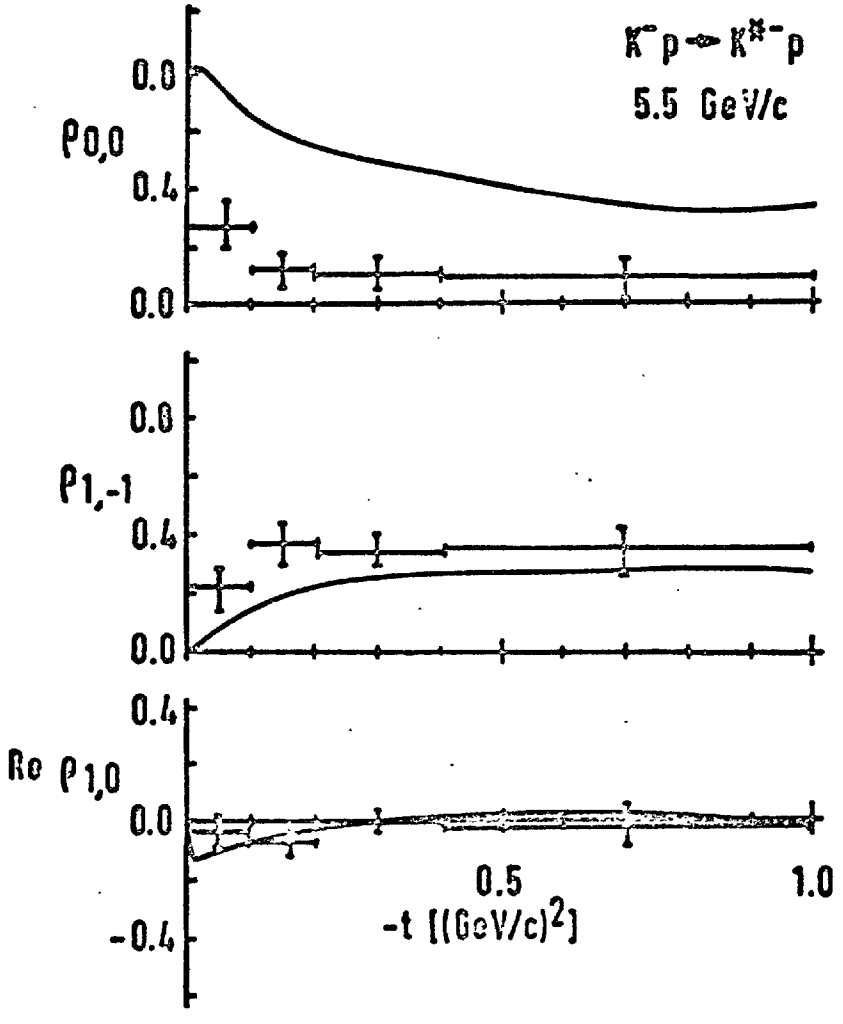


Fig. 27

Density matrix elements of the K^* resonance in $K^-p \to K^{*-}p$.

Data from Ref. 61.

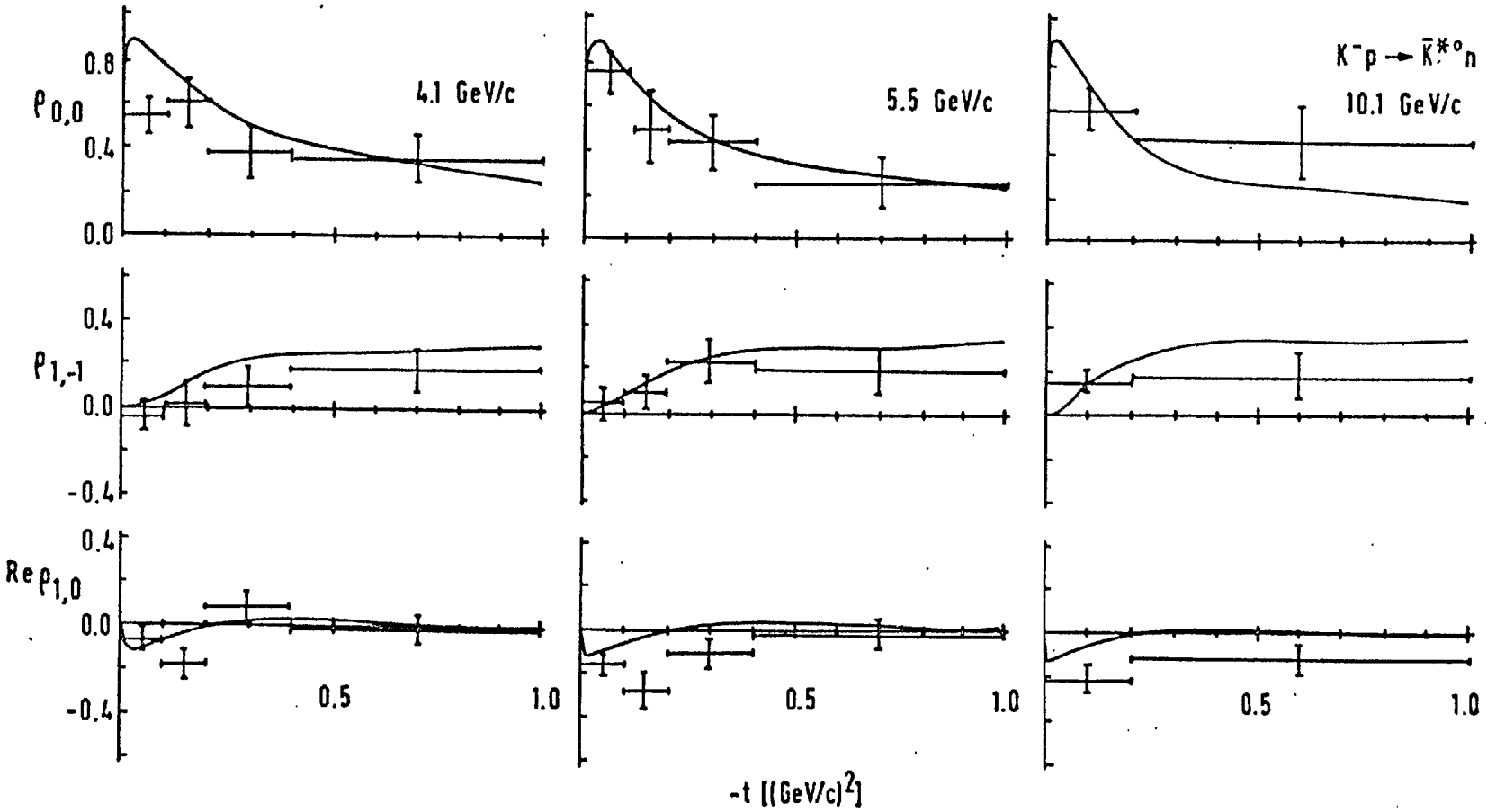


Fig. 28

Density matrix elements of the K^* resonance in $K^-p \to \bar{K}^{*o}n$. Data from Ref. 61 and 63.

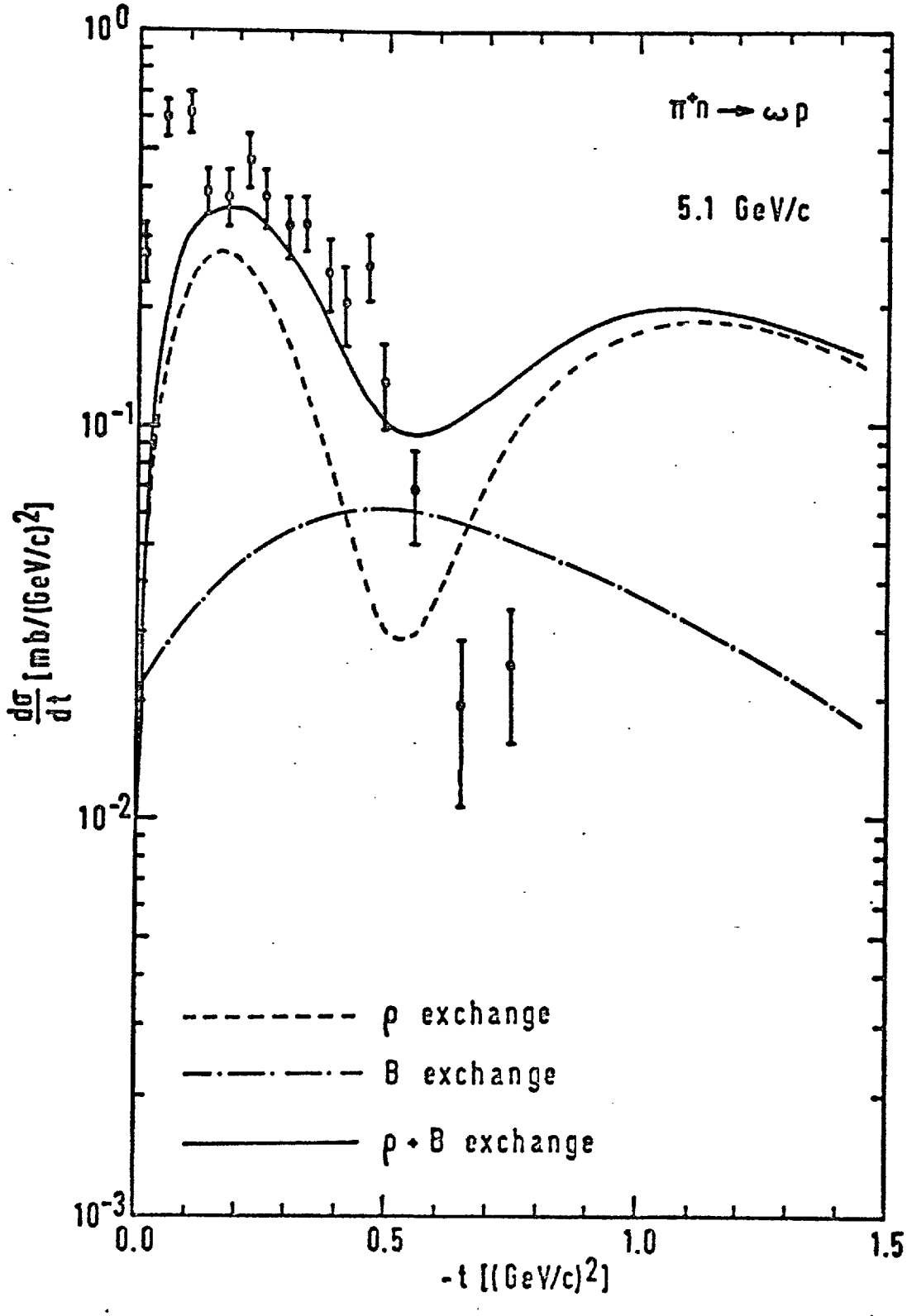


Fig. 29

Contributions to the differential cross section for $\pi^+ n \rightarrow \omega p$ from ρ, B and ρ+B exchanges. Data from Ref. 64.

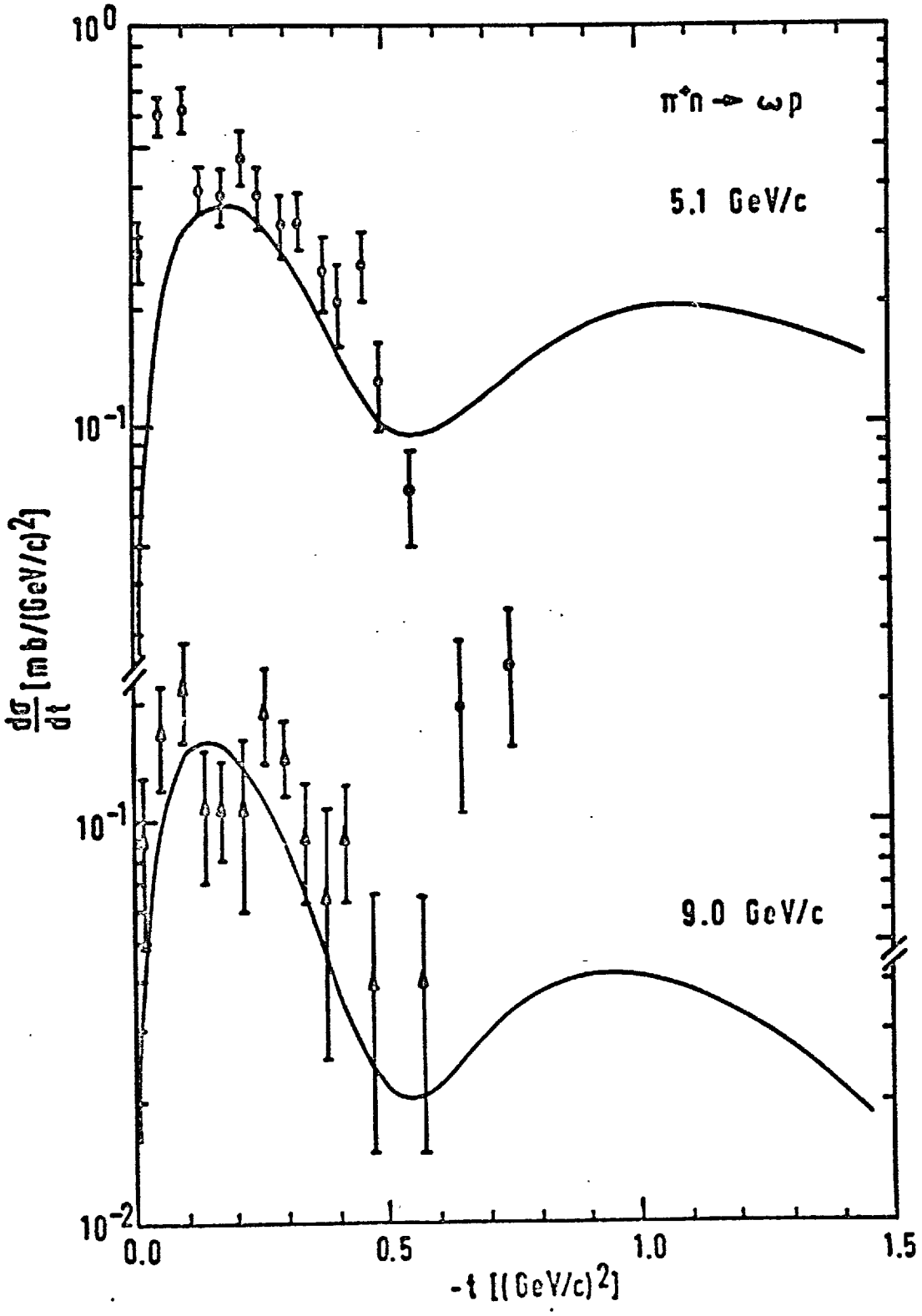


Fig. 30

Differential cross section for $\pi^+ n \rightarrow \omega p$. Data from Ref. 64.

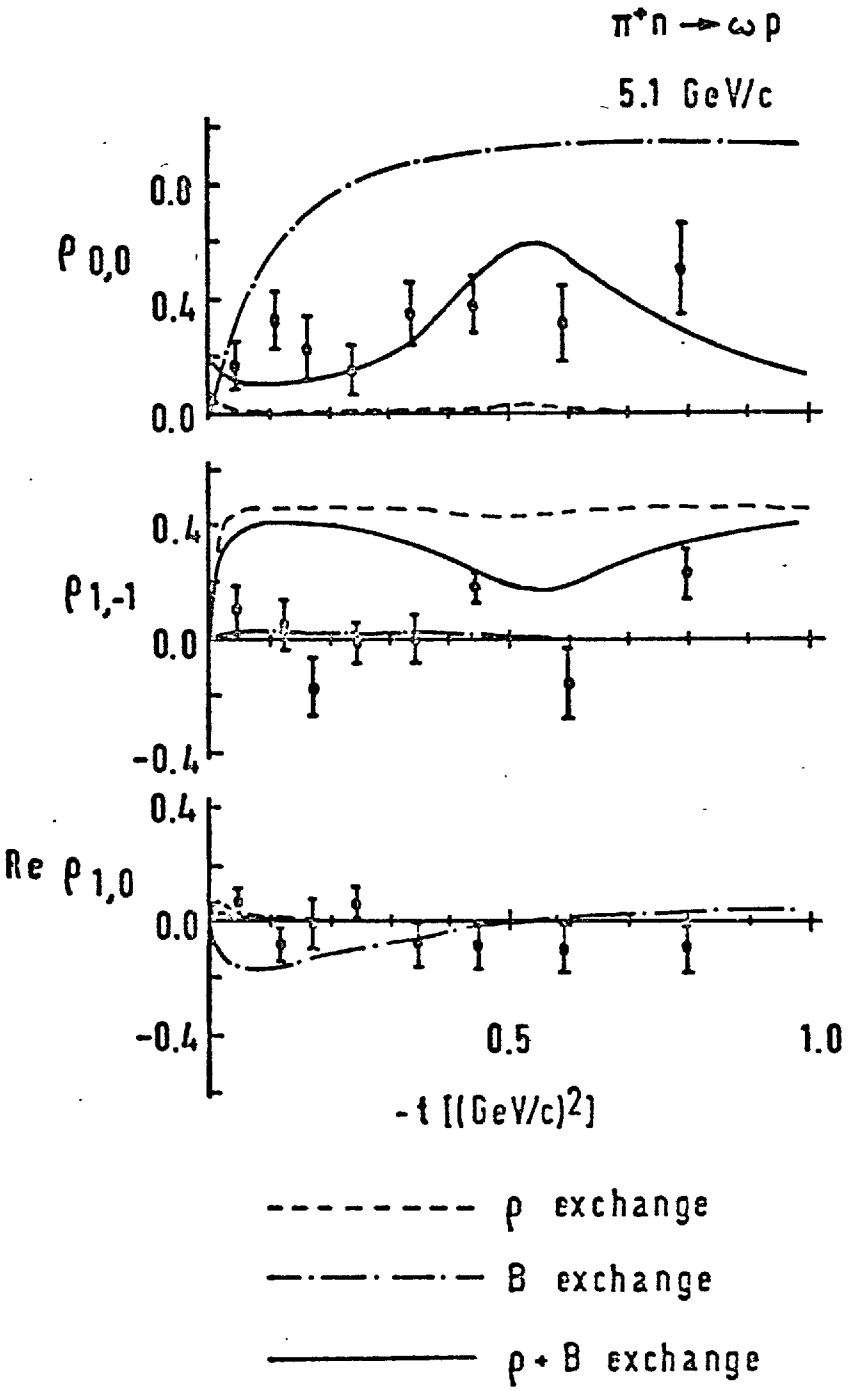


Fig. 31

Density matrix elements of the ω resonance in $\pi^+ n \to \omega p$. The contributions from ρ, B and ρ+B exchanges are shown. Data from Ref. 64.

CHAPTER IV

APPLICATION TO BARYON-BARYON SCATTERING

4.1 Introduction

Results are presented for reactions of the type

$$1/2^+\ 1/2^+ \rightarrow 3/2^+\ 1/2^+$$

$$1/2^+\ 1/2^+ \rightarrow 3/2^+\ 3/2^+$$

and which proceed by the exchange of non-strange mesons. The large number of helicity amplitudes makes it desirable to employ a scheme to avoid the introduction of an extremely large number of parameters.

Data on the production of the $\Delta(1236)$ isobar in proton-proton reactions is available from various counter and bubble chamber experiments for

$$pp \rightarrow n\Delta^{++}$$

$$pp \rightarrow p\Delta^{+}$$

$$pp \rightarrow \Delta^{++}\Delta^{o}.$$

The model is applied to these single and double $\Delta(1236)$-production reactions in the energy range 5 - 24 GeV/c [65]. Extremely favourable agreement is obtained between the theoretical predictions and the experimental data on differential cross sections and density matrix elements.

4.2 Formalism

We have assumed that the principal trajectories exchanged in these reactions correspond to the π, ρ and A_2 mesons.

Denoting the pseudoscalar-exchange and vector-exchange amplitudes by T_P and T_V, respectively, we have for $1/2^+\ 1/2^+ \to 3/2^+\ 1/2^+$

$$T_P = J_5'(D)\ \frac{1}{t-M^2}\ J_5(0)$$

$$T_V = J_\mu'(D)\ \frac{-g_{\mu\nu} + Q_\mu Q_\nu/M^2}{t-M^2}\ J_\nu(0)$$

and for $1/2^+\ 1/2^+ \to 3/2^+\ 3/2^+$

$$T_P = J_5'(D)\ \frac{1}{t-M^2}\ J_5(D)$$

$$T_V = J_\mu'(D)\ \frac{-g_{\mu\nu} + Q_\mu Q_\nu/M^2}{t-M^2}\ J_\nu(D)\ ,$$

where the primed and unprimed quantities distinguish the two vertices.

Reggeizing and introducing the 2^+-exchange contribution, the amplitude for $1/2^+\ 1/2^+ \to 3/2^+\ 1/2^+$ then becomes

$$T = -\ \alpha_\pi' \Gamma(-\alpha_\pi)\ \frac{1 + e^{-i\pi\alpha_\pi}}{2}\ \left(\frac{s + \frac{1}{2}t - \frac{1}{2}\sum_{i=1}^{4} m_i^2}{s_o}\right)^{\alpha_\pi}$$

$$\times\ g^2 g_G'\ g_{D+\frac{2}{3}F}\ \frac{1}{m_B'}\ \left(1 + \frac{2m}{\mu}\right)^2 \left(1 - \frac{\mu^2}{4m_B^2}\right) Q_\lambda' \bar{\psi}_\lambda' u' \bar{u} \gamma_5 u$$

$$-\Big[\ \alpha_\rho'\ \Gamma(1-\alpha_\rho)\ \frac{1 - e^{-i\pi\alpha_\rho}}{2}\ \left(\frac{s + \frac{1}{2}t - \frac{1}{2}\sum_{i=1}^{4} m_i^2}{s_o}\right)^{\alpha_\rho - 1}$$

$$+\ \alpha_{A_2}'\ \Gamma(1-\alpha_{A_2})\ \frac{1 + e^{-i\pi\alpha_{A_2}}}{2}\ \left(\frac{s + \frac{1}{2}t - \frac{1}{2}\sum_{i=1}^{4} m_i^2}{s_o}\right)^{\alpha_{A_2} - 1}\ \Big]$$

$$\times g^2 g'_G \frac{1}{2m'^2_B}\left(1+\frac{2m}{\mu}\right)$$

$$\times\Big[\frac{1}{2m_B}\Big[\Big(1+\frac{\mu}{2m}\Big)g_F-\Big(1+\frac{2m}{\mu}\Big)g_{D+\frac{2}{3}F}\Big]\varepsilon_{\mu\kappa\lambda\rho}P_\mu P'_\kappa Q'_\lambda\bar{\psi}'_\rho u'\bar{u}u$$

$$+\Big(1-\frac{t}{4m_B^2}\Big)\Big(1+\frac{2m}{\mu}\Big)g_{D+\frac{2}{3}F}\varepsilon_{\mu\kappa\lambda\rho}P'_\kappa Q'_\lambda\bar{\psi}_\rho u'\bar{u}\gamma_\mu u\Big],$$

while the amplitude for $1/2^+\ 1/2^+ \to 3/2^+\ 3/2^+$ becomes

$$T=-\alpha'_\pi\,\Gamma(-\alpha_\pi)\,\frac{1+e^{-i\pi\alpha_\pi}}{2}\left(\frac{s+\frac{1}{2}t-\frac{1}{2}\sum_{i=1}^{4}m_i^2}{s_o}\right)^{\alpha_\pi}$$

$$\times g^2 g_G g'_G\,\frac{1}{m_B^2}\left(1+\frac{2m}{\mu}\right)^2 Q'_\lambda\bar{\psi}'_\lambda u' Q_\kappa\bar{\psi}_\kappa u$$

$$+\Big[\alpha'_\rho\,\Gamma(1-\alpha_\rho)\,\frac{1-e^{-i\pi\alpha_\rho}}{2}\left(\frac{s+\frac{1}{2}t-\frac{1}{2}\sum_{i=1}^{4}m_i^2}{s_o}\right)^{\alpha_\rho-1}$$

$$+\alpha'_{A_2}\,\Gamma(1-\alpha_{A_2})\,\frac{1+e^{-i\pi\alpha_{A_2}}}{2}\left(\frac{s+\frac{1}{2}t-\frac{1}{2}\sum_{i=1}^{4}m_i^2}{s_o}\right)^{\alpha_{A_2}-1}\Big]$$

$$\times g^2 g_G g'_G\,\frac{1}{4m_B^4}\left(1+\frac{2m}{\mu}\right)^2\varepsilon_{\mu\alpha\beta\gamma}P'_\alpha Q'_\beta\bar{\psi}'_\gamma u'\varepsilon_{\mu\kappa\lambda\rho}P_\kappa Q_\lambda\bar{\psi}_\rho u.$$

Explicit expressions for the helicity amplitudes are evaluated using standard techniques and are given in Appendix D.

4.3 Discussion and Results

The theoretical momentum transfer distributions are identical in the forward and backward directions. In some cases the experimental distributions have been folded, therefore necessitating the multiplication of the data by a factor of one half, since the theoretical calculations consider Δ production in one hemisphere only.

(i) $1/2^+ \; 1/2^+ \rightarrow 3/2^+ \; 1/2^+$

Fig. 32 compares the contributions to the differential cross section for the reaction $pp \rightarrow n\Delta^{++}$ from absorbed π exchange before and after Reggeization in this model. We note that near the forward direction the Reggeized exchange gives a normalization lower by about 30% than the elementary exchange. This difference becomes more marked with increasing momentum transfer, the Reggeized exchange being more steeply t dependent. The contributions from ρ and A_2 exchanges are also shown. The relative couplings given by the model predict pion dominance, particularly near the forward direction, the other exchanges making relatively small contributions except at large angles. This is in keeping with the data, since Ma et al [66] found the energy dependence of this reaction up to 24 GeV/c to be consistent with π exchange.

Fig. 33 shows the energy dependence of the momentum transfer distribution for this reaction. Our theoretical results are quite consistent with the s dependence of the data over the energy range 5.5 - 24.2 GeV/c. The t dependence is also satisfactory. The sets of data at 6.6 and 6.92 GeV/c confirm the presence of the predicted

turnover near the forward direction. This turnover persists in the 6.6 GeV/c data when analysed as a function of $t' = t - t_{min}$, showing that this is not simply a kinematic effect. The data for this reaction at and above 13.0 GeV/c were analysed experimentally as a function of t'. Because of the small value of t_{min} for this reaction at these energies, we have, for consistency, plotted the data as a function of t.

With no absorption we obtain

$$\rho_{3,3} = \text{Re } \rho_{3,-1} = \text{Re } \rho_{3,1} = 0$$

for the spin density matrix elements of a Δ resonance produced by π exchange. The ρ and A_2 exchanges give

$$\rho_{3,3} = 3/8 = .375, \quad \text{Re } \rho_{3,-1} = \sqrt{3}/8 = .216, \quad \text{Re } \rho_{3,1} = 0.$$

Our results for the spin density matrix elements of the Δ resonance produced in the reaction $pp \to n\Delta^{++}$ are compared with the data in Fig. 34. The data strongly indicates that π exchange is the dominant mechanism. This is given by the model, the values of the density matrix elements being almost entirely due to π exchange.

The predictions of the model are compared in Fig. 35 with representative data on the differential cross section for the reaction $pp \to p\Delta^{+}$ at four different incident momenta in the range 5.52 - 15.0 GeV/c. More data is available, but this is poorer and for this reason it has not been included in the analysis. We observe that both the s and t dependence of the theoretical distributions are

consistent with experiment. It should be noted that the data at 6.0, 10.0 and 15.0 GeV/c have an additional possible 50% uncertainty in overall normalization. The theoretical differential cross section shows a turnover near the forward direction but the experimental statistics are not sufficiently good to test this point. However, charge independence gives the relation

$$\frac{d\sigma}{dt}(pp \to p\Delta^{+}) = \frac{1}{3}\frac{d\sigma}{dt}(pp \to n\Delta^{++})$$

independent of any particular model and, within the experimental errors, the data appears to bear this out. In view of this it would be surprising if improved statistics do not show the presence of a forward turnover in $p\Delta^{+}$ production.

Ignoring the slight p-n mass difference, the theoretical predictions for the spin density matrix elements of the Δ resonance produced in the reaction $pp \to p\Delta^{+}$ are identical to those from $n\Delta^{++}$ production. No data is currently available to test this.

(ii) $\underline{1/2^{+}\ 1/2^{+} \to 3/2^{+}\ 3/2^{+}}$

Our results for the differential cross section for the reaction $pp \to \Delta^{++}\ \Delta^{o}$ are shown in Fig. 36. We note that both the s and t dependence are well represented over the energy range 5.0 - 16.08 GeV/c. The differential cross section peaks before and after absorption. The effect of the absorption is to decrease the forward normalization, and also to give a sharper fall-off with

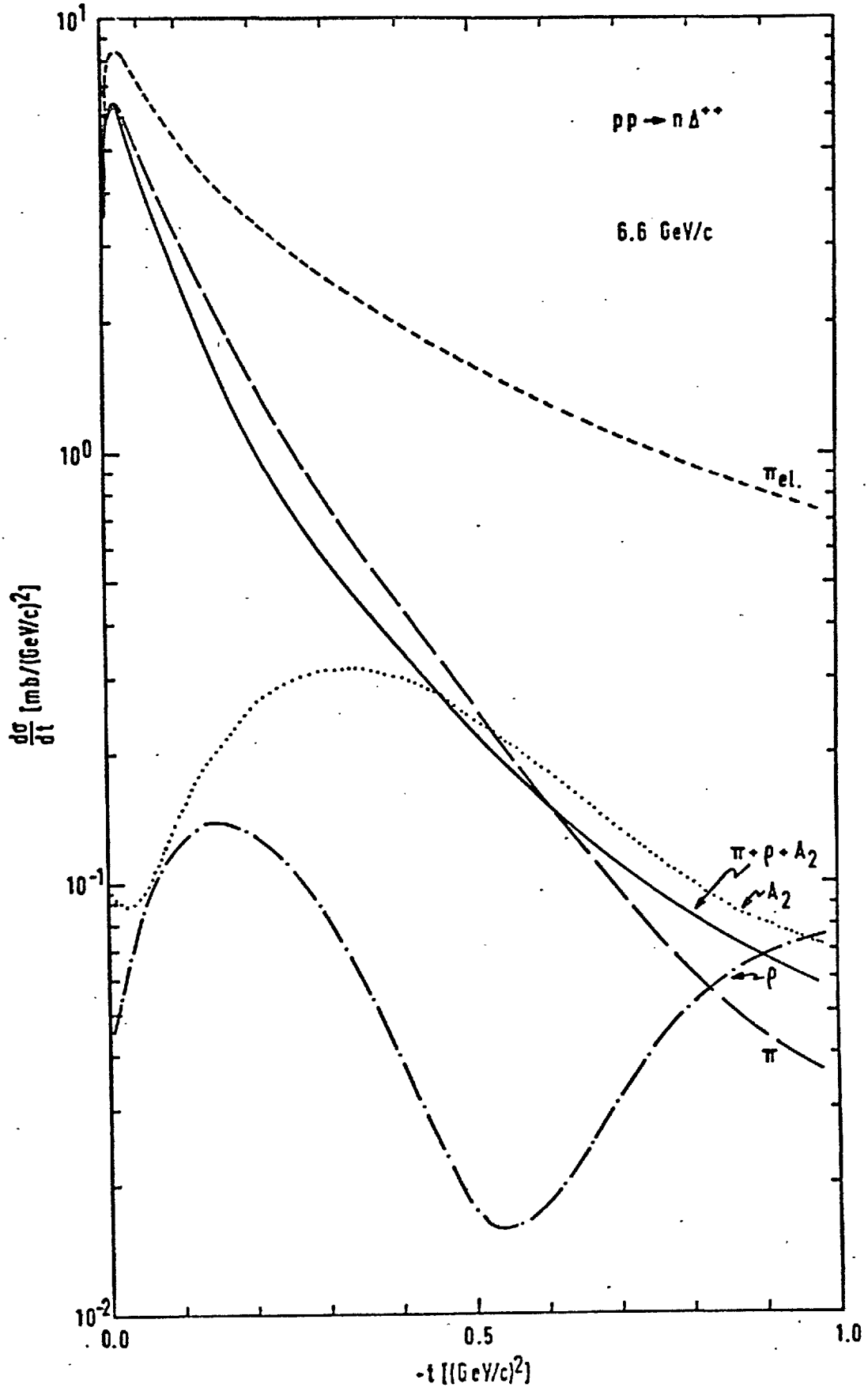


Fig. 32

Contributions to the differential cross section for $pp \to n\Delta^{++}$ from absorbed elementary π, Reggeized π, ρ, A_2 and $\pi+\rho+A_2$ exchanges.

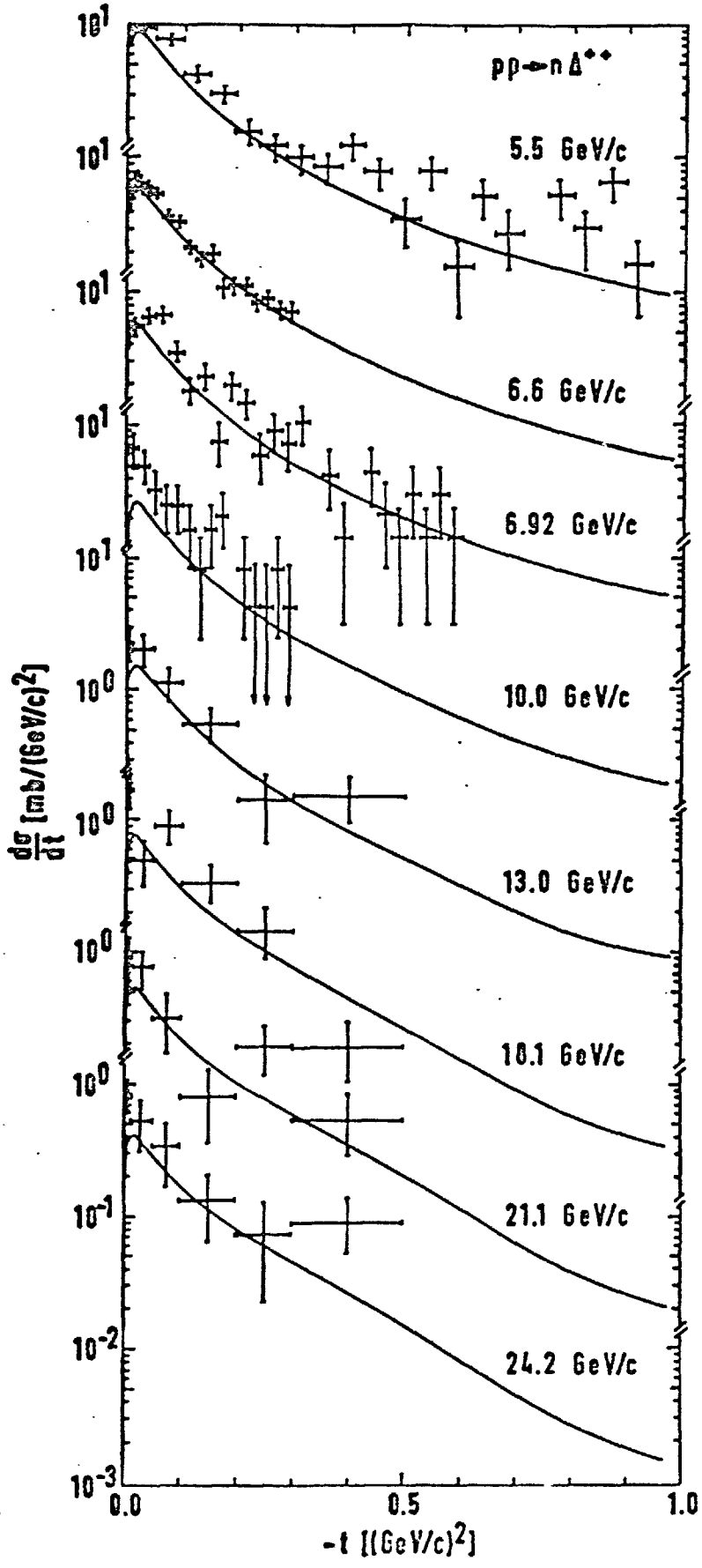


Fig. 33

Differential cross section for $pp \to n\Delta^{++}$.

Data from Ref. 66, 67, 68, 69 and 70.

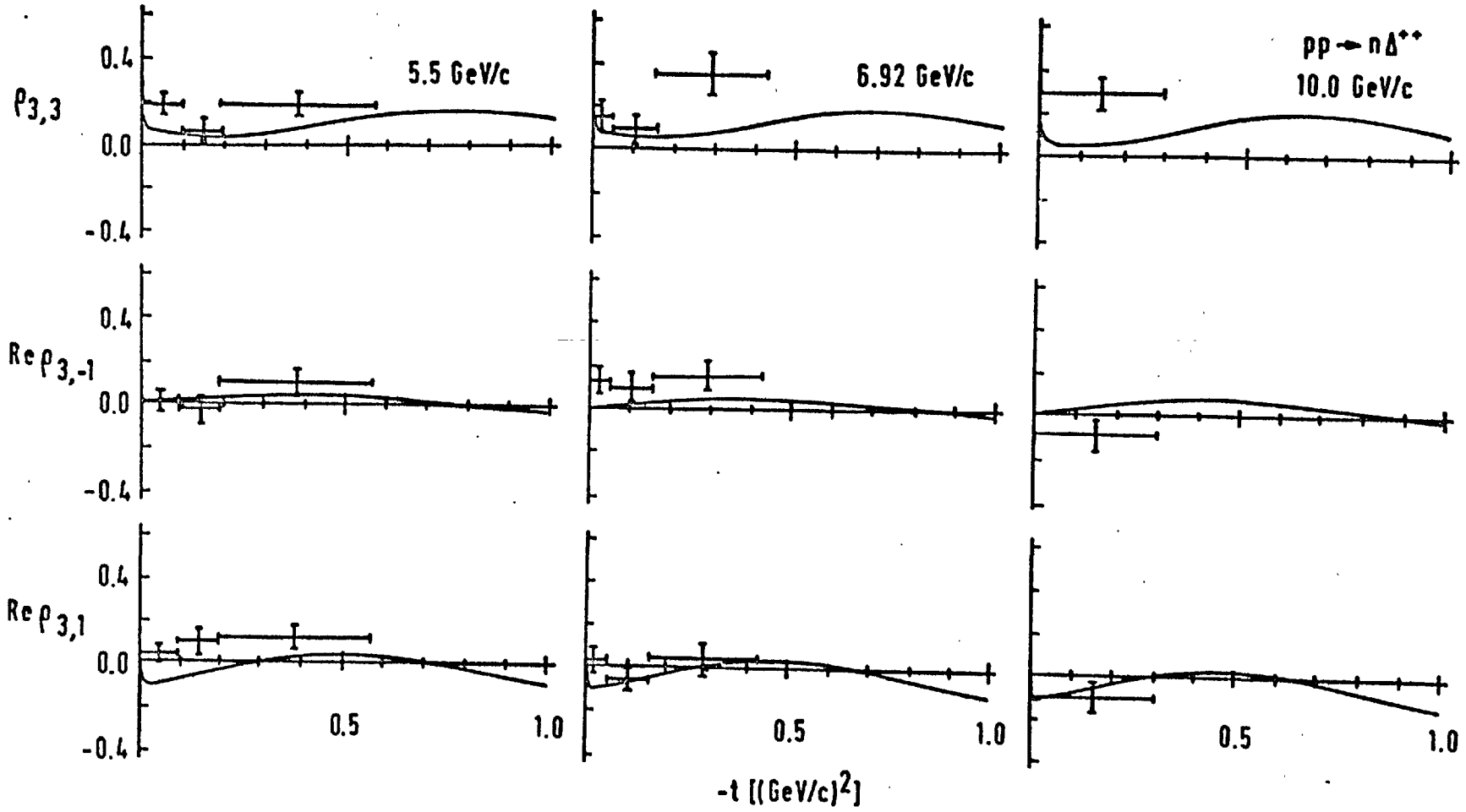


Fig. 34

Density matrix elements of the Δ resonance in $pp \to n\Delta^{++}$. Data from Ref. 67, 69 and 70.

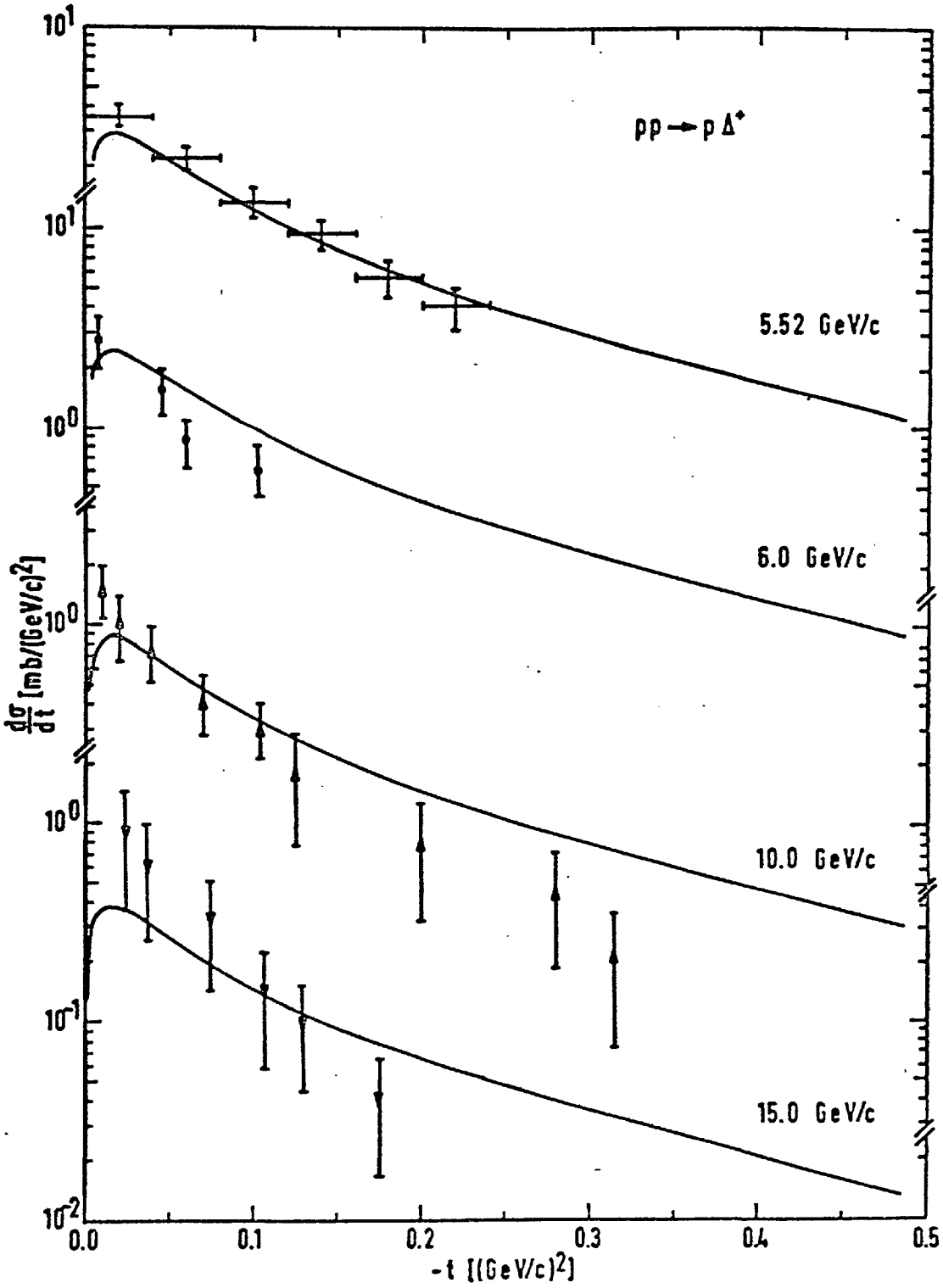


Fig. 35

Differential cross section for $pp \to p\Delta^+$.

Data from Ref. 71 and 72.

increasing momentum transfer. The experimental data at 5.0 and 10.0 GeV/c were analysed as functions of t rather than t'. Since t_{min} is large for this reaction, the fact that t = 0 is not the forward direction gives a misleading appearance to the first bin. To approximately correct for this we have equated the areas between t = 0 and the edge of the first bin and t = t_{min} and the edge of the first bin. This procedure is exact for zero-width resonances. A true correction for this kinematic effect would require a re-analysis of the original experimental data [73].

The density matrix elements of the Δ^{++} resonance produced in this reaction are shown in Fig. 37. Our results, which are in satisfactory agreement with the data, indicate that π exchange is the dominant mechanism.

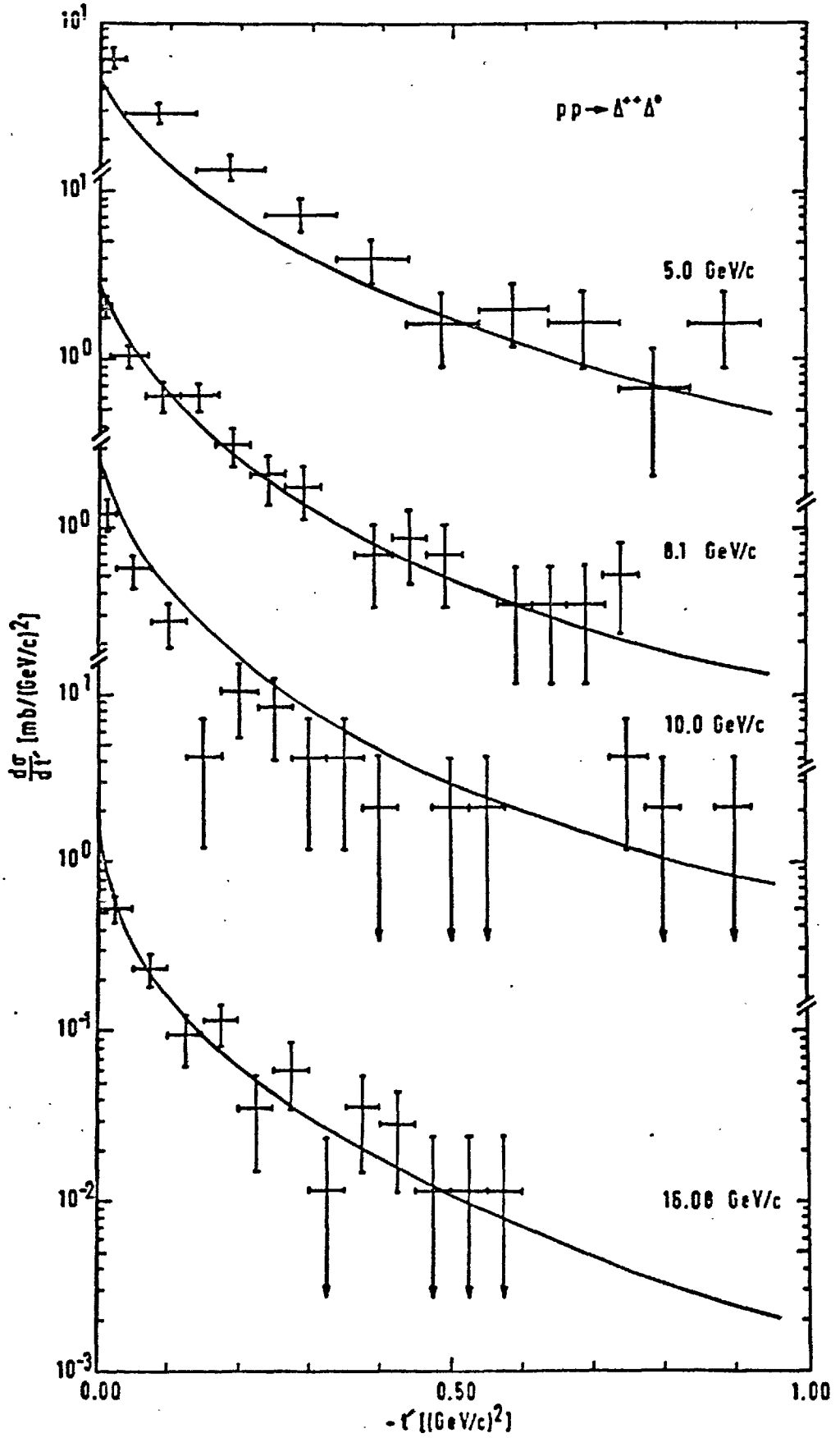


Fig. 36

Differential cross section for $pp \to \Delta^{++}\Delta^{\circ}$.

Data from Ref. 74, 75, 76 and 77.

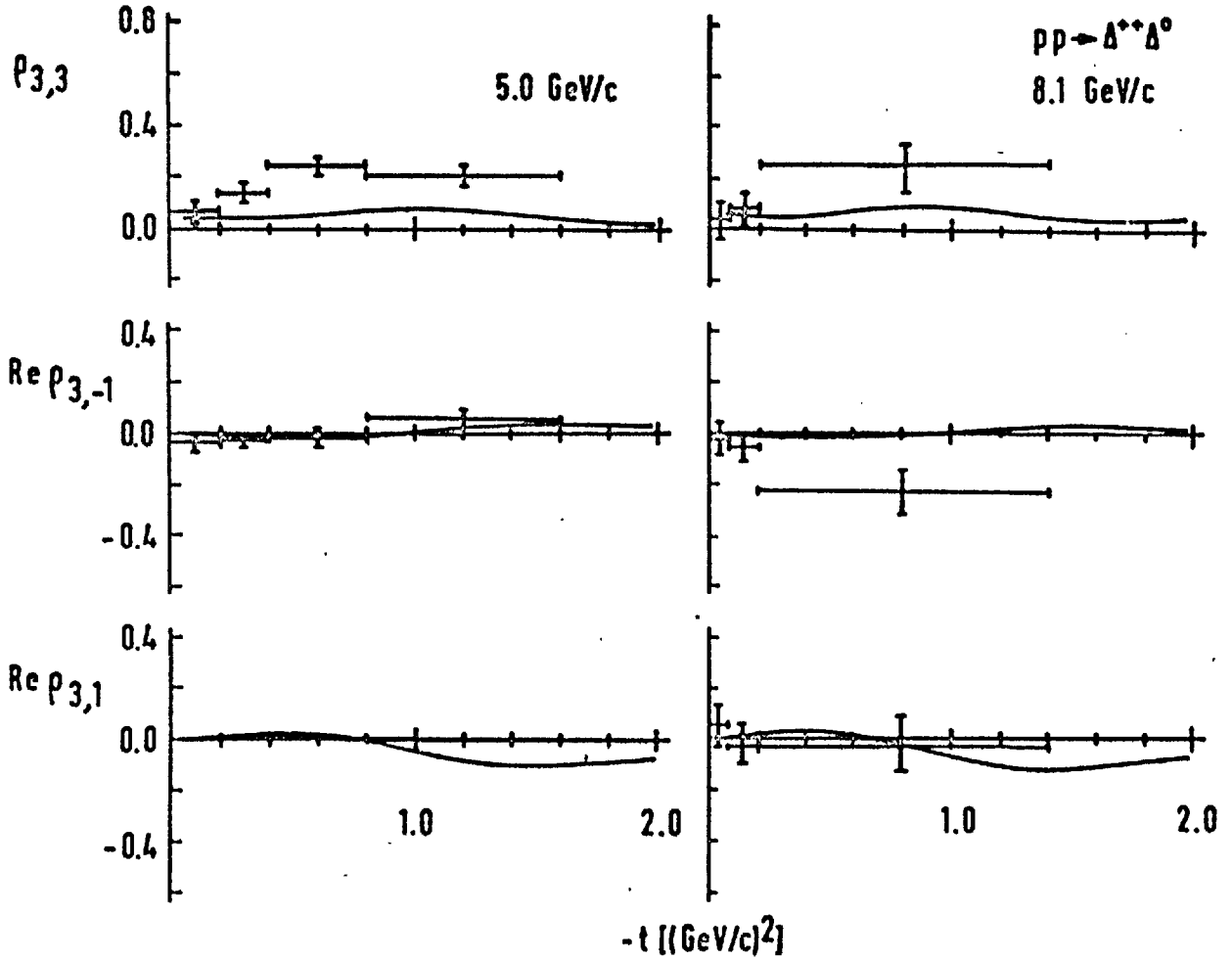


Fig. 37

Density matrix elements of the Δ^{++} resonance in $pp \to \Delta^{++}\Delta^{0}$. Data from Ref. 74 and 75.

CHAPTER V

CONCLUSIONS

5.1 Summary

With the exception of the $K^{*\pm}$ - and ω-production reactions, for the processes we have analysed the angular dependence of the differential cross sections predicted by the model agrees with the essential features of the experimental data, in particular, forward peaks, turnovers and dips, in all cases where the data is sufficiently good to enable such comparisons to be made. General agreement is also obtained for the density matrix elements. Although the dips in the differential cross sections arise originally from the nonsense zeros introduced in the Reggeization procedure, this feature is largely due to the influence of the symmetry scheme, which determines the ratios of the helicity amplitudes and the relative strengths of the couplings at the vertices.

The energy dependence of the model derives mainly from the replacement of s^J by s^α in the Reggeization of the amplitudes, although there is an addition slow s dependence in the absorption parameters. This is in general agreement with experiment.

One not entirely unexpected shortcoming of the model we have found is in the prediction of absolute normalizations, which do not always coincide with the data. This may not be unconnected with the difficulty of obtaining absolute normalizations experimentally. It should be remembered that the quoted normalization errors on experimental data are often in the region of 20 - 30% and frequently higher. When data is available for a particular process from different experimental groups, agreement may be reasonable good for one set of data but poor for another.

Although such a procedure is justified, we have not smoothed the data within the stated normalization errors in order to improve the appearance of our results. We should also remark that this difficulty of relative normalization errors makes the extraction of meaningful parameters from data extremely difficult.

It should be emphasized that in this model we are in a theoretical strait-jacket, in that the symmetry scheme and strong exchange degeneracy fix completely the pole graphs. Since SU(3) is well known to be broken, we certainly do not expect a higher symmetry scheme to give perfect agreement with experiment. However, rather than at this point introduce a few arbitrary parameters and perform curve fitting procedures to bring about detailed agreement between theory and experiment, we feel that effort could more profitably be directed towards investigating a better consistent and physically plausible scheme for mass-splitting in U(6,6) $\otimes$ O(3,1) and a method of breaking strong exchange degeneracy.

Discrepancies between the predictions of the model and the experimental data, particularly the steepness of the t dependence, could be reduced by allowing the final-state absorption to be different from the initial-state absorption. However, the coefficients cannot be determined experimentally and we feel that little real insight is to be gained by making these arbitrary parameters to be fitted to the data.

It must also be borne in mind that while the general concept of the absorption model is probably correct, the exact procedure for including such corrections is not at all clear at present, and that although our Reggeization procedure seems very natural other reasonable schemes could be devised.

Calculations have also been performed using this model for reactions of the type $0^- 1/2^+ \to 1^- 3/2^+$ i.e.

$$\pi^+ p \to \rho^o \Delta^{++}$$
$$K^+ p \to K^{*o} \Delta^{++}$$
$$K^- n \to \bar{K}^{*o} \Delta^-$$
$$\pi^+ p \to \omega \Delta^{++}.$$

The first three of these reactions exhibit a sharp forward pion peak. Considering the severe restrictions of the model, the agreement obtained with the experimental data is encouraging [37]. The results of the model as applied to spin-2 production processes will be published shortly.

We feel that a useful test of this model would be its application to the processes

$$pn \to np$$
$$\bar{p}p \to \bar{n}n.$$

Here the pion contribution tends to exhibit, in addition to the sharp forward peak, a secondary maximum just beyond this peak. This is absent from the data but its phenomenological elimination presents difficulty.

A similar problem arises in π-exchange photoproduction processes. However, additional complications not present in other processes result from the requirement of gauge invariance and the presence in some photoproduction processes of diffractive-type terms as well as exchange-type terms in the amplitudes. Calculations with fixed-pole exchange and U(6,6) symmetry have already been published [27].

This model is currently being applied to backward scattering processes. An elementary-particle exchange model incorporating U(6,6)

symmetry has previously been reported [78].

Encouraging results have been obtained by applying the Veneziano model to 3-particle production processes both in the spinless approximation [79] and taking some account of spin [80]. U(6,6) has been included in such B_5 calculations to produce a Veneziano model with spin with favourable results for the reactions

$$K^- p \rightarrow \pi^- \pi^+ \Lambda$$
$$K^- p \rightarrow \bar{K}^o \pi^- p. \quad (81)$$

More sophisticated models are currently being developed [82]. Since most of the assumptions of the present work are consistent with the Veneziano model, a Venezianoized U(6,6) absorptive peripheral model has been developed with applications to KN and $\bar{K}N$ charge-exchange [83] and to $K^*(890)$ and $\Delta(1236)$ production [84].

5.2 Calculational Procedure

As discussed in Appendix E, for the numerical work we used an exact partial-wave series [85] rather than suffer the laboriousness and inaccuracies of the impact-parameter representation. We employed a 48-point Gaussian quadrature to calculate explicitly 30 partial waves. Previous experience has shown this to be extremely accurate. To perform the partial-wave expansions, modify the partial waves, resum the series and calculate the results for all the reactions considered here took less than 300 seconds on a CDC 6600. Along with Lovelace [86], we find it easier to be exact.

APPENDIX A

NOTATION

We employ 2-particle helicity states $|p\theta\phi;\lambda_1\lambda_2>$ to describe a system of two particles in the c.m. frame. Particle 1 has 3-momentum $\underline{p}_1$, where in polar coordinates $\underline{p}_1 = (p,\theta,\phi)$, and helicity λ_1. Particle 2 moves in the opposite direction with helicity λ_2. The 2-particle state is constructed from two single-particle states with covariant normalization

$$<\underline{p}'|\underline{p}> = 2\, E_{\underline{p}}\, \delta^3(\underline{p}'-\underline{p}).$$

The S and T operators are related by

$$S = 1 - iT.$$

When taking matrix elements we separate out from T the overall energy-momentum conservation delta function

$$<f|S|i> = <f|i> - i\, \delta^4(p_i-p_f)\, <f|T|i>,$$

where p_i and p_f are the initial and final state 4-momenta, respectively.

We distinguish between the incoming meson (baryon), target baryon, outgoing meson (baryon) and outgoing baryon by the label $i = 1,2,3$ and 4, respectively. The c.m. coordinate system is defined such that particle 1 is travelling along the +z direction and particle 3 is travelling at an angle θ to this direction in the x-z plane. The quantities m_i, E_i, s_i and λ_i denote the mass, c.m. energy, spin and

helicity, respectively, of particle i, and k and q are the magnitudes of the c.m. 3-momenta in the initial and final states, respectively.

We thus obtain the covariantly normalized c.m. scattering amplitudes

$$\langle\lambda_3\lambda_4|\phi(s,\cos\theta)|\lambda_1\lambda_2\rangle = \langle q\theta 0;\lambda_3\lambda_4|T|k00;\lambda_1\lambda_2\rangle.$$

The differential cross section is then

$$\frac{d\sigma}{d\Omega} = \frac{1}{(2s_1+1)(2s_2+1)}\frac{q}{k}\frac{1}{64\pi^2 s}\sum_i |\phi_i|^2,$$

where the summation is over all helicity amplitudes, and

$$\frac{d\sigma}{dt} = \frac{\pi}{kq}\frac{d\sigma}{d\Omega}.$$

For calculations carried out in units of GeV, the differential cross section must be multiplied by the conversion factor .389336 to obtain $d\sigma/dt$ in units of $mb/(GeV/c)^2$.

APPENDIX B

DENSITY MATRIX AND POLARIZATION

In a 2-body scattering reaction where either of the final particles is a resonance, information concerning the production process may be obtained from the spin density matrix elements of the resonance.

Taking particle 3 to be the resonance, in the c.m. frame the density matrix elements are given by

$$\rho_{\lambda_3'\lambda_3} = \frac{\sum_{\lambda_1\lambda_2\lambda_4} \langle\lambda_3'\lambda_4|\phi'|\lambda_1\lambda_2\rangle\langle\lambda_3\lambda_4|\phi'|\lambda_1\lambda_2\rangle^*}{\sum_i |\phi_i'|^2} .$$

Experimental results are usually quoted in the Jackson frame i.e. the rest frame of the decaying resonance, particle 3, in which the z axis is taken parallel to the momentum of the incident particle, particle 1, in this frame, and the y axis is perpendicular to the production plane. The reason for this choice is that in a peripheral-type model the change of momentum and angular momentum is carried by an exchanged particle. In the rest frame of particle 3, particle 1 and the exchanged particle approach each other with equal and opposite momenta and hence with no relative orbital angular momentum. The population of spin states of particle 3 is therefore directly related in this frame to the spin of the exchanged particle. With respect to this new reference frame, the density matrix elements are given by

$$\rho_{m'm} = \sum_{\lambda_3\lambda_3'} d^{s_3}_{m'\lambda_3'}(\psi_3)\, d^{s_3}_{m\lambda_3}(\psi_3)\, \rho_{\lambda_3'\lambda_3},$$

where s_3 is the spin of particle 3, ψ_3 is the angle between the

directions of particles 1 and 4 as seen in the rest frame of particle 3, and, with the coordinate system and notation defined in Appendix A,

$$\tan \psi_3 = \frac{m_3 \sqrt{1 - \cos^2 \theta}}{E_3(\cos \theta - \frac{qE_1}{kE_3})} .$$

Similar expressions hold when particle 4 is the resonance, with

$$\tan \psi_4 = - \frac{m_4 \sqrt{1 - \cos^2 \theta}}{E_4(\cos \theta - \frac{qE_2}{kE_4})} .$$

Explicit expressions for the rotation functions are given in Appendix C.

Not all the elements of the density matrix are independent, since the matrix is Hermitian and has unit trace i.e.

$$\rho_{m'm} = \rho_{mm'}^{*}$$

$$\sum_m \rho_{mm} = 1,$$

and parity is conserved in the production process, which, from the symmetry properties of the rotation functions, implies

$$\rho_{m'm} = (-1)^{m'-m} \rho_{-m',-m} .$$

Imposing these constraints gives for the spin-1 density matrix

$$\rho_{m'm} = \begin{pmatrix} \frac{1}{2}(1-\rho_{00}) & \rho_{10} & \rho_{1,-1} \\ \rho_{10}^{*} & \rho_{00} & -\rho_{10}^{*} \\ \rho_{1,-1} & -\rho_{10} & \frac{1}{2}(1-\rho_{00}) \end{pmatrix}$$

with real ρ_{00} and $\rho_{1,-1}$, and for the spin-3/2 density matrix

$$\rho_{m'm} = \begin{pmatrix} \rho_{33} & \rho_{31} & \rho_{3,-1} & \rho_{3,-3} \\ \rho_{31}^{*} & \frac{1}{2}-\rho_{33} & \rho_{1,-1} & \rho_{3,-1}^{*} \\ \rho_{3,-1}^{*} & -\rho_{1,-1} & \frac{1}{2}-\rho_{33} & -\rho_{31}^{*} \\ -\rho_{3,-3} & \rho_{3,-1} & -\rho_{31} & \rho_{33} \end{pmatrix}$$

with real ρ_{33} and imaginary $\rho_{3,-3}$ and $\rho_{1,-1}$.

The polarization of the nucleons produced in the $0^{-}\frac{1}{2}^{+} \to 0^{-}\frac{1}{2}^{+}$ processes is given by

$$P(t) = \frac{2\ \mathrm{Im}(\phi'_{++}\phi'^{*}_{-+})}{|\phi'_{++}|^2 + |\phi'_{-+}|^2} \quad ,$$

where ϕ'_{++} and ϕ'_{-+} are the helicity nonflip and helicity flip amplitudes, respectively.

APPENDIX C

ROTATION FUNCTIONS

The functions $d_{\lambda\mu}^{j}(x)$, where $x = \cos\theta$, are evaluated by first writing these functions in terms of Jacobi polynomials,

$$d_{\lambda\mu}^{j}(x) = \left[\frac{(j+\lambda)!(j-\lambda)!}{(j+\mu)!(j-\mu)!}\right]^{\frac{1}{2}}(\cos\tfrac{1}{2}\theta)^{\lambda+\mu}\ (-\sin\tfrac{1}{2}\theta)^{\lambda-\mu}\ P_{j-\lambda}^{\lambda-\mu,\lambda+\mu}(\cos\theta),$$

where $\lambda-\mu$ and $\lambda+\mu \geq 0$. The Jacobi polynomials obey the two recurrence relations

$$\tfrac{1}{2}(2+\alpha+\beta+2n)(x+1)P_n^{\alpha,\beta+1}(x)$$

$$=(n+1)P_{n+1}^{\alpha,\beta}(x) + (1+\beta+n)P_n^{\alpha,\beta}(x)$$

and

$$\tfrac{1}{2}(2+\alpha+\beta+2n)(x-1)P_n^{\alpha+1,\beta}(x)$$

$$=(n+1)P_{n+1}^{\alpha,\beta}(x) - (1+\alpha+n)P_n^{\alpha,\beta}(x).$$

By application of these relations the Jacobi polynomials can be reduced to Legendre polynomials, since

$$P_n^{0,0}(x) = P_n(x).$$

The resulting expressions for the rotation functions therefore contain no derivatives of Legendre polynomials.

This procedure gives, for the functions required in the partial-wave expansions,

$$d_{1/2,\pm 1/2}^{\;\;j}(x) = \frac{1}{\left[2(1\pm x)\right]^{\frac{1}{2}}}\left[P_{\ell+1}(x) \pm P_{\ell}(x)\right]$$

$$d_{3/2,\pm 1/2}^{\;\;j}(x) = \frac{\left[\frac{1}{2}(\ell+2)\ell\right]^{\frac{1}{2}}}{(2\ell+3)(2\ell+1)} \frac{1}{(1\pm x)(1\mp x)^{\frac{1}{2}}}$$

$$\times \left[(2\ell+1)\{P_{\ell+2}(x) - P_{\ell}(x)\} \pm (2\ell+3)\{P_{\ell+1}(x) - P_{\ell-1}(x)\}\right]$$

$$d_{5/2,\pm 1/2}^{\;\;j}(x) = \frac{\left[\frac{1}{2}(\ell+3)(\ell+2)\ell(\ell-1)\right]^{\frac{1}{2}}}{(2\ell+5)(2\ell+3)(2\ell+1)(2\ell-1)} \frac{1}{(1\pm x)^{3/2}(1\mp x)}$$

$$\times \left[(2\ell-1)\{(2\ell+1)P_{\ell+3}(x) - 2(2\ell+3)P_{\ell+1}(x) + (2\ell+5)P_{\ell-1}(x)\}\right.$$

$$\left. \pm (2\ell+5)\{(2\ell-1)P_{\ell+2}(x) - 2(2\ell+1)P_{\ell}(x) + (2\ell+3)P_{\ell-2}(x)\}\right]$$

where $j = \ell+\frac{1}{2}$, and

$$d_{0,0}^{\;\;j}(x) = P_j(x)$$

$$d_{1,0}^{\;\;j}(x) = \frac{\left[j(j+1)\right]^{\frac{1}{2}}}{2j+1} \frac{1}{(1+x)^{\frac{1}{2}}(1-x)^{\frac{1}{2}}}\left[P_{j+1}(x) - P_{j-1}(x)\right]$$

$$d_{1,\pm 1}^{\;\;j}(x) = \frac{1}{2j+1}\frac{1}{1\pm x}\left[jP_{j+1}(x) \pm (2j+1)P_j(x) + (j+1)P_{j-1}(x)\right]$$

$$d_{2,0}^{\;\;j}(x) = \frac{\left[(j+2)(j+1)j(j-1)\right]^{\frac{1}{2}}}{(2j+3)(2j+1)(2j-1)} \frac{1}{(1+x)(1-x)}$$

$$\times \left[(2j-1)P_{j+2}(x) - 2(2j+1)P_j(x) + (2j+3)P_{j-2}(x)\right]$$

$$d_{2,\pm 1}^{\ j}(x) = \frac{\left[(j+2)(j-1)\right]^{\frac{1}{2}}}{(2j+3)(2j+1)(2j-1)} \frac{1}{(1\pm x)^{3/2}(1\mp x)^{1/2}}$$

$$\times\Big[\, j(2j-1)P_{j+2}(x) + 3(2j+1)P_{j}(x) - (j+1)(2j+3)P_{j-2}(x)$$

$$\pm (2j+3)(2j-1)\{P_{j+1}(x) - P_{j-1}(x)\}\,\Big]$$

$$d_{3,0}^{\ j}(x) = \frac{\left[(j+3)(j+2)(j+1)j(j-1)(j-2)\right]^{\frac{1}{2}}}{(2j+5)(2j+3)(2j+1)(2j-1)(2j-3)} \frac{1}{(1+x)^{3/2}(1-x)^{3/2}}$$

$$\times\Big[\, (2j-1)(2j-3)P_{j+3}(x) - 3(2j+3)(2j-3)P_{j+1}(x)$$

$$+ 3(2j+5)(2j-1)P_{j-1}(x) - (2j+5)(2j+3)P_{j-3}(x)\,\Big]$$

$$d_{3,\pm 1}^{\ j}(x) = \frac{\left[(j+3)(j+2)(j-1)(j-2)\right]^{\frac{1}{2}}}{(2j+5)(2j+3)(2j+1)(2j-1)(2j-3)} \frac{1}{(1\pm x)^{2}(1\mp x)}$$

$$\times\Big[\, j(2j-1)(2j-3)P_{j+3}(x) - (j-5)(2j+3)(2j-3)P_{j+1}(x)$$

$$- (j+6)(2j+5)(2j-1)P_{j-1}(x) + (j+1)(2j+5)(2j+3)P_{j-3}(x)$$

$$\pm (2j+5)(2j-3)\{(2j-1)P_{j+2}(x) - 2(2j+1)P_{j}(x)$$

$$+(2j+3)P_{j-2}(x)\}\Big].$$

The Legendre polynomials appearing in these expressions are evaluated using the recurrence relation

$$(n+1)P_{n+1}(x) = (2n+1)xP_{n}(x) - nP_{n-1}(x)$$

given that

$$P_0(x) = 1$$

$$P_1(x) = x.$$

For transforming the density matrices from the c.m. frame to the Jackson frame, the independent elements of the rotation matrices are, for spin 1

$$d_{11}(\cos\psi) = \tfrac{1}{2}(1+\cos\psi)$$

$$d_{01}(\cos\psi) = \frac{1}{\sqrt{2}}\sin\psi$$

$$d_{-11}(\cos\psi) = \tfrac{1}{2}(1-\cos\psi)$$

$$d_{00}(\cos\psi) = \cos\psi$$

and for spin 3/2

$$d_{33}(\cos\psi) = \tfrac{1}{2}(1+\cos\psi)\cos\tfrac{1}{2}\psi$$

$$d_{13}(\cos\psi) = \frac{\sqrt{3}}{2}(1+\cos\psi)\sin\tfrac{1}{2}\psi$$

$$d_{-13}(\cos\psi) = \frac{\sqrt{3}}{2}(1-\cos\psi)\cos\tfrac{1}{2}\psi$$

$$d_{-33}(\cos\psi) = \tfrac{1}{2}(1-\cos\psi)\sin\tfrac{1}{2}\psi$$

$$d_{11}(\cos\psi) = \tfrac{1}{2}(3\cos\psi-1)\cos\tfrac{1}{2}\psi$$

$$d_{-11}{}^{1}(\cos\psi) = \tfrac{1}{2}(3\cos\psi+1)\sin\tfrac{1}{2}\psi.$$

The other $d_{\lambda\mu}{}^{j}(x)$ may be obtained from the relations

$$d_{\lambda\mu}{}^{j}(x) = (-1)^{\lambda-\mu}d_{\mu\lambda}{}^{j}(x) = d_{-\mu,-\lambda}{}^{j}(x).$$

APPENDIX D

HELICITY AMPLITUDES

We employ the Pauli representation of the γ matrices i.e.

$$\gamma_0 = \begin{pmatrix} 1 & 0 \\ 0 & -1 \end{pmatrix} \otimes 1$$

$$\underline{\gamma} = \begin{pmatrix} 0 & 1 \\ -1 & 0 \end{pmatrix} \otimes \underline{\sigma}$$

$$\gamma_5 = \gamma_0\gamma_1\gamma_2\gamma_3 = \begin{pmatrix} 0 & -i \\ -i & 0 \end{pmatrix} \otimes 1$$

where

$$1 = \begin{pmatrix} 1 & 0 \\ 0 & 1 \end{pmatrix} \quad \sigma_1 = \begin{pmatrix} 0 & 1 \\ 1 & 0 \end{pmatrix} \quad \sigma_2 = \begin{pmatrix} 0 & -i \\ i & 0 \end{pmatrix} \quad \sigma_3 = \begin{pmatrix} 1 & 0 \\ 0 & -1 \end{pmatrix}.$$

The following wave functions are used for a particle travelling at an angle θ to the +z axis in the x-z plane with 4-momentum $p = (E,\underline{p})$, mass m and helicity λ.

1. Spin-1/2

$$u^{(\lambda)}(p) = \frac{1}{\sqrt{E+m}} \begin{pmatrix} E+m \\ 2\lambda|\underline{p}| \end{pmatrix} \otimes e^{-i\sigma_2 \frac{1}{2}\theta} \chi^{(\lambda)}$$

where

$$\chi^{(\lambda=+\frac{1}{2})} = \begin{pmatrix} 1 \\ 0 \end{pmatrix} \qquad \chi^{(\lambda=-\frac{1}{2})} = \begin{pmatrix} 0 \\ 1 \end{pmatrix}$$

2. Spin-1

$$\varepsilon_\mu^{(\lambda=+1)}(p) = \frac{1}{\sqrt{2}} \left(0 \; ; \; -\cos\theta \; , \; -i \; , \; \sin\theta \right)$$

$$\varepsilon_\mu^{(\lambda=0)}(p) = \left(\frac{|p|}{m} \; ; \; \frac{E}{m}\sin\theta \; , \; 0 \; , \; \frac{E}{m}\cos\theta \right)$$

$$\varepsilon_\mu^{(\lambda=-1)}(p) = \frac{1}{\sqrt{2}} \left(0 \; ; \; \cos\theta \; , \; -i \; , \; -\sin\theta \right)$$

3. Spin-3/2

$$\psi_\mu^{(\lambda=+3/2)}(p) = \left(0 \; ; \; -\frac{1}{\sqrt{2}}\cos\theta u_+ \; , \; -\frac{i}{\sqrt{2}}u_+ \; , \; \frac{1}{\sqrt{2}}\sin\theta u_+ \right)$$

$$\psi_\mu^{(\lambda=+1/2)}(p) = \left(\frac{\sqrt{2}}{\sqrt{3}}\frac{|p|}{m}u_+ \; ; \; \frac{\sqrt{2}}{\sqrt{3}}\frac{E}{m}\sin\theta u_+ - \frac{1}{\sqrt{6}}\cos\theta u_- \; , \right.$$

$$\left. -\frac{i}{\sqrt{6}}u_- \; , \; \frac{\sqrt{2}}{\sqrt{3}}\frac{E}{m}\cos\theta u_+ + \frac{1}{\sqrt{6}}\sin\theta u_- \right)$$

$$\psi_\mu^{(\lambda=-1/2)}(p) = \left(\frac{\sqrt{2}}{\sqrt{3}}\frac{|p|}{m}u_- \; ; \; \frac{1}{\sqrt{6}}\cos\theta u_+ + \frac{\sqrt{2}}{\sqrt{3}}\frac{E}{m}\sin\theta u_- \; , \right.$$

$$\left. -\frac{i}{\sqrt{6}}u_+ \; , \; -\frac{1}{\sqrt{6}}\sin\theta u_+ + \frac{\sqrt{2}}{\sqrt{3}}\frac{E}{m}\cos\theta u_- \right)$$

$$\psi_\mu^{(\lambda=-3/2)}(p) = \left(0 \; ; \; \frac{1}{\sqrt{2}}\cos\theta u_- \; , \; -\frac{i}{\sqrt{2}}u_- \; , \; -\frac{1}{\sqrt{2}}\sin\theta u_- \right)$$

where $u_+ = u^{(\lambda=+\frac{1}{2})}(p)$ and $u_- = u^{(\lambda=-\frac{1}{2})}(p)$.

To obtain the wave-functions for a particle travelling in the opposite direction we put $\theta \to \theta+\pi$ and insert the phase factor $(-1)^{s-\lambda}$, where s is the spin of the particle.

In addition to the notation already introduced, the following expressions are used

$$C_{\pm} = \frac{(E_4+m_4)(E_2+m_2) \pm kq}{\sqrt{(E_4+m_4)(E_2+m_2)}}$$

$$H_{\pm} = \frac{(E_4+m_4)k \pm (E_2+m_2)q}{\sqrt{(E_4+m_4)(E_2+m_2)}}$$

and

$$F_1 = \frac{1}{2m_B}\left[\left(1 + \frac{\mu}{2m}\right)g_{F+3S} - \left(1 + \frac{2m}{\mu}\right)g_{D+\frac{2}{3}F-S}\right]$$

$$F_2 = \left(1 - \frac{t}{4m_B^2}\right)\left(1 + \frac{2m}{\mu}\right)g_{D+\frac{2}{3}F-S}.$$

We also define

$$P_P = \alpha_P' \, \Gamma(-\alpha_P) \, \frac{1 + e^{-i\pi\alpha_P}}{2} \left(\frac{s + \frac{1}{2}t - \frac{1}{2}\Sigma}{s_o}\right)^{\alpha_P}$$

$$P_A = \alpha_A' \, \Gamma(-\alpha_A) \, \frac{1 - e^{-i\pi\alpha_A}}{2} \left(\frac{s + \frac{1}{2}t - \frac{1}{2}\Sigma}{s_o}\right)^{\alpha_A}$$

$$P_V = \alpha_V' \, \Gamma(1-\alpha_V) \, \frac{1 - e^{-i\pi\alpha_V}}{2} \left(\frac{s + \frac{1}{2}t - \frac{1}{2}\Sigma}{s_o}\right)^{\alpha_V - 1}$$

$$P_T = \alpha_T' \, \Gamma(1-\alpha_T) \, \frac{1 + e^{-i\pi\alpha_T}}{2} \left(\frac{s + \frac{1}{2}t - \frac{1}{2}\Sigma}{s_o}\right)^{\alpha_T - 1}$$

where the labels P,A,V and T refer to 0^-, 1^+, 1^- and 2^+ exchanges, respectively, and

$$\Sigma = \sum_{i=1}^{4} m_i^2 .$$

The g's and h's with subscripts which are combinations of D, F, S and G are the appropriate U(3) Clebsch-Gordan coefficients at the baryon and meson vertices, respectively. These are given in Tables 3 - 7.

The helicity amplitudes are related in pairs by parity according to the relation

$$\langle\lambda_3\lambda_4|\phi|\lambda_1\lambda_2\rangle = \frac{\eta_3\eta_4}{\eta_1\eta_2}\,(-1)^{s_3+s_4-s_1-s_2}\,(-1)^{\lambda-\mu}\,\langle-\lambda_3-\lambda_4|\phi|-\lambda_1-\lambda_2\rangle,$$

where the η_i are the intrinsic parities and $\lambda = \lambda_1-\lambda_2$, $\mu = \lambda_3-\lambda_4$. The helicity dependence of the amplitudes is shown in Tables 8 - 12. With this notation, the following expressions are obtained.

1. $0^- \; 1/2^+ \to 0^- \; 1/2^+$

Defining

$$A_1 = \frac{3}{2}gh\,\left(h_F P_V + h_D P_T \right)$$

and

$$E_{\pm} = (E_1+E_3)C_{\pm} + (k\pm q)H_{\pm}$$

we obtain

$$\phi_1 = A_1\left[F_1(2s+t-\Sigma)C_- + F_2E_+ \right]\cos\tfrac{1}{2}\theta$$

$$\phi_2 = A_1 \left[F_1(2s+t-\Sigma)C_+ + F_2 E_- \right] \sin\tfrac{1}{2}\theta \,.$$

2. $0^- \; 1/2^+ \to 0^- \; 3/2^+$

Defining

$$A_2 = -i \frac{3gh}{\sqrt{2}m_B^2} g_G \left(1 + \frac{2m}{\mu}\right) (E_1+E_2)\, qk \sin\theta \,(h_F P_V + h_D P_T)$$

we obtain

$$\phi_1 = A_2 \, C_- \cos\tfrac{1}{2}\theta$$

$$\phi_2 = \frac{1}{\sqrt{3}} A_2 \, C_+ \sin\tfrac{1}{2}\theta$$

$$\phi_3 = \frac{1}{\sqrt{3}} \phi_1$$

$$\phi_4 = \sqrt{3} \, \phi_2 \,.$$

3. $0^- \; 1/2^+ \to 1^- \; 1/2^+$

Defining

$$A_3 = i3gh \left(1 + \frac{2m}{\mu}\right)\left(1 - \frac{\mu^2}{4m_B^2}\right) g_{D+\frac{2}{3}F-S} \,(h_F P_P + h_{D+2S} P_A)$$

$$A_4 = \frac{i3gh}{2m_M} \,(h_{D+2S} P_V + h_F P_T)$$

we obtain

$$\phi_1 = A_3 \frac{1}{\sqrt{2}} k \sin\theta \, H_- \cos\tfrac{1}{2}\theta$$

$$+ \sqrt{2} A_4 \left[2F_1(E_1+E_2) C_- qk \sin\theta \cos\tfrac{1}{2}\theta \right.$$

$$\left. + F_2 \left(C_+ qk \sin\theta \cos\tfrac{1}{2}\theta + H_+ \{2E_1 q + E_3 k(1-\cos\theta)\} \sin\tfrac{1}{2}\theta \right) \right]$$

$$\phi_2 = - A_3 \frac{E_1 q - E_3 k \cos\theta}{m_3} H_- \cos\tfrac{1}{2}\theta$$

$$+ 2 A_4 F_2 H_+ m_3 k \sin\theta \sin\tfrac{1}{2}\theta$$

$$\phi_3 = - A_3 \frac{1}{\sqrt{2}} k \sin\theta \, H_- \cos\tfrac{1}{2}\theta$$

$$+ \sqrt{2} A_4 \left[2F_1(E_1+E_2) C_- qk \sin\theta \cos\tfrac{1}{2}\theta \right.$$

$$\left. + F_2 \left(C_+ qk \sin\theta \cos\tfrac{1}{2}\theta + H_+ E_3 k(1+\cos\theta) \sin\tfrac{1}{2}\theta \right) \right]$$

$$\phi_4 = A_3 \frac{1}{\sqrt{2}} k \sin\theta \, H_+ \sin\tfrac{1}{2}\theta$$

$$+ \sqrt{2} A_4 \left[2F_1(E_1+E_2) C_+ qk \sin\theta \sin\tfrac{1}{2}\theta \right.$$

$$\left. + F_2 \left(C_- qk \sin\theta \sin\tfrac{1}{2}\theta - H_- E_3 k(1-\cos\theta) \cos\tfrac{1}{2}\theta \right) \right]$$

$$\phi_5 = - A_3 \frac{E_1 q - E_3 k \cos\theta}{m_3} H_+ \sin\tfrac{1}{2}\theta$$

$$- 2 A_4 F_2 H_- m_3 k \sin\theta \cos\tfrac{1}{2}\theta$$

$$\phi_6 = - A_3 \frac{1}{\sqrt{2}} k \sin\theta H_+ \sin\tfrac{1}{2}\theta$$

$$+ \sqrt{2} A_4 \left[2F_1(E_1+E_2) C_+ qk \sin\theta \sin\tfrac{1}{2}\theta \right.$$

$$\left. + F_2 \left(C_- qk \sin\theta \sin\tfrac{1}{2}\theta + H_-\{2E_1 q - E_3 k(1+\cos\theta)\}\cos\tfrac{1}{2}\theta \right) \right] .$$

Since in the baryon-baryon scattering reactions explicitly considered here it is not possible in principle to distinguish from which vertex a particular final-state baryon emerges, the total amplitudes are obtained by antisymmetrizing the following amplitudes.

4. $1/2^+ \; 1/2^+ \rightarrow \; 3/2^+ \; 1/2^+$

Defining

$$A_5 = - ig^2 \, g'_G \, g_{D+\frac{2}{3}F} \frac{1}{m'_B} \left(1 + \frac{2m}{\mu}\right)^2 \left(1 - \frac{\mu^2}{4m_B^2}\right) P_P$$

$$A_6 = - ig^2 \, g'_G \frac{1}{2m'^2_B} \left(1 + \frac{2m}{\mu}\right)(P_V + P_T)$$

and

$$C'_{\pm} = \frac{(E_3+m_3)(E_1+m_1) \pm kq}{\sqrt{(E_3+m_3)(E_1+m_1)}}$$

$$B_1 = \frac{E_1 q - E_3 k \cos\theta}{m_3} C'_+ \sin\tfrac{1}{2}\theta - \tfrac{1}{2} k \sin\theta \, C'_- \cos\tfrac{1}{2}\theta$$

$$B_2 = \frac{E_1 q - E_3 k \cos\theta}{m_3} C'_- \cos\tfrac{1}{2}\theta + \tfrac{1}{2} k \sin\theta \, C'_+ \sin\tfrac{1}{2}\theta$$

$$B_3 = qk \sin\theta\, C_+ \cos\tfrac{1}{2}\theta + E_3 k(1+\cos\theta)\, H_+ \sin\tfrac{1}{2}\theta$$

$$B_4 = qk \sin\theta\, C_- \sin\tfrac{1}{2}\theta - E_3 k(1-\cos\theta)\, H_- \cos\tfrac{1}{2}\theta$$

$$B_5 = qk \sin\theta\, C_+ \cos\tfrac{1}{2}\theta + \{2E_1 q + E_3 k(1-\cos\theta)\}\, H_+ \sin\tfrac{1}{2}\theta$$

$$B_6 = qk \sin\theta\, C_- \cos\tfrac{1}{2}\theta + \{2E_1 q - E_3 k(1+\cos\theta)\}\, H_- \cos\tfrac{1}{2}\theta$$

we obtain

$$\phi_1 = \frac{1}{\sqrt{2}} A_5\, k \sin\theta\, C'_-\, H_- \cos^2\tfrac{1}{2}\theta$$

$$+ \sqrt{2}\, A_6 \Big[F_1 2(E_1+E_2)\, qk \sin\theta\, C'_-\, C_- \cos^2\tfrac{1}{2}\theta$$

$$+ F_2\, C'_-\, B_5 \cos\tfrac{1}{2}\theta \Big]$$

$$\phi_2 = -\frac{\sqrt{2}}{\sqrt{3}} A_5\, B_2\, H_- \cos\tfrac{1}{2}\theta$$

$$-\frac{\sqrt{2}}{\sqrt{3}} A_6 \Big[F_1 2(E_1+E_2)\, qk \sin\theta\, C'_+\, C_- \sin\tfrac{1}{2}\theta \cos\tfrac{1}{2}\theta$$

$$+ F_2 \Big(C'_+\, B_5 \sin\tfrac{1}{2}\theta - 2m_3 k \sin\theta\, C'_-\, H_+ \sin\tfrac{1}{2}\theta \cos\tfrac{1}{2}\theta \Big) \Big]$$

$$\phi_3 = \frac{\sqrt{2}}{\sqrt{3}} A_5\, B_1\, H_- \cos\tfrac{1}{2}\theta$$

$$+ \frac{\sqrt{2}}{\sqrt{3}} A_6 \Big[F_1 2(E_1+E_2)\, qk \sin\theta\, C'_-\, C_- \cos^2\tfrac{1}{2}\theta$$

$$+ F_2 \Big(C'_-\, B_3 \cos\tfrac{1}{2}\theta - 2m_3 k \sin\theta\, C'_+\, H_+ \sin^2\tfrac{1}{2}\theta \Big) \Big]$$

$$\phi_4 = \frac{1}{\sqrt{2}} A_5 \, k \sin\theta \, C'_+ \, H_- \sin\tfrac{1}{2}\theta \cos\tfrac{1}{2}\theta$$

$$- \sqrt{2} \, A_6 \left[F_1 2(E_1+E_2) \, qk \sin\theta \, C'_+ \, C_- \sin\tfrac{1}{2}\theta \cos\tfrac{1}{2}\theta \right.$$

$$\left. + F_2 \, C'_+ \, B_3 \sin\tfrac{1}{2}\theta \right]$$

$$\phi_5 = \frac{1}{\sqrt{2}} A_5 \, k \sin\theta \, C'_- \, H_+ \sin\tfrac{1}{2}\theta \cos\tfrac{1}{2}\theta$$

$$+ \sqrt{2} \, A_6 \left[F_1 2(E_1+E_2) \, qk \sin\theta \, C'_- \, C_+ \sin\tfrac{1}{2}\theta \cos\tfrac{1}{2}\theta \right.$$

$$\left. + F_2 \, C'_- \, B_4 \cos\tfrac{1}{2}\theta \right]$$

$$\phi_6 = - \frac{\sqrt{2}}{\sqrt{3}} A_5 \, B_2 \, H_+ \sin\tfrac{1}{2}\theta$$

$$- \frac{\sqrt{2}}{\sqrt{3}} A_6 \left[F_1 2(E_1+E_2) \, qk \sin\theta \, C'_+ \, C_+ \sin^2\tfrac{1}{2}\theta \right.$$

$$\left. + F_2 \left(C'_+ \, B_4 \sin\tfrac{1}{2}\theta + 2m_3 k \sin\theta \, C'_- \, H_- \cos^2\tfrac{1}{2}\theta \right) \right]$$

$$\phi_7 = \frac{\sqrt{2}}{\sqrt{3}} A_5 \, B_1 \, H_+ \sin\tfrac{1}{2}\theta$$

$$+ \frac{\sqrt{2}}{\sqrt{3}} A_6 \left[F_1 2(E_1+E_2) \, qk \sin\theta \, C'_- \, C_+ \sin\tfrac{1}{2}\theta \cos\tfrac{1}{2}\theta \right.$$

$$\left. + F_2 \left(C'_- \, B_6 \cos\tfrac{1}{2}\theta + 2m_3 k \sin\theta \, C'_+ \, H_- \sin\tfrac{1}{2}\theta \cos\tfrac{1}{2}\theta \right) \right]$$

$$\phi_8 = \frac{1}{\sqrt{2}} A_5 \, k \sin\theta \, C'_+ \, H_+ \sin^2\tfrac{1}{2}\theta$$

$$- \sqrt{2} \, A_6 \left[F_1 2(E_1+E_2) \, qk \sin\theta \, C'_+ \, C_+ \sin^2\tfrac{1}{2}\theta \right.$$

$$\left. + F_2 \, C'_+ \, B_6 \sin\tfrac{1}{2}\theta \right]$$

$$\phi_9 = \frac{1}{\sqrt{2}} A_5 \, k \sin\theta \, C'_+ \, H_- \sin\tfrac{1}{2}\theta \cos\tfrac{1}{2}\theta$$

$$+ \sqrt{2} \, A_6 \left[F_1 2(E_1+E_2) \, qk \sin\theta \, C'_+ \, C_- \sin\tfrac{1}{2}\theta \cos\tfrac{1}{2}\theta \right.$$

$$\left. + F_2 \, \dot{C}'_+ \, B_5 \sin\tfrac{1}{2}\theta \right]$$

$$\phi_{10} = - \frac{\sqrt{2}}{\sqrt{3}} A_5 \, B_1 \, H_- \cos\tfrac{1}{2}\theta$$

$$+ \frac{\sqrt{2}}{\sqrt{3}} A_6 \left[F_1 2(E_1+E_2) \, qk \sin\theta \, C'_- \, C_- \cos^2\tfrac{1}{2}\theta \right.$$

$$\left. + F_2 \left(C'_- \, B_5 \cos\tfrac{1}{2}\theta + 2m_3 k \sin\theta \, C'_+ \, H_+ \sin^2\tfrac{1}{2}\theta \right) \right]$$

$$\phi_{11} = - \frac{\sqrt{2}}{\sqrt{3}} A_5 \, B_2 \, H_- \cos\tfrac{1}{2}\theta$$

$$+ \frac{\sqrt{2}}{\sqrt{3}} A_6 \left[F_1 2(E_1+E_2) \, qk \sin\theta \, C'_+ \, C_- \sin\tfrac{1}{2}\theta \cos\tfrac{1}{2}\theta \right.$$

$$\left. + F_2 \left(C'_+ \, B_3 \sin\tfrac{1}{2}\theta + 2m_3 k \sin\theta \, C'_- \, H_+ \sin\tfrac{1}{2}\theta \cos\tfrac{1}{2}\theta \right) \right]$$

$$\phi_{12} = - \frac{1}{\sqrt{2}} A_5 \, k \sin\theta \, C'_- \, H_- \cos^2\tfrac{1}{2}\theta$$

$$+ \sqrt{2} \, A_6 \left[F_1 2(E_1+E_2) \, qk \sin\theta \, C'_- \, C_- \cos^2\tfrac{1}{2}\theta + F_2 \, C'_- \, B_3 \cos\tfrac{1}{2}\theta \right]$$

$$\phi_{13} = \frac{1}{\sqrt{2}} A_5 \, k \sin\theta \, C'_+ \, H_+ \sin^2\tfrac{1}{2}\theta$$

$$+ \sqrt{2} \, A_6 \left[F_1 2(E_1+E_2) \, qk \sin\theta \, C'_+ \, C_+ \sin^2\tfrac{1}{2}\theta + F_2 \, C'_+ \, B_4 \sin\tfrac{1}{2}\theta \right]$$

$$\phi_{14} = -\frac{\sqrt{2}}{\sqrt{3}} A_5 B_1 H_+ \sin\tfrac{1}{2}\theta$$

$$+ \frac{\sqrt{2}}{\sqrt{3}} A_6 \left[F_1 2(E_1+E_2)\, qk \sin\theta\, C'_- C_+ \sin\tfrac{1}{2}\theta \cos\tfrac{1}{2}\theta \right.$$

$$\left. + F_2 \left(C'_- B_4 \cos\tfrac{1}{2}\theta - 2m_3 k \sin\theta\, C'_+ H_- \sin\tfrac{1}{2}\theta \cos\tfrac{1}{2}\theta \right) \right]$$

$$\phi_{15} = -\frac{\sqrt{2}}{\sqrt{3}} A_5 B_2 H_+ \sin\tfrac{1}{2}\theta$$

$$+ \frac{\sqrt{2}}{\sqrt{3}} A_6 \left[F_1 2(E_1+E_2)\, qk \sin\theta\, C'_+ C_+ \sin^2\tfrac{1}{2}\theta \right.$$

$$\left. + F_2 \left(C'_+ B_6 \sin\tfrac{1}{2}\theta - 2m_3 k\, C'_- H_- \cos^2\tfrac{1}{2}\theta \right) \right]$$

$$\phi_{16} = -\frac{1}{\sqrt{2}} A_5 k \sin\theta\, C'_- H_+ \sin\tfrac{1}{2}\theta \cos\tfrac{1}{2}\theta$$

$$+ \sqrt{2}\, A_6 \left[F_1 2(E_1+E_2)\, qk \sin\theta\, C'_- C_+ \sin\tfrac{1}{2}\theta \cos\tfrac{1}{2}\theta \right.$$

$$\left. + F_2\, C'_- B_6 \cos\tfrac{1}{2}\theta \right].$$

5. $1/2^+\ 1/2^+ \rightarrow 3/2^+\ 3/2^+$

Defining

$$A_7 = -g^2\, g'_G\, g_G \frac{1}{m_B^2} \left(1 + \frac{2m}{\mu}\right)^2 P_P$$

$$A_8 = g^2\, g'_G\, g_G \frac{1}{4m_B^4} \left(1 + \frac{2m}{\mu}\right)^2 (P_V + P_T)$$

and

$$D_1 = \frac{E_1 q - E_3 k \cos\theta}{m_3} C_+ \sin\tfrac{1}{2}\theta - \tfrac{1}{2} k \sin\theta \, C_- \cos\tfrac{1}{2}\theta$$

$$D_2 = \frac{E_1 q - E_3 k \cos\theta}{m_3} C_- \cos\tfrac{1}{2}\theta + \tfrac{1}{2} k \sin\theta \, C_+ \sin\tfrac{1}{2}\theta$$

$$D_3 = \frac{(E_1+2E_3) q + E_3 k \cos\theta}{m_3} C_+ \sin\tfrac{1}{2}\theta + \tfrac{1}{2} C_- \cos\tfrac{1}{2}\theta$$

$$D_4 = \frac{(E_1+2E_3) q + E_3 k \cos\theta}{m_3} C_- \cos\tfrac{1}{2}\theta - \tfrac{1}{2} C_+ \sin\tfrac{1}{2}\theta$$

and assuming $m_1 = m_2$ and $m_3 = m_4$ we obtain

$$\phi_1 = \tfrac{1}{2} A_7 k^2 \sin^2\theta \, C_-^2 \cos^2\tfrac{1}{2}\theta$$

$$+ A_8 \left[(s-2m_3^2) k^2 \sin^2\theta + \{(2s+t-\Sigma)t + (m_1^2-m_3^2)^2\} \right] C_-^2 \cos^2\tfrac{1}{2}\theta$$

$$\phi_2 = -\frac{1}{\sqrt{3}} A_7 D_2 \, k \sin\theta \, C_- \cos\tfrac{1}{2}\theta$$

$$-\frac{1}{\sqrt{3}} A_8 \left[\{(2s+t-\Sigma)D_2 + tD_4 + (m_1^2-m_3^2)(D_2-D_4)\} \, k \sin\theta \right.$$

$$\left. + \{(2s+t-\Sigma)t + (m_1^2-m_3^2)^2\} \, C_+ \sin\tfrac{1}{2}\theta \right] C_- \cos\tfrac{1}{2}\theta$$

$$\phi_3 = \frac{1}{\sqrt{3}} A_7 D_1 \, k \sin\theta \, C_- \cos\tfrac{1}{2}\theta$$

$$+ \frac{1}{\sqrt{3}} A_8 \left[(2s+t-\Sigma)D_1 + tD_3 + (m_1^2-m_3^2)(D_1-D_3) \right]$$

$$\times k \sin\theta \, C_- \cos\tfrac{1}{2}\theta$$

$$\phi_4 = \tfrac{1}{2} A_7 k^2 \sin^2\theta C_+C_- \sin\tfrac{1}{2}\theta \cos\tfrac{1}{2}\theta$$

$$+ A_8 (s-2m_3^2) k^2 \sin^2\theta C_+ C_- \sin\tfrac{1}{2}\theta \cos\tfrac{1}{2}\theta$$

$$\phi_5 = \frac{1}{\sqrt{3}} A_7 D_2 k \sin\theta C_- \cos\tfrac{1}{2}\theta$$

$$+ \frac{1}{\sqrt{3}} A_8 \Big[\{(2s+t-\Sigma)D_2 + tD_4 + (m_1^2-m_3^2)(D_2-D_4)\} k \sin\theta$$

$$+ \{(2s+t-\Sigma)t + (m_1^2-m_3^2)^2\} C_+ \sin\tfrac{1}{2}\theta \Big] C_- \cos\tfrac{1}{2}\theta$$

$$\phi_6 = -\frac{2}{3} A_7 D_2^2$$

$$- \frac{2}{3} A_8 \Big[(2s+t-\Sigma)D_2^2 - tD_4^2 - 2(m_1^2-m_3^2)D_2D_4$$

$$+ \{(2s+t-\Sigma)t + (m_1^2-m_3^2)^2\}\Big(\frac{E_3^2+q^2}{m_3^2} C_-^2 \cos^2\tfrac{1}{2}\theta + \tfrac{1}{2} C_+^2 \sin^2\tfrac{1}{2}\theta\Big)\Big]$$

$$\phi_7 = \frac{2}{3} A_7 D_1 D_2$$

$$+ \frac{2}{3} A_8 \Big[(2s+t-\Sigma)D_1D_2 - tD_3D_4 - (m_1^2-m_3^2)(D_1D_4+D_2D_3)$$

$$+ \{(2s+t-\Sigma)t + (m_1^2-m_3^2)^2\} \frac{E_3^2+q^2}{m_3^2} C_+ C_- \sin\tfrac{1}{2}\theta \cos\tfrac{1}{2}\theta \Big]$$

$$\phi_8 = \frac{1}{\sqrt{3}} A_7 D_2 k \sin\theta C_+ \sin\tfrac{1}{2}\theta$$

$$+ \frac{1}{\sqrt{3}} A_8 \Big[(2s+t-\Sigma)D_2 + tD_4 + (m_1^2-m_3^2)(D_2-D_4) \Big]$$

$$\times k \sin\theta C_+ \sin\tfrac{1}{2}\theta$$

$$\phi_9 = \frac{1}{\sqrt{3}} A_7 D_1 k \sin\theta C_- \cos\tfrac{1}{2}\theta$$

$$+ \frac{1}{\sqrt{3}} A_8 \left[(2s+t-\Sigma)D_1 + tD_3 + (m_1^2-m_3^2)(D_1-D_3) \right]$$

$$\times k \sin\theta C_- \cos\tfrac{1}{2}\theta$$

$$\phi_{10} = -\frac{2}{3} A_7 D_1 D_2$$

$$-\frac{2}{3} A_8 \left[(2s+t-\Sigma)D_1D_2 - tD_3D_4 - (m_1^2-m_3^2)(D_1D_4+D_2D_3) \right.$$

$$\left. + \{(2s+t-\Sigma)t + (m_1^2-m_3^2)^2\} \frac{E_3^2+q^2}{m_3^2} C_+ C_- \sin\tfrac{1}{2}\theta \cos\tfrac{1}{2}\theta \right]$$

$$\phi_{11} = \frac{2}{3} A_7 D_1^2$$

$$+ \frac{2}{3} A_8 \left[(2s+t-\Sigma)D_1^2 - tD_3^2 - 2(m_1^2-m_3^2)D_1D_3 \right.$$

$$\left. + \{(2s+t-\Sigma)t + (m_1^2-m_3^2)^2\} \left(\frac{E_3^2+q^2}{m_3^2} C_+^2 \sin^2\tfrac{1}{2}\theta + \tfrac{1}{2} C_-^2 \cos^2\tfrac{1}{2}\theta \right) \right]$$

$$\phi_{12} = \frac{1}{\sqrt{3}} A_7 D_1 k \sin\theta C_+ \sin\tfrac{1}{2}\theta$$

$$+ \frac{1}{\sqrt{3}} A_8 \left[\{(2s+t-\Sigma)D_1 + tD_3 + (m_1^2-m_3^2)(D_1-D_3)\} k \sin\theta \right.$$

$$\left. - \{(2s+t-\Sigma)t + (m_1^2-m_3^2)^2\} C_- \cos\tfrac{1}{2}\theta \right] C_+ \sin\tfrac{1}{2}\theta$$

$$\phi_{13} = -\tfrac{1}{2} A_7 k^2 \sin^2\theta C_+ C_- \sin\tfrac{1}{2}\theta \cos\tfrac{1}{2}\theta$$

$$- A_8 (s-2m_3^2) k^2 \sin^2\theta C_+ C_- \sin\tfrac{1}{2}\theta \cos\tfrac{1}{2}\theta$$

$$\phi_{14} = \frac{1}{\sqrt{3}} A_7 D_2 k \sin\theta C_+ \sin\tfrac{1}{2}\theta$$

$$+ \frac{1}{\sqrt{3}} A_8 \left[(2s+t-\Sigma)D_2 + tD_4 + (m_1^2-m_3^2)(D_2-D_4) \right]$$

$$\times k \sin\theta C_+ \sin\tfrac{1}{2}\theta$$

$$\phi_{15} = -\frac{1}{\sqrt{3}} A_7 D_1 k \sin\theta C_+ \sin\tfrac{1}{2}\theta$$

$$- \frac{1}{\sqrt{3}} A_8 \left[\{(2s+t-\Sigma)D_1 + tD_3 + (m_1^2-m_3^2)(D_1-D_3)\} k \sin\theta \right.$$

$$\left. - \{(2s+t-\Sigma)t + (m_1^2-m_3^2)^2\} C_- \cos\tfrac{1}{2}\theta \right] C_+ \sin\tfrac{1}{2}\theta$$

$$\phi_{16} = -\tfrac{1}{2} A_7 k^2 \sin^2\theta C_+^2 \sin^2\tfrac{1}{2}\theta$$

$$- A_8 \left[(s-2m_3^2) k^2 \sin^2\theta + \{(2s+t-\Sigma)t + (m_1^2-m_3^2)^2\} \right] C_+^2 \sin^2\tfrac{1}{2}\theta$$

$$\phi_{17} = \tfrac{1}{2} A_7 k^2 \sin^2\theta C_+ C_- \sin\tfrac{1}{2}\theta \cos\tfrac{1}{2}\theta$$

$$+ A_8 \left[(s-2m_3^2) k^2 \sin^2\theta + \{(2s+t-\Sigma)t + (m_1^2-m_3^2)^2\} \right]$$

$$\times C_+ C_- \sin\tfrac{1}{2}\theta \cos\tfrac{1}{2}\theta$$

$$\phi_{18} = -\frac{1}{\sqrt{3}} A_7 D_1 k \sin\theta C_- \cos\tfrac{1}{2}\theta$$

$$- \frac{1}{\sqrt{3}} A_8 \left[\{(2s+t-\Sigma)D_1 + tD_3 + (m_1^2-m_3^2)(D_1-D_3)\} k \sin\theta \right.$$

$$\left. - \{(2s+t-\Sigma)t + (m_1^2-m_3^2)^2\} C_- \cos\tfrac{1}{2}\theta \right] C_- \cos\tfrac{1}{2}\theta$$

$$\phi_{19} = -\frac{1}{\sqrt{3}} A_7 D_2 k \sin\theta C_- \cos\tfrac{1}{2}\theta$$

$$-\frac{1}{\sqrt{3}} A_8 \left[(2s+t-\Sigma)D_2 + tD_4 + (m_1^2-m_3^2)(D_2-D_4) \right]$$

$$\times k \sin\theta C_- \cos\tfrac{1}{2}\theta$$

$$\phi_{20} = -\tfrac{1}{2} A_7 k^2 \sin^2\theta C_-^2 \cos^2\tfrac{1}{2}\theta$$

$$- A_8 (s-2m_3^2) k^2 \sin^2\theta C_-^2 \cos^2\tfrac{1}{2}\theta$$

$$\phi_{21} = \frac{1}{\sqrt{3}} A_7 D_2 k \sin\theta C_+ \sin\tfrac{1}{2}\theta$$

$$+\frac{1}{\sqrt{3}} A_8 \left[\{(2s+t-\Sigma)D_2 + tD_4 + (m_1^2-m_3^2)(D_2-D_4)\} k \sin\theta \right.$$

$$\left. + \{(2s+t-\Sigma)t + (m_1^2-m_3^2)^2\} C_+ \sin\tfrac{1}{2}\theta \right] C_+ \sin\tfrac{1}{2}\theta$$

$$\phi_{22} = -\frac{2}{3} A_7 D_1 D_2$$

$$-\frac{2}{3} A_8 \left[(2s+t-\Sigma)D_1D_2 - t D_3D_4 - (m_1^2-m_3^2)(D_1D_4+D_2D_3) \right.$$

$$\left. + \{(2s+t-\Sigma)t + (m_1^2-m_3^2)^2\} \left(\frac{E_3^2+q^2}{m_3^2} - \frac{1}{2} \right) C_+ C_- \sin\tfrac{1}{2}\theta \cos\tfrac{1}{2}\theta \right]$$

$$\phi_{23} = -\frac{2}{3} A_7 D_2^2$$

$$-\frac{2}{3} A_8 \left[(2s+t-\Sigma)D_2^2 - tD_4^2 - 2(m_1^2-m_3^2)D_2D_4 \right.$$

$$\left. + \{(2s+t-\Sigma)t + (m_1^2-m_3^2)^2\} \frac{E_3^2+q^2}{m_3^2} C_-^2 \cos^2\tfrac{1}{2}\theta \right]$$

$$\phi_{24} = -\frac{1}{\sqrt{3}} A_7 D_2 \, k \sin\theta \, C_- \cos\tfrac{1}{2}\theta$$

$$-\frac{1}{\sqrt{3}} A_8 \left[(2s+t-\Sigma)D_2 + tD_4 + (m_1^2-m_3^2)(D_2-D_4) \right]$$

$$\times k \sin C_- \cos\tfrac{1}{2}\theta$$

$$\phi_{25} = \frac{1}{\sqrt{3}} A_7 D_1 \, k \sin\theta \, C_+ \sin\tfrac{1}{2}\theta$$

$$+\frac{1}{\sqrt{3}} A_8 \left[(2s+t-\Sigma)D_1 + tD_3 + (m_1^2-m_3^2)(D_1-D_3) \right]$$

$$\times k \sin\theta \, C_+ \sin\tfrac{1}{2}\theta$$

$$\phi_{26} = -\frac{2}{3} A_7 D_1^2$$

$$-\frac{2}{3} A_8 \left[(2s+t-\Sigma)D_1^2 - tD_3^2 - 2(m_1^2-m_3^2)D_1D_3 \right.$$

$$\left. + \{(2s+t-\Sigma)t + (m_1^2-m_3^2)^2\} \frac{E_3^2+q^2}{m_3^2} C_+^2 \sin^2\tfrac{1}{2}\theta \right]$$

$$\phi_{27} = -\frac{2}{3} A_7 D_1 D_2$$

$$-\frac{2}{3} A_8 \left[(2s+t-\Sigma)D_1D_2 - tD_3D_4 - (m_1^2-m_3^2)(D_1D_4+D_2D_3) \right.$$

$$\left. + \{(2s+t-\Sigma)t + (m_1^2-m_3^2)^2\} \left(\frac{E_3^2+q^2}{m_3^2} - \frac{1}{2} \right) C_+ C_- \sin\tfrac{1}{2}\theta \cos\tfrac{1}{2}\theta \right]$$

$$\phi_{28} = -\frac{1}{\sqrt{3}} A_7 D_1 k \sin\theta C_- \cos\tfrac{1}{2}\theta$$

$$-\frac{1}{\sqrt{3}} A_8 \Big[\{ (2s+t-\Sigma)D_1 + tD_3 + (m_1^2-m_3^2)(D_1-D_3) \} k \sin\theta$$

$$+ \{(2s+t-\Sigma)t + (m_1^2-m_3^2)^2\} C_- \cos\tfrac{1}{2}\theta \Big] C_- \cos\tfrac{1}{2}\theta$$

$$\phi_{29} = -\tfrac{1}{2} A_7 k^2 \sin^2\theta C_+^2 \sin^2\tfrac{1}{2}\theta$$

$$- A_8 (s-2m_3^2) k^2 \sin^2\theta C_+^2 \sin^2\tfrac{1}{2}\theta$$

$$\phi_{30} = \frac{1}{\sqrt{3}} A_7 D_1 k \sin\theta C_+ \sin\tfrac{1}{2}\theta$$

$$+ \frac{1}{\sqrt{3}} A_8 \Big[(2s+t-\Sigma)D_1 + tD_3 + (m_1^2-m_3^2)(D_1-D_3) \Big]$$

$$\times k \sin\theta C_+ \sin\tfrac{1}{2}\theta$$

$$\phi_{31} = \frac{1}{\sqrt{3}} A_7 D_2 k \sin\theta C_+ \sin\tfrac{1}{2}\theta$$

$$+ \frac{1}{\sqrt{3}} A_8 \Big[\{ (2s+t-\Sigma)D_2 + tD_4 + (m_1^2-m_3^2)(D_2-D_4) \} k \sin\theta$$

$$+ \{(2s+t-\Sigma)t + (m_1^2-m_3^2)^2\} C_+ \sin\tfrac{1}{2}\theta \Big] C_+ \sin\tfrac{1}{2}\theta$$

$$\phi_{32} = \tfrac{1}{2} A_7 k^2 \sin^2\theta C_+ C_- \sin\tfrac{1}{2}\theta \cos\tfrac{1}{2}\theta$$

$$+ A_8 \Big[(s-2m_3^2) k^2 \sin^2\theta + \{ (2s+t-\Sigma)t + (m_1^2-m_3^2)^2 \} \Big]$$

$$\times C_+ C_- \sin\tfrac{1}{2}\theta \cos\tfrac{1}{2}\theta.$$

Reaction	Exchange	Baryon Vertex		Meson Vertex	
		F	$D+\frac{2}{3}F$	D	F
$\pi^- p \to \pi^o n$	ρ	$\sqrt{2}$	$5\sqrt{2}/3$		2
$\pi^- p \to \eta n$	A_2	$\sqrt{2}$	$5\sqrt{2}/3$	$2/\sqrt{3}$	
$K^- p \to \bar{K}^o n$	ρ	$\sqrt{2}$	$5\sqrt{2}/3$		$-\sqrt{2}$
	A_2	$\sqrt{2}$	$5\sqrt{2}/3$	$\sqrt{2}$	
$K^+ n \to K^o p$	ρ	$\sqrt{2}$	$5\sqrt{2}/3$		$\sqrt{2}$
	A_2	$\sqrt{2}$	$5\sqrt{2}/3$	$\sqrt{2}$	

Table 3

Clebsch-Gordan coefficients for $0^- 1/2^+ \to 0^- 1/2^+$

Reaction	Exchange	Baryon Vertex	Meson Vertex	
		G	D	F
$\pi^+ p \to \pi^o \Delta^{++}$	ρ	$-\sqrt{2}$		-2
$\pi^+ p \to \eta \Delta^{++}$	A_2	$-\sqrt{2}$	$2/\sqrt{3}$	
$K^+ p \to K^o \, ^{++}$	ρ	$-\sqrt{2}$		$\sqrt{2}$
	A_2	$-\sqrt{2}$	$\sqrt{2}$	

Table 4

Clebsch-Gordan coefficients for $0^- 1/2^+ \to 0^- 3/2^+$

Reaction	Exchange	Baryon Vertex		Meson Vertex	
		F+3S	$D+\frac{2}{3}F-S$	D+2S	F
$\pi^+ p \to \rho^+ p$	π, A_2	1	5/3		2
	ω	3	-1/3	2	
$\pi^- p \to \rho^- p$	π, A_2	1	5/3		-2
	ω	3	-1/3	2	
$\pi^- p \to \rho^o n$	π, A_2	$\sqrt{2}$	$5\sqrt{2}/3$		2
$K^+ p \to K^{*+} p$	π, A_2	1	5/3		1
	η	$\sqrt{3}$	$1/\sqrt{3}$		$\sqrt{3}$
	ρ, B	1	5/3	1	
	ω	3	-1/3	1	
	ϕ	0	$-2\sqrt{2}/3$	$\sqrt{2}$	
$K^- p \to K^{*-} p$	π, A_2	1	5/3		-1
	η	$\sqrt{3}$	$1/\sqrt{3}$		$-\sqrt{3}$
	ρ, B	1	5/3	1	
	ω	3	-1/3	1	
	ϕ	0	$-2\sqrt{2}/3$	$\sqrt{2}$	
$K^- p \to \bar{K}^{*o} n$	π, A_2	$\sqrt{2}$	$5\sqrt{2}/3$		$-\sqrt{2}$
	ρ, B	$\sqrt{2}$	$5\sqrt{2}/3$	$\sqrt{2}$	
$\pi^+ n \to \omega p$	ρ, B	$\sqrt{2}$	$5\sqrt{2}/3$	2	

Table 5

Clebsch-Gordan coefficients for $0^- \; 1/2^+ \to 1^- \; 1/2^+$

Reaction	Exchange	F	$D+\frac{2}{3}F$	G'
$pp \to n\Delta^{++}$	π, ρ, A_2	$\sqrt{2}$	$5\sqrt{2}/3$	$-\sqrt{2}$
$pp \to p\Delta^{+}$	π, ρ, A_2	1	5/3	$2/\sqrt{3}$

Table 6

Clebsch-Gordan coefficients for $1/2^+\ 1/2^+ \to 3/2^+\ 1/2^+$

Reaction	Exchange	G	G'
$pp \to \Delta^{++}\Delta^{o}$	π, ρ, A_2	$\sqrt{2}/\sqrt{3}$	$-\sqrt{2}$

Table 7

Clebsch-Gordan coefficients for $1/2^+\ 1/2^+ \to 3/2^+\ 3/2^+$

$\lambda_3\ \lambda_4$ \ $\lambda_1\ \lambda_2$	$0\quad \frac{1}{2}$	$0\quad -\frac{1}{2}$
$0\quad \frac{1}{2}$	ϕ_1	$-\phi_2$
$0\quad -\frac{1}{2}$	ϕ_2	ϕ_1

Table 8

Helicity dependence of amplitudes for $0^-\ 1/2^+ \to 0^-\ 1/2^+$

$\lambda_3\ \lambda_4$ \ $\lambda_1\ \lambda_2$	$0\quad \frac{1}{2}$	$0\quad -\frac{1}{2}$
$0\quad {}^3/_2$	ϕ_1	$-\phi_4$
$0\quad {}^1/_2$	ϕ_2	ϕ_3
$0\quad -{}^1/_2$	ϕ_3	$-\phi_2$
$0\quad -{}^3/_2$	ϕ_4	ϕ_1

Table 9

Helicity dependence of amplitudes for $0^-\ 1/2^+ \to 0^-\ 3/2^+$

λ_3 λ_4 \ λ_1 λ_2	0 $\frac{1}{2}$	0 $-\frac{1}{2}$
1 $\frac{1}{2}$	ϕ_1	$-\phi_6$
0 $\frac{1}{2}$	ϕ_2	ϕ_5
-1 $\frac{1}{2}$	ϕ_3	$-\phi_4$
1 $-\frac{1}{2}$	ϕ_4	ϕ_3
0 $-\frac{1}{2}$	ϕ_5	$-\phi_2$
-1 $-\frac{1}{2}$	ϕ_6	ϕ_1

Table 10

Helicity dependence of amplitudes for $0^- \; 1/2^+ \to 1^- \; 1/2^+$

λ_3 λ_4 \ λ_1 λ_2	$\frac{1}{2}$ $\frac{1}{2}$	$-\frac{1}{2}$ $\frac{1}{2}$	$\frac{1}{2}$ $-\frac{1}{2}$	$-\frac{1}{2}$ $-\frac{1}{2}$
$^3/_2$ $^1/_2$	ϕ_1	ϕ_9	$-\phi_{16}$	ϕ_8
$^1/_2$ $^1/_2$	ϕ_2	ϕ_{10}	ϕ_{15}	$-\phi_7$
$-^1/_2$ $^1/_2$	ϕ_3	ϕ_{11}	$-\phi_{14}$	ϕ_6
$-^3/_2$ $^1/_2$	ϕ_4	ϕ_{12}	ϕ_{13}	$-\phi_5$
$^3/_2$ $-^1/_2$	ϕ_5	ϕ_{13}	ϕ_{12}	$-\phi_4$
$^1/_2$ $-^1/_2$	ϕ_6	ϕ_{14}	$-\phi_{11}$	ϕ_3
$-^1/_2$ $-^1/_2$	ϕ_7	ϕ_{15}	ϕ_{10}	$-\phi_2$
$-^3/_2$ $-^1/_2$	ϕ_8	ϕ_{16}	$-\phi_9$	ϕ_1

Table 11

Helicity dependence of amplitudes for $1/2^+ \; 1/2^+ \to 3/2^+ \; 1/2^+$

$\lambda_3\ \lambda_4$ \ $\lambda_1\ \lambda_2$	$\frac{1}{2}\ \ \frac{1}{2}$	$-\frac{1}{2}\ \ \frac{1}{2}$	$\frac{1}{2}\ \ -\frac{1}{2}$	$-\frac{1}{2}\ \ -\frac{1}{2}$
$^3/_2\ \ ^3/_2$	ϕ_1	ϕ_{17}	$-\phi_{32}$	ϕ_{16}
$^1/_2\ \ ^3/_2$	ϕ_2	ϕ_{18}	ϕ_{31}	$-\phi_{15}$
$^{-1}/_2\ \ ^3/_2$	ϕ_3	ϕ_{19}	$-\phi_{30}$	ϕ_{14}
$^{-3}/_2\ \ ^3/_2$	ϕ_4	ϕ_{20}	ϕ_{29}	$-\phi_{13}$
$^3/_2\ \ ^1/_2$	ϕ_5	ϕ_{21}	ϕ_{28}	$-\phi_{12}$
$^1/_2\ \ ^1/_2$	ϕ_6	ϕ_{22}	$-\phi_{27}$	ϕ_{11}
$^{-1}/_2\ \ ^1/_2$	ϕ_7	ϕ_{23}	ϕ_{26}	$-\phi_{10}$
$^{-3}/_2\ \ ^1/_2$	ϕ_8	ϕ_{24}	$-\phi_{25}$	ϕ_9
$^3/_2\ \ ^{-1}/_2$	ϕ_9	ϕ_{25}	$-\phi_{24}$	ϕ_8
$^1/_2\ \ ^{-1}/_2$	ϕ_{10}	ϕ_{26}	ϕ_{23}	$-\phi_7$
$^{-1}/_2\ \ ^{-1}/_2$	ϕ_{11}	ϕ_{27}	$-\phi_{22}$	ϕ_6
$^{-3}/_2\ \ ^{-1}/_2$	ϕ_{12}	ϕ_{28}	ϕ_{21}	$-\phi_5$
$^3/_2\ \ ^{-3}/_2$	ϕ_{13}	ϕ_{29}	ϕ_{20}	$-\phi_4$
$^1/_2\ \ ^{-3}/_2$	ϕ_{14}	ϕ_{30}	$-\phi_{19}$	ϕ_3
$^{-1}/_2\ \ ^{-3}/_2$	ϕ_{15}	ϕ_{31}	ϕ_{18}	$-\phi_2$
$^{-3}/_2\ \ ^{-3}/_2$	ϕ_{16}	ϕ_{32}	$-\phi_{17}$	ϕ_1

Table 12

Helicity dependence of amplitudes for $1/2^+\ 1/2^+ \to 3/2^+\ 3/2^+$

APPENDIX E

NUMERICAL PROCEDURE

Owing to the impossibility of performing the required partial-wave expansions analytically, this work was performed numerically using a computer. Some of the work carried out by the collaboration involved models containing free parameters to be determined by fitting experimental data. The computer program was therefore written in such a manner as to allow it, if desired, to be used in conjunction with the minimization program MINUITS (CERN Program Library No. D506). In view of the general paucity of data on polarizations and spin density matrix elements, and the weak constraints imposed by such data on a fit, this facility for data-fitting was confined to differential cross sections. The procedure, when obtaining parameters, was to allow MINUITS to vary these parameters in order to reduce to a minimum the quantity χ^2 defined by

$$\chi^2 = \sum_{\substack{\text{All data} \\ \text{points}}} \left[\frac{\left(\frac{d\sigma}{dt}\right)_{\text{experiment}} - \left(\frac{d\sigma}{dt}\right)_{\text{theory}}}{\text{standard deviation of } \left(\frac{d\sigma}{dt}\right)_{\text{experiment}}} \right]^2 .$$

For a particular point a $\chi^2<1$ represents a theoretical value within the statistical error. Overall normalization errors are not taken into account in this formula.

Now, the partial-wave expansion is

$$\langle\lambda_3\lambda_4|\phi(s,t)|\lambda_1\lambda_2\rangle = \sum_{j=j_{min}}^{\infty} (2j+1)\ \langle\lambda_3\lambda_4|T^j(s)|\lambda_1\lambda_2\rangle\ d_{\lambda\mu}{}^j(\cos\theta),$$

where $j_{min} = \max(|\lambda|,|\mu|)$, $\lambda = \lambda_1 - \lambda_2$, $\mu = \lambda_3 - \lambda_4$, and θ is the c.m.

scattering angle. The partial waves are given by

$$\langle\lambda_3\lambda_4|T^j(s)|\lambda_1\lambda_2\rangle = \tfrac{1}{2}\int_{-1}^{+1}\langle\lambda_3\lambda_4|\phi(s,t)|\lambda_1\lambda_2\rangle\, d_{\lambda\mu}{}^j(\cos\theta)\, d(\cos\theta).$$

The integration was performed using an N-point Gaussian quadrature, according to which

$$\int_{-1}^{+1} f(x)\, dx = \sum_{n=1}^{N} w_n\, f(x_n),$$

where w_n is the quadrature weight associated with the point x_n. This integrates exactly a polynomial of degree 2N-1, and also does not require evaluation of the integrand at the end-points $\cos\theta = \pm 1$, which presents computational difficulties. In our case, we obtain

$$\langle\lambda_3\lambda_4|T^j(s)|\lambda_1\lambda_2\rangle = \sum_{n=1}^{N} \tfrac{1}{2}\langle\lambda_3\lambda_4|\phi(s,\cos\theta_n)|\lambda_1\lambda_2\rangle\, d_{\lambda\mu}{}^j(\cos\theta_n)\, w_n.$$

The rotation functions depend only on $\cos\theta$ and, for the integration, need to be evaluated only at certain points $\cos\theta_n$ depending on the order N of the quadrature. This enables us to write the integration in terms of new weights

$$w_n'(j,\lambda,\mu) = \tfrac{1}{2}\, d_{\lambda\mu}{}^j(\cos\theta_n)\, w_n,$$

which may be evaluated just once, thus saving a very considerable amount of computing time. We therefore obtain

$$\langle\lambda_3\lambda_4|T^j(s)|\lambda_1\lambda_2\rangle = \sum_{n=1}^{N} \langle\lambda_3\lambda_4|\phi(s,\cos\theta_n)|\lambda_1\lambda_2\rangle\, w'_n(j,\lambda,\mu).$$

By using the symmetry properties of the functions $d_{\lambda\mu}{}^j(\cos\theta)$, the number of sets of new weights which must be calculated and stored may be reduced.

Once the partial waves have been obtained, they are modified according to the prescription

$$\langle\lambda_3\lambda_4|T'^j(s)|\lambda_1\lambda_2\rangle = \tfrac{1}{2}\left[S_{final}{}^j(s) + S_{initial}{}^j(s)\right] \langle\lambda_3\lambda_4|T^j(s)|\lambda_1\lambda_2\rangle,$$

and resummed to obtain the absorbed amplitudes

$$\langle\lambda_3\lambda_4|\phi'(s,t)|\lambda_1\lambda_2\rangle = \sum_{j=j_{min}}^{\infty} (2j+1)\, \langle\lambda_3\lambda_4|T'^j(s)|\lambda_1\lambda_2\rangle\, d_{\lambda\mu}{}^j(\cos\theta).$$

The partial waves need be evaluated explicitly only until for some $j = j_{max}$ we find $S^j = 1$. Partial waves corresponding to $j > j_{max}$ are unaltered by the absorption. This "tail" may then be added, since, in an abbreviated notation,

$$\sum_{j=j_{min}}^{\infty} T'^j = \sum_{j=j_{min}}^{j_{max}} T'^j + \phi(s,t) - \sum_{j=j_{min}}^{j_{max}} T^j .$$

The value of j_{max} increases with increasing energy, and hence the higher the order of Gaussian quadrature required to give the high partial waves accurately. For the energies considered $j_{max} = 30$ and a 48-point Gaussian quadrature were found to be quite sufficient. As a check, calculations have been performed with $j_{max} = 50$ and a 512-point Gaussian quadrature. These results were found not to change significantly.

REFERENCES

1. J.D. Jackson, invited talk, Proceedings of the International Conference on High-Energy Physics, Berkeley, 1966.

2. M. Froissart, Phys. Rev. 123, 1053 (1961).

3. T. Regge, Nuovo Cimento 14, 951 (1959); 18, 947 (1960).

4. L. Bertocchi, review talk, Proceedings of the International Conference on Elementary Particles, Heidelberg, 1967.

5. V. Barger, Regge Analysis of High-Energy Scattering Data, invited talk presented at the Regge Pole Conference, University of California, Irvine, 1969.

6. G.E. Hite, Rev. Mod. Phys. 41, 669 (1969); Proceedings of the IX Internationale Universitätswochen für Kernphysik der Universität, Schladming, 1970;
A. Krzywicki, Duality and Regge Cuts in Inelastic 2-Body Processes, invited paper presented at the 5th. Moriond Meeting, 1970.

7. P. Sonderegger, Proceedings of the International School of Elementary Particle Physics, Herceg Novi, 1968.

8. P.T. Matthews, Brandeis Summer School Report, Vol. I, 1963.

9. N.J. Sopkovich, Nuovo Cimento 26, 186 (1962).

10. L. Durand and Y.T. Chiu, Phys. Rev. Letters 12, 399 (1964).

11. H.D.D. Watson, Phys. Letters 17, 72 (1965); Ph.D. thesis, Imperial College, London, 1965.

12. D. Amati, S. Fubini and A. Stanghellini, Nuovo Cimento 26, 896 (1962).

13. S. Mandelstam, Nuovo Cimento 30, 1127 (1963); 30, 1148 (1963).

14. P.V. Landshoff, Regge Cuts: A Review of the Theory, invited talk presented at the Oxford International Conference on Elementary Particles, Oxford, England, 1971;
C. Risk, The Derivation of the Absorption Model from Feynman Diagrams, Lawrence Radiation Laboratory Report No. UCRL-19453.

15. J.D. Jackson and C. Quigg, Phys. Letters 29B, 236 (1969);
M. Biyajima, Prog. Theor. Phys. 43, 61 (1970).

16. R.J.N. Phillips, Proceedings of the IX Internationale Universitätswochen für Kernphysik der Universität, Schladming, 1970.

17. M.L. Blackmon, G. Kramer and K. Schilling, Nucl. Phys. B12, 495 (1969), and references contained therein.

18. B.J. Hartley, R.W. Moore and K.J.M. Moriarty, Phys. Rev. 187, 1921 (1969); D1, 954 (1970);
P.A. Collins, B.J. Hartley, R.W. Moore and K.J.M. Moriarty, Nucl. Phys. B20, 381 (1970); Phys. Rev. D1, 3195 (1970).

19. P.A. Collins, B.J. Hartley, J.D. Jenkins, R.W. Moore and K.J.M. Moriarty, Phys. Rev. D1, 2619 (1970).

20. C. Lovelace, Proc. Roy. Soc. Lond. A. 318, 321 (1970).

21. G.L. Kane, F. Henyey, D.R. Richards, M. Ross and G. Williamson, Phys. Rev. Letters 25, 1519 (1970);
M. Ross, F.S. Henyey and G.L. Kane, Nucl. Phys. B23, 269 (1970).

22. F. Drago, A. Love, R.J.N. Phillips and G.A. Ringland, Phys. Letters 31B, 647 (1970).

23. C. Michael, Proceedings of the Ruhestein Meeting on Low-Energy Hadron Interactions and Coupling Constants.

24. A. Salam, R. Delbourgo and J. Strathdee, Proc. Roy. Soc. Lond. 284A, 146 (1965);
M.A.B. Bég and A. Pais, Phys. Rev. Letters 14, 267 (1965);
B. Sakita and K.C. Wali, Phys. Rev. Letters 14, 404 (1965); Phys. Rev. 139, B1355 (1965);
R. Delbourgo, M.A. Rashid, A. Salam and J. Strathdee, Seminar on High-Energy Physics and Elementary Particles, Trieste (International Atomic Energy Agency, Vienna, 1965).

25. K. Mahanthappa and E.C. Sudarshan, Phys. Rev. Letters 14, 163 (1965);
E. Borchi and R. Gatto, Phys. Letters 14, 352 (1964).

26. J.H.R. Migneron and K. Moriarty, Phys. Rev. Letters 18, 978 (1967);

H.D.D. Watson, R. Migneron, K. Moriarty, D. Fincham and A.P. Hunt, Nuovo Cimento 62A, 127 (1969).

27. D.G. Fincham, A.P. Hunt, J.H.R. Migneron and K. Moriarty, Nucl. Phys. B13, 161 (1969).

28. D.G. Fincham, Ph.D. thesis, Imperial College, London, 1970.

29. G. Ebel, H. Pilkuhn and F. Steiner, Proceedings of the International Conference on Elementary Particles, Lund, 1969.

30. Particle Data Group, Rev. Mod. Phys. 42, 87 (1970).

31. J.D. Jackson, review talk, Proceedings of the International Conference on Elementary Particles, Lund, 1969.

32. M. Roos, Lettere al Nuovo Cimento 3, 257 (1970).

33. M. Jacob and G.C. Wick, Annals of Physics 7, 404 (1959).

34. S.J. Lindenbaum, Proceedings of the Oxford International Conference on Elementary Particles, Oxford, England, 1965.

35. J.D. Hansen, D.R.O. Morrison, N. Tovey and E. Flaminio, Compilation of Cross Sections, I-Proton Induced Reactions, Report No. CERN-HERA 70-2 (1970).

36. J.D. Jackson, J.T. Donohue, K. Gottfried, R. Keyser and B.E.Y. Svensson, Phys. Rev. 139, B428 (1965);
H. Pilkuhn and B.E.Y. Svensson, Nuovo Cimento 38, 518 (1965).

37. S.A. Adjei, P.A. Collins, B.J. Hartley, R.W. Moore and K.J.M. Moriarty, A Parameter-Free Reggeized Absorption Model for Meson-Baryon Scattering, Imperial College Report No. ICTP/70/19.

38. Since this work was completed new data has become available: O. Guisan, Polarization in Charge-Exchange Reactions. This preliminary data shows that the polarization of the recoil neutron in $\pi^- p \to \pi^o n$ is positive out to at least $t = -.5$. The same experiment will give better data on the polarization in $\pi^- p \to \eta n$. Another experiment has been designed to measure the polarization in $K^- p \to \bar{K}^o n$.

39. A. Krzywicki and J. Tran Thanh Van, Phys. Letters 30B, 185 (1969).

40. Saclay-Orsay Collaboration, Phys. Rev. Letters 14, 763 (1965); Phys. Letters 20, 75 (1966).

41. Saclay-Orsay-Pisa Collaboration, Nucl. Phys. B16, 335 (1970).

42. Saclay-Orsay Collaboration, Phys. Letters 18, 200 (1965).

43. CERN-Zürich Collaboration, Phys. Letters 23, 396 (1966).

44. D. Cline, J. Penn and D.D.Reeder, University of Wisconsin Report, 1969; D. Cline, J. Matos and D.D. Reeder, Phys. Rev. Letters 23, 1318 (1969); A. Firestone, G. Goldhaber, A. Hirata, D. Lissauer and G.H. Trilling, Phys. Rev. Letters 25, 958 (1970).

45. M. Abolins, D.D. Carmony, Duong-N Hoa, R.L. Lander, C. Rindfleisch and Nguyen-Hun Xuong, Phys. Rev. 136, B195 (1964).

46. Aachen-Berlin-Birmingham-Bonn-Hamburg-London(I.C.)-München Collaboration, Phys. Rev. 138, B897 (1965).

47. Aachen-Berlin-CERN Collaboration, Phys. Letters 19, 608 (1965).

48. N. Schmitz, Proceedings of the Easter School for Physicists, CERN, Vol. I, 1965.

49. Private communication from Aachen-Berlin-CERN Collaboration to M. Krammer and U. Maor, Nuovo Cimento 50A, 963 (1967).

50. R.D. Matthews, Nucl. Phys. B11, 339 (1969).

51. Aachen-Berlin-CERN Collaboration, Nucl. Phys. B24, 509 (1970).

52. Private communication from CERN-Bruxelles Collaboration to M. Krammer and U. Maor, Nuovo Cimento 52A, 308 (1967).

53. D.J. Mellema, University of California Report No. UCLA-1047.

54. R.S. Holmes, J.C. Berlinghieri, M. Farber, T. Ferbel, P. Slattery, B. Werner and H. Yuta, University of Rochester Report No. UR-875-313.

55. E. Leader, invited paper, Institute of Physics and the Physical Society, Conference on Elementary Particle Physics, Cambridge, England, 1969.

56. R.L. Eisner, P.B. Johnson, P.R. Klein, R.E. Peters, R.J. Sahni, W.L. Yen and G.W. Tantfest, Phys. Rev. 164, 1699 (1967).

57. I. Derado, J.A. Poirier,N.N. Biswas, N.M. Cason, V.P. Kenney and W.D. Shepard, Phys. Letters 24B, 112 (1967).

58. J.A. Poirier,N.N. Biswas, N.M. Cason, I. Derado, V.P. Kenney, W.D. Shephard, E.H. Synn, H. Yuta, W. Selove, R. Ehrlich and A.L. Baker, Phys. Rev 163, 1462 (1967); CERN-Munich Collaboration, Nucl. Phys. B7, 1 (1968).

59. Orsay-Milan-Berkeley Collaboration, Nuovo Cimento 53A, 798 (1968).

60. Bruxelles-CERN Collaboration, paper submitted to the International Conference on High-Energy Physics, Vienna, 1968. Our data is from Ref. 53.

61. F. Schweingruber, M. Derrick, T. Fields, D. Griffiths, L.G. Hyman, R.J. Jabbur, J. Loken, R. Ammar, R.E.P. Davis, W. Kropac and J. Mott, Phys. Rev. 166, 1317 (1968).

62. Birmingham-Glasgow-London(I.C.)-München-Oxford-Rutherford Laboratory Collaboration, Nuovo Cimento 53A, 522 (1968).

63. Aachen-Berlin-CERN-London(I.C.)-Vienna Collaboration, Nucl. Phys. B5, 567 (1968).

64. F.D. Gault (private communication).

65. S.A. Adjei, P.A. Collins, B.J. Hartley, R.W. Moore and K.J.M. Moriarty, A Parameter-Free Reggeized Absorption Model for Δ(1236) Production in Proton-Proton Reactions, Imperial College Report No. ICTP/70/20.

66. Z. Ming Ma, G.A. Smith, R.J. Sprafka and G.T. Williamson, Phys. Rev. Letters 24, 1031 (1970).

67. G. Alexander, O. Benary, G. Czapek, B. Haber, N. Kidron, B. Reuter, A. Shapira, E. Simopoulou and G. Yekutieli, Phys. Rev. 154, 1284 (1967).

68. Z.Ming Ma, G.A. Smith, R.J. Sprafka, E. Colton and P.E. Schlein, Phys. Rev. Letters 23, 342 (1969).

69. G. Alexander, Z. Carmel, Y. Eisenberg, E.E. Ronat, A. Shapira, G. Yekutieli, A. Fridman, G. Maurer, J. Oudet, C. Zech and P. Cüer, Phys. Rev. 173, 1322 (1968).

70. H.-C. Dehne, J. Díaz, K. Strömer, A. Schmitt, W.P. Swanson, I. Borecka, G. Knies and G. Wolf, Nuovo Cimento 53A, 232 (1968).

71. G.B. Chadwick, G.B. Collins, P.J. Duke, T. Fujii, N.C. Hien, M.A.R. Kemp and F.Turkot, Phys. Rev. 128, 1823 (1962).

72. E.W. Anderson, E.J. Bleser, G.B. Collins, T. Fujii, J. Menes, F. Turkot, R.A. Carrigan, Jr., R.M. Edelstein, N.C. Hien, T.J. McMahon and I. Nadelhaft, Phys. Rev. Letters, 16, 855 (1966).

73. D.C. Colley, review paper, Topical Conference on High-Energy Collisions of Hadrons, CERN, 1968.

74. A.P. Colleraine and U. Nauenberg, Phys. Rev. 161, 1387 (1967).

75. Orsay-Saclay Collaboration, Nucl. Phys. B5, 169 (1968).

76. J.G. Rushbrooke (private communication).

77. Cambridge-London(I.C.) Collaboration (private communication).

78. F.D. Gault, B.J. Hartley, J.H.R. Migneron and K.J.M. Moriarty, Nuovo Cimento 62A, 269 (1969).

79. B. Petersson and N.A. Törnqvist, Nucl. Phys. B13, 629 (1969); P.A. Collins, B.J. Hartley, R.W. Moore and K.J.M. Moriarty, Phys. Rev. D1, 3134 (1970); Nucl. Phys. B22, 150 (1970).

80. S.A. Adjei, P.A. Collins, B.J. Hartley, R.W. Moore and K.J.M. Moriarty, A Veneziano Model for $K^- p \to K^{*-} \pi^+ n$ and $K^- p \to \bar{K}^{*0} n$ Taking Some Account of Spin, Phys. Rev. D (to be published).

81. S.A. Adjei, P.A. Collins, B.J. Hartley, R.W. Moore and K.J.M. Moriarty, Phys. Rev. D3, 150 (1971); An Approach to the Inclusion of Spin in the Veneziano Model for $K^- p \to \bar{K}^0 \pi^- p$ and $K^- p \to K^{*-} p$, Imperial College Report No. ICTP/70/21.

82. S.A. Adjei, P.A. Collins, B.J. Hartley, R.W. Moore and K.J.M. Moriarty, The Removal of Baryon Parity Doublets in the

Veneziano Model for Meson-Baryon Scattering, Phys. Rev. D3, May (1971); Residue Recurrence Relations for the Veneziano Model, Lettere al Nuovo Cimento (to be published); A Daughterless Dual Model, Imperial College Report No. ICTP/70/12.

83. S.A. Adjei, P.A. Collins, B.J. Hartley, R.W. Moore and K.J.M. Moriarty, A Veneziano Model with Cuts for $\bar{K}N$ and KN Charge-Exchange Scattering, Imperial College Report No. ICTP/70/1.

84. P.A. Collins, B.J. Hartley, R.W. Moore, K.J.M. Moriarty and G.W. Parry, A Veneziano Model with Absorptive Corrections for Higher-Spin Production, Imperial College Report No. ICTP/70/26.

85. S.A. Adjei, P.A. Collins, B.J. Hartley, R.W. Moore and K.J.M. Moriarty, An Efficient Partial-Wave Analyser with Application to the Reggeized Absorption Model, invited paper, Institute of Physics and the Physical Society, Conference on Computational Physics, London, 1970.

86. C. Lovelace, Nucl. Phys. B12, 253 (1969).